24. Aerospace Engineering

Hamid Hefazi

This chapter focuses on the commercial aviation sector of the aerospace industry. Following a brief introduction, basic definitions and terminology are discussed in Sects. 24.1–24.5. Sections 24.6 and 24.7 focus on the aerodynamic characteristics of flight, followed by the general configuration of airplanes in Sect. 24.8. Weight definitions and the related performance of aircrafts are discussed in Sects. 24.9 and 24.10. Section 24.11 is on the stability and control of airplanes, followed by a description of loads in Sect. 24.12. Finally, Sect. 24.13 reviews aircraft structure and Sect. 24.14 describes basic maintenance checks for commercial airplanes.

K.-H. Grote, H. Hefazi (Eds.), *Springer Handbook of Mechanical Engineering*, Springer Handbooks,
https://doi.org/10.1007/978-3-030-47035-7_24

24.1 Aerospace Industry

Aerospace engineering is a branch of engineering that deals with the design, construction, and operation of aerospace vehicles.

The aerospace industry comprises a collection of organizations involved in the research, design, construction, testing, and operation of aerospace vehicles. In the USA, the aerospace industry consists of 20 prime contractors, 18 major airlines carriers that posted more than US $1 billion in revenue during the fiscal year 2016 (consisting of mainline, regional, and freight carriers), a large government-supported research agency, and thousands of smaller companies that supply special components to these primary contractors. A number of private space flight companies have also been added to this mix since the year 2000. The total (direct and induced) employment by the industry varies somewhat with changing business conditions, but in recent years has averaged about 2.5 million people, of whom approximately 70 000 are employed as engineers. According to a 2016 report by the Aerospace Industry Association [24.1], the total direct employment by the US aerospace and defense (A&D) sector in 2015 was 1.65 million. Additionally, the induced employment by the sector was estimated at 1.13 million. The aerospace industries in developed countries such as Russia, Japan, and European countries are not quite as large as that of the USA in terms of number of employees, but are similar in nearly every respect. Aerospace industries are also growing rapidly in populous countries such as China and India.

The products of the aerospace industry are many and varied, meeting a number of mission requirements. The broadest product classifications are related to the customer purchasing the product, giving rise to a classification into civil and military products. More specific product classifications can be derived from the type of aerospace vehicle and the particular use to which it is put. This section is organized in this manner.

Globally, more than 45 countries have notable levels of aerospace industry activities (Fig. 24.1). These activities include aircraft manufacturing, spacecraft manufacturing, missile and unmanned air vehicle (UAV) manufacturing (including engines, systems, aerostructures, and subtier suppliers), airborne defense electronics, simulator and ground support equipment, research and development, as well as maintenance and repair operations (MRO) for transport, military, and business and general aviation (BGA) aircraft.

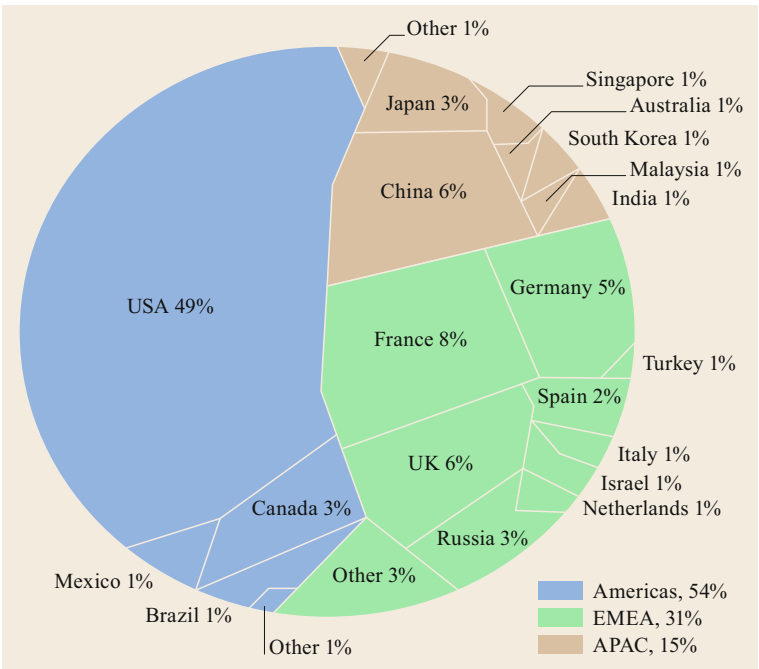

Fig. 24.1 The 2017 global aerospace industry – US$ 838 billion (Source: AeroDynamic Advisory & Teal Group 2018) [24.1–3]

24.2 Aerospace Technology and Development

24.2.1 Aerospace and Society

The wealth of any modern society is to a large extent based on fast and reliable transport of information, passengers, and freight in an environmentally acceptable way. Aerospace is a mandatory part of the overall transportation system: satellites provide weather information, navigation signals, and transmit messages worldwide; transport aircraft provide fast and safe transportation of passengers and/or freight across borders; and military aerospace will be part of any strategy for many years to come. In commercial terms, the future of aeronautics is bright: the increase of passenger traffic has been stable at some 5% per year over the past three decades, and is forecast to continue this trend over the coming decades. The International Air Transport Association (IATA) passenger growth forecast projects that passenger numbers are expected to reach 8.2 billion by 2031 with a 3.7% average annual growth in demand (2014 baseline year). This is more than double the 3.8 billion who flew in 2016. Cargo growth is even higher, at 6% per year [24.2]. From Fig. 24.2 it can be seen that, in Europe, passenger transport by aeronautics has exceeded that by rail and public transport since 2015.

In addition, aeronautics has always touched the human imagination: from the story of Daedalus through Leonardo da Vinci to Antoine de Saint-Exupéry. It is an ancient wish of mankind to be able to fly, and space has inspired human thought for a long time as well, from ancient cultures, which already knew much about the stars, up to today, where we think about an ever-expanding or finally collapsing universe.

In some fields of activity, aeronautics and space systems merge. After launch, space payload carriers not built in space have to cross the atmosphere, coping with gravity and air friction, similar to aeronautic vehicles. More specifically, common interests include space tourism, hypersonic transport, and rail guns as satellite launchers.

The launch of space vehicles is somehow spectacular and, in the past, has been limited to government agencies and a few places in the world. Therefore, the public takes quite some interest in such launches, because they are linked to the above-mentioned dream of mankind. Furthermore, since the year 2000, a robust and competitive commercial space sector has developed, promising to generate new global markets and innovation-driven entrepreneurship. On the other hand, and even though aeronautic vehicles are also part of that dream and are mandatory for modern life, their operation is more heavily criticized. Whereas, for example, railway noise is accepted even in the heart of cities at midnight, aircraft noise seems to be annoying even if hardly noticeable. The public is used to all other kinds of traffic and has accepted their drawbacks, but noise and emissions from aeronautics are more in the focus of today's discussion than merited by their share of the overall transport system. This may be due to the fact that the basis of one's desire to fly is the

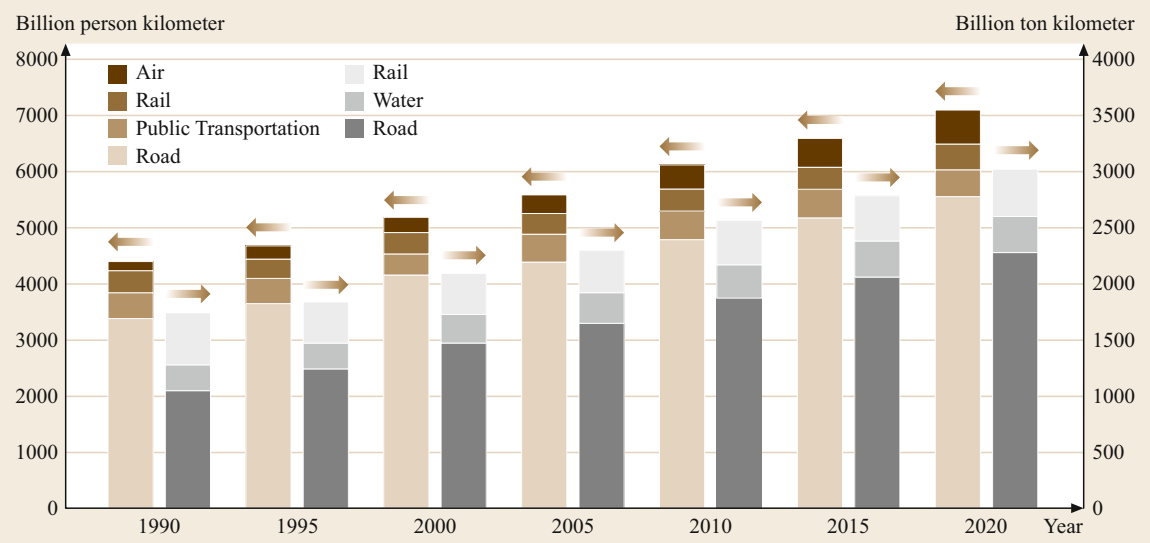

Fig. 24.2 Share of different modes of passenger and freight transportation in Europe (EU-25) (source: European Commission)

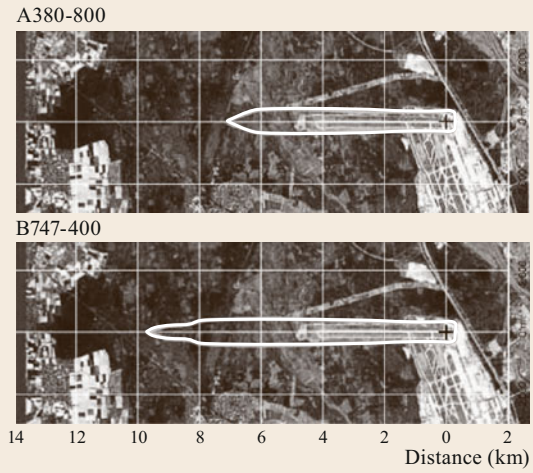

Fig. 24.3 Noise carpet at Frankfurt airport. The sound pressure is 85 dB(A) or higher within the marked region (source: DLH)

ease and weightlessness of a bird soaring in the sky. Thus, humans react more sensitively to aircraft noise and pollution than to pollution from any other means of transport. In reality, much progress has been made over recent decades. Noise has been drastically reduced with the target of keeping the major part of the noise carpet within the airport area (Fig. 24.3). While the amount of exhaust emissions has even been decoupled from the number of aircraft, overall aviation emissions remain a challenge due to increased demand for air travel (Fig. 24.4) [24.3].

As in other fields, there are many ways to look at aerospace engineering. Firstly, there is the work of specialists in many fields, but one can also consider a system approach, combining disciplines into increasingly complex components up to the level of the final vehicles; finally, there is the system-of-systems approach, when talking about the air transport system (ATS). In astronautics, this system-of-systems approach includes the vehicle, payload, transfer, and ground support. In any case, the total life cycle has to be addressed, from the first flight or launch via planned operation up to the disposal of the vehicle. The importance of the last topic is increasing, in aeronautics due to the issue of global resource management and in astronautics due to the issue of space debris.

24.2.2 Aerospace Disciplines and the Design Process

Aerospace in general is an integrated or so-called integration subject, with aeronautics and astronautics as particular fields of activity. Vehicle design is based on inputs from the fundamental engineering disciplines, namely aerodynamics, structures, and systems. As subgroups, flight mechanics, propulsion, guidance navigation and control (GNC), and others are found but can be allocated to the first three disciplines. In addition, combinations of the original disciplines have emerged, such as aeroelastics and aeroacoustics. Within each of these disciplines, progress has been made in the past, such as new flow control means, new materials, and new electronics systems.

Building on the foundations laid by work in the individual disciplines, components are created. This is already an interdisciplinary task; e.g., for an aircraft flap, aerodynamic performance is needed as well as the structure, including the kinematics and actuators on the systems side. Today, in aeronautics the largest components are the complete aircraft structure and the engines, which are developed and manufactured sepa-

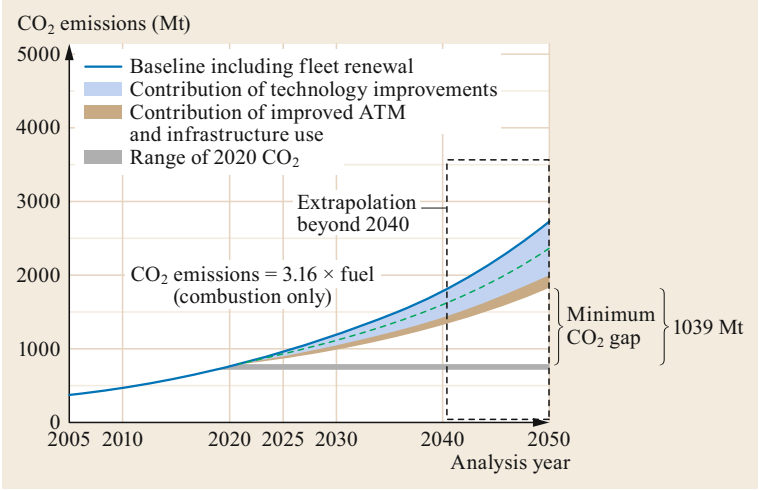

Fig. 24.4 CO_2 emissions trends from international aviation, 2005–2050

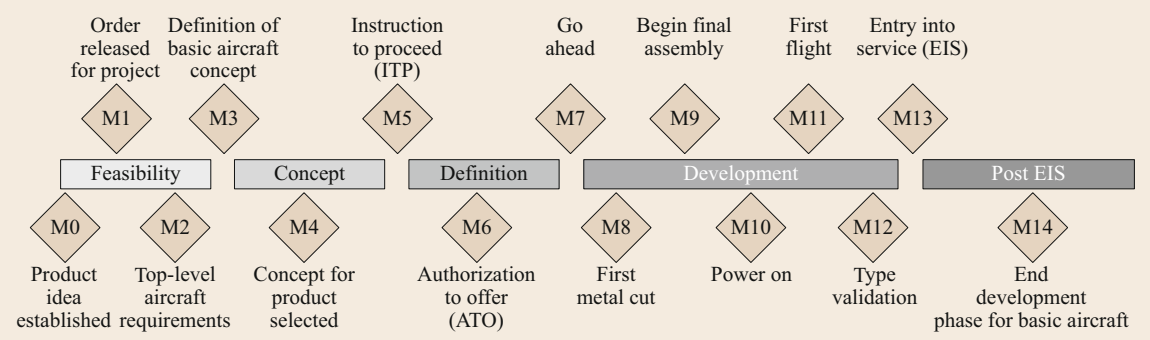

Fig. 24.5 Development process

rately. As for components, their development and final composition into a complete vehicle is a multidisciplinary and interdisciplinary task.

As for most other product developments, aircraft or spacecraft design follows a process which has been set up throughout recent decades. Initially, there is a market analysis, looking for what is missing in the present set of products. In aeronautics, this may be defined by the so-called transport task, i.e., the requirement to move a given payload in a given time across a given distance. In astronautics, apart from the vehicle, the payload itself can be the product to be developed, such as a satellite.

From these general requirements set by the market demands, the so-called top-level aircraft requirements (TLAR) can be derived as a basis for the future project office (FPO) work that will construct the general arrangement (GA) of the vehicle to be designed, working with tools mainly based on statistics and/or simple calculation methods.

This GA will then be given to various departments, such as flight dynamics or structures. Together with the aircraft program management, they will start component development, accompanied by tests using wind tunnels, test rigs, or simulators. At this stage, new technologies already available in the respective disciplines can be included in the design process. Increasingly, digital mock-ups (DMU) are used in the first part of the development phase instead of hardware.

With the GA and first performance estimates available, launching customers have to be found. They will influence the final design by their own needs. Depending on the product size and cost, with a certain number of products sold, the actual development starts with the program go-ahead, almost in parallel with the production of the first parts. At the end, specific tests will be carried out on prototypes, which may require some final, hopefully minor, changes to the design. The last step is the certification process, which ends with entry into service (EIS).

The whole development process as outlined above is almost the same for any aircraft manufacturer, and can be seen as a series of milestones as shown in Fig. 24.5.

At present, the market analysis may last for 2 years, the predevelopment for some 3 years, the development and manufacture for about 5 years, and the certification for another year. Just before the committed start of a program, technology development may take place, with technology feasibility or prematurity as a first step, and technology application studies as the final step. Overall, the time between the first thought about a new aircraft and the EIS is approximately 10–15 years.

For example, first thoughts on the Airbus A380 were published in 1989; at that time it was called the megaliner, ultrahigh-capacity aircraft (UHCA). Later it became the very large commercial transport (VLCT), as a common Airbus–Boeing feasibility study.

The committed program start occurred in 2000, and finally the A380 was introduced into airline service in 2007, corresponding to a total of 18 years. Of course, all manufacturers try to speed up this process. For the given and already highly optimized standard aircraft configuration, i.e., the fuselage, wing, engines, and tailplane as present in today's aircraft, further optimization is possible mainly by improving the design chain, including supplier management. However, for a completely new design, such as a blended wing body (BWB) (Fig. 24.6) or an oblique flying wing (OFW), the exhaustive time scale as described above is likely to remain.

Apart from monodisciplinary technologies such as new materials, actuators, or a specific aerodynamic vortex generator, integrated technologies make their way into the product, too; for example, fly-by-wire technology was a must for the European supersonic transport aircraft Concorde in the 1960s. Without it, it would not have been possible for the pilots to fly this aircraft in all the different flight regimes, in each of which the aircraft control behavior is different. Afterwards, in a first attempt, this technology was introduced into the

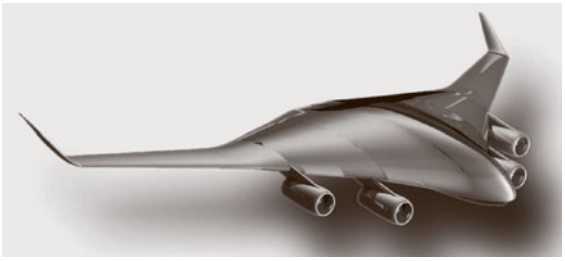

Fig. 24.6 Blended wing body (source: DLR)

Airbus A310, until it finally became mature in the Airbus A320, which made its maiden flight in 1987. Flow control technology or artificial instability are other examples of technology development, and manufacturing technologies such as friction stir welding or laser beam welding, advanced bonding or surface coating have been developed in the past and are part of the production process today.

Following its complete assembly, the vehicle will be operated in a larger system. Aircraft navigate with the help of air-traffic control, they are linked to other traffic in the air, and on the ground, especially in the vicinity of airports, they need to be loaded and unloaded, and they are part of a so-called intermodality concept that links personal and public transport on the ground with air or sea transport.

Design integration and connectivity of aircraft systems through the Internet of Things (IoT) are among the key enablers that impact the next-generation aircraft design process. Multidisciplinary design and optimization (MDO) and digital design are among the technologies that are at various levels of maturity in order to support the next-generation aircraft design process. Furthermore, a new area of the industry, focused on unmanned aircraft systems (UASs) – commonly know as drones or unmanned aerial vehicles (UAVs) – has also emerged in recent years. However, applications of these systems have mostly been limited to military and a few other commercial activities, as opposed to passenger or cargo transportation.

24.2.3 Challenges in Aeronautical Engineering

Looking at the history of aeronautics, it can be structured into three blocks. From its beginning until the end of World War II, physical understanding was the dominant driver. This began with daring pilots in fantastic flying machines, permanently hunting for records in range, speed, and altitude. As the next phase, coinciding with the introduction of jet engines, commercial aeronautics emerged. Many different configurations have been studied, including vertical take-off and landing (VTOL) aircraft such as the Dornier Do 31, supersonic transport in the shape of Concorde, and flying wings such as the Northrop YB-49. This led to the third phase, which is based on today's configuration of a commercial transport aircraft, all looking very much the same regardless of the manufacturing company. This configuration has reached a high level of maturity, so after all the expensive configuration studies, finally civil transport aircraft design and manufacturing has paid off.

However, with the success of commercial transport, three other issues have emerged. Firstly, airports are increasingly operating at their capacity limits, so it is questionable whether there is any chance to increase air traffic, even if there is a demand for it. Secondly, linked to this, environmental aspects play a leading role, even though the contribution of aeronautics to global emissions may be small, i.e., about 2% today. However, the 2015 Intergovernmental Panel on Climate Change (IPCC) estimated that aviation's contribution could grow to 5% of the total by 2050 if action is not taken to tackle these emissions. Thirdly, and still linked to growth, safety issues are of increasing importance. Today's reliability rate of 10^{-9} failures per flight hour for critical components will not be sufficient if the number of aircraft doubles within a decade. In order to reduce the number of accidents in parallel with an increasing number of vehicles, functional hazard analysis must yield greater reliability. This holds true for single components such as an actuator, up to subsystems such as an aileron, and also the complete aircraft system and structure.

Almost at the same time, the European Commission published its Vision 2020 [24.4] on aeronautics and the National Aeronautics and Space Administration (NASA) published its Aeronautics Blueprint on these issues. Both came to similar conclusions: with aeronautics being a vital element for the wealth of society on one side, and the environmental issues linked to it on the other side, in the future there will be additional TLAR, in order to balance transport needs, societal needs in terms of safety and security, and environment protection. These additional TLAR may ask for totally different vehicle configurations as well as for new ways of operating these vehicles. In addition, all of these issues ask for a system approach; for example, in contrast to road and rail transport, security will play an increasingly important role in aeronautics. There are an increasing number of studies on seamless air transport which ask for new ground procedures and probably even new vehicle designs. To define and finally solve all the new TLAR will be a demanding task for any discipline as well as for the overall vehicle and system composition, in aeronautics as well as in astronautics. Therefore, a fourth phase can be expected, aiming for sustainable growth.

24.3 Aircraft

The term "aircraft" is an all-inclusive term for any form of craft designed for navigation in the air. In the years since the first actual man-carrying flight in a hot-air balloon in the late 1700s, there have been a number of types of aircraft that have provided the means for aerial navigation. A brief recap includes the hot-air balloon ascension of de Rozier and d'Arlandes in 1783, the hydrogen balloon flight of J.A.C. Charles and M.N. Robert in 1783, and the successful steam-engine-powered airship (balloon) of Giffard in 1852. The German Otto Lilienthal developed a man-carrying glider that made over 2000 glides before suffering a fatal crash in 1896 [24.5]. As has been well documented, it was the Wright brothers, Orville and Wilbur, who made the first controlled powered flights of an airplane in 1903. Progress in aircraft design was slow in the first few years after the Wright flights, but by the start of World War I (WWI), many flying machines of various types and configurations had been successfully built and flown. During WWI, military requirements gave rise to the development of numerous types of aircraft with very specialized capabilities, which were produced in their thousands. Following the war, aircraft for the transportation of passengers came into widespread use, with the establishment of airline companies and air routes, first between major European cities, but later in America and other parts of the world as well. In the period between World War I and World War II, specialized aircraft were used to set nonstop distance records between continents, while other specialized aircraft set records for speed and altitude. World War II saw the introduction of new technology in aircraft design with the advent of practical helicopters, jet engines, rocket propulsion systems, and guided missiles. Following World War II, there was significant growth in private, recreational flying, expansion of the international commercial air transportation system, as well as continuing development of experimental aircraft that flew higher, faster, and farther than previous aircraft. With the creation of the National Aeronautics and Space Administration (NASA) in 1958, a variety of unique aircraft and spacecraft were designed to meet very specific mission objectives laid down by the agency. In recent years, there has been increasing military interest in unmanned combat air vehicles (UCAVs).

24.3.1 Aircraft Types

The two major categories of aircraft types are lighter than air (LTA) and heavier than air (HTA). A lighter-than-air craft is one that rises aloft by making use of Archimedes' principle, that is, by displacing a weight of air that is greater than the weight of the craft itself, thus creating a buoyant force. A heavier-than-air aircraft is one that rises aloft due to Bernoulli's principle acting on the aircraft's lifting surfaces, creating suction on the upper surface and pressure on the lower surface relative to the ambient air pressure. The design and operation of civil aircraft in the USA is subject to numerous regulations promulgated by the Federal Aviation Administration (FAA) of the Department of Transportation [24.6]. Table 24.1 presents a summary of the various types of FAA regulations.

Table 24.1 Summary of Federal Aviation Regulatory (FAR) categories

Regulatory category	FAR part
Certification procedures for products and parts	21
Airworthiness standards, normal, utility, acrobatic, and commuters	23
Airworthiness standards, transport category airplanes	25
Airworthiness standards, normal category rotorcraft	27
Airworthiness standards, transport category rotorcraft	29
Airworthiness standards, manned free balloons	31
Airworthiness standards, aircraft engines	33
Airworthiness standards, propellers	35
Noise standards, aircraft type, and airworthiness standards	36
Airworthiness directives	39
Maintenance, preventive maintenance, rebuilding, and alteration	43
Identification and registration marking	45
Aircraft registration	47
General operating and flight rules	91
Special air-traffic rules and airport traffic patterns	93
Instrument flight rules (IFR) altitudes	95
Standard instrument approach procedures	97
Ultralight vehicles	103
Certification and operation, domestic, flag, and supplemental air carriers, and commercial operators of large aircraft	121
Certification and operation, airplanes having seating capacity of 20 or more passengers, or a maximum payload capacity of 6000 lb or more	125
Certification and operation of scheduled air carrier helicopters	127
Air taxi operators and commercial operators	135
Agricultural aircraft operations	139

Lighter-than-Air Aircraft

One can distinguish between the following types of LTA aircraft:

- Hot-air balloon, which consists of a large envelope made of lightweight fabric to contain the hot air, a burner located below the envelope, usually fueled by kerosene, to heat ambient air, causing it to rise into the envelope. A basket hung underneath the burner is provided for the pilot and passengers.
- Light-gas balloon, which is similar in arrangement to a hot-air balloon, but without the burner. The buoyant force is generated by the use of light gases such as helium in the envelope, which displace the relatively heavier ambient air.
- Blimp or nonrigid airship, which is basically a large gas balloon whose streamlined shape is maintained by internal gas pressure. In addition to the gas envelope, the blimp has a car attached to the lower part of the envelope for the crew and passengers, engines and propellers to develop forward speed, and fins with hinged aft portions for control.
- Rigid airship, a lighter-than-air aircraft with a rigid frame to maintain its shape and provide a volume for the internal placement of light gasbags. The rigid airship also has a car attached to the lower part of the rigid frame for the crew and passengers, engines, propellers, and tail fins similar to the blimp. Rigid airships reached the peak of their development in the mid-1930s, but several spectacular accidents curtailed further development.

Heavier-than-Air Craft

HTA aircraft can be divided into three main categories.

A *glider* is an aircraft that flies without an engine. The simplest form of a glider is the hang glider, which consists of a wing, a control frame, and a pilot harness. The pilot is zipped into the harness and literally hangs beneath the wing, with his hands on the control bar of the control frame. The wing has an aluminum frame that supports the wing fabric, and internal battens to provide a proper shape to the fabric. Hang gliders are usually launched from a very steep hill or a cliff that affords sufficient altitude for gliding flight. Simple utility gliders which have rigid structural elements similar to an airplane are used primarily for training. These gliders are launched into the air by being towed by a power winch, an automobile, or an airplane. Extremely refined sailplanes, usually made of very lightweight materials and featuring very long thin wings, take advantage of rising air currents, and can soar for a long time and cover distances of hundred of miles in a single flight. A variation of the sailplane is the *motorglider*, basically a sailplane with a small motor and propeller, which is used for take-off and climb to soaring altitude, whereupon the motor is shut off, and then retracted along with the propeller to revert to the sailplane configuration.

An *airplane* is an air vehicle that incorporates a propulsion system and fixed wings, and is supported by aerodynamic forces acting on the wings. Airplane propulsion systems may be a piston engine driving a propeller, a turbojet engine, or a rocket engine, depending on the required mission. Airplanes range in form from small general aviation aircraft, usually privately owned, with one or two engines, to larger commercially operated air transport aircraft that can carry from 20 to upwards of 500 passengers and can fly distances from 500 to over 8000 miles nonstop. In addition to these civil aircraft types, there a number of military aircraft types designed for different missions, such as fighter, attack, bomber, reconnaissance, transport, and trainer. A very small class of airplanes, known as experimental research aircraft, usually powered by rocket engines, has been built to obtain flight test data at extremely high speeds and altitudes. The ultimate development in this area is the US Space Shuttle, which is a rocket-powered spacecraft for most of its mission, and an unpowered glider for the approach and landing phase of the flight. A number of supersonic transport aircrafts such as Lockheed Martin's X-59 (QueSST, quiet supersonic transport) and Boom Technology's Overture (https://boomsupersonic.com/overture) are at various stages of development.

A *helicopter* is an aircraft that is supported by aerodynamic forces generated by long thin blades rotating about a vertical axis. The rotor blades are driven by the helicopter's propulsion system, usually a piston or gas turbine engine. Helicopters range in size from small, two-seat personal utility models to large transport types that can carry up to 40 people. Large heavy-lift helicopters are often used in specialized hauling and construction tasks, where their ability to remain airborne over a fixed spot for extended periods of time is unique. Helicopters have also been used in several military applications such as air–sea rescue, medical evacuation, as battlefield gunships, and for special-operations troop transport. Recent developments in helicopter technology have led to hybrid helicopter craft called the tilt rotor. In this machine, there are two rotors to provide the vertical forces required for take-off and landing, but as the name implies, these rotors may be tilted to varying degrees until they are aligned in the direction of flight, acting like the propellers on a conventional airplane. The tilt rotor has small wings to provide the aerodynamic lift required during cruise flight, during which the rotors are used to provide forward thrust.

24.4 Spacecraft

Spacecraft fall into two major categories, unmanned, with no humans aboard, and manned, with humans aboard. Examples of unmanned spacecraft include civil communication satellites, military reconnaissance satellites, and scientific probes that gather information on our solar system. Examples of unmanned spacecraft include the Eutelsat civil communication satellites, the Aquila and Kosmos military reconnaissance satellites, the Hubble Space Telescope and Mars Global Surveyor and Starlink satellites. Examples of manned spacecraft include the Soyuz, Mir, Mercury, Gemini, Apollo, Space Shuttle SpaceX's Crew Dragon and Boeing's Starlines.

24.5 Definitions

The following are some important definitions related to a good understanding of aerospace engineering.

24.5.1 Units

Although there has been a policy in the USA in recent years to convert to the International System of Units (SI), the US aerospace industry continues to use English units in its work. This publication will use English units as primary, since most American engineers are familiar with this terminology. A list of conversion factors between SI and English units is given in Table 24.2.

24.5.2 Flight Speed Terminology

One of the key performance parameters for an airplane is its maximum level-flight speed [24.7]. For a variety of technical and economic reasons, various airplanes are designed to operate at speeds most appropriate to their design missions. Modern airplanes operate at speeds ranging from a low of around 60 kn to highs of around 1450 kn. Over such a wide range of flight speeds, the characteristics of the airflow around the airplane change dramatically. These changes, associated with the compressible nature of air, are directly related to the flight Mach number, defined as the flight speed divided by the speed of sound in the ambient air in which the airplane is flying. This situation has given rise to some general terms to describe airplane flight speeds in terms of Mach number, as shown in Fig. 24.7 [24.8]. Also shown are the types of airplanes having maximum level-flight speeds within the various speed regimes.

Standard Atmosphere

For design and performance calculations, it is appropriate to establish a standard set of characteristics for the Earth's atmosphere in which aircraft operate. The US standard atmosphere is a widely used set whose essential characteristics, that is, the temperature, pressure, density, and viscosity, as a function of altitude have been derived using

$$p = \rho RT \,,$$
$$\mathrm{d}p = -\rho g \,\mathrm{d}h \,,$$

where

p = pressure in $\mathrm{lb/ft^2}$,
ρ = density in $\mathrm{slug/ft^3}$,
T = absolute temperature in °Ra ,
R = gas constant (1718 ft lb/(slug °Ra)) for air ,
g = gravitational constant ($32.17\,\mathrm{ft/s^2}$),
h = height above sea level in feet.

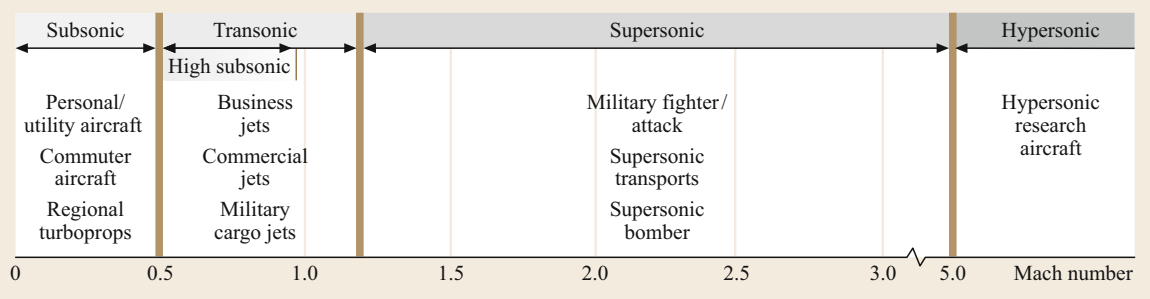

Fig. 24.7 Flight speed terminology

Table 24.2 Conversion factors between SI and English units

Conversion factor	
Mass	1.00 kg = 0.06852 slug 1.00 slug = 14.594 kg At the surface of the Earth, an object with a mass of 1.00 kg weighs 9.80 N or 2.205 lb, and an object with a mass of 1.00 slug weighs 32.17 lb or 143.10 N
Length	1.00 m = 3.2808 ft 1.00 ft = 0.3048 m = 30.48 cm
Force	1.00 N = 0.2248 lb 1.00 lb = 4.4482 N
Temperature	1.00 K = 1.8 °R °R = °F + 460 1.0 °R = 0.5556 K K = °C + 273
Pressure	$1.00\,N/m^2 = 1.4504 \times 10^{-4}\,lb/in^2 = 2.0886 \times 10^{-2}\,lb/ft^2$ $1.00\,lb/in^2 = 6.8947 \times 10^{3}\,N/m^2$ $1.00\,lb/ft^2 = 47.88\,N/m^2$
Velocity	1.00 m/s = 3.2808 ft/s = 2.2369 mi/h 1.00 ft/s = 0.6818 mi/h = 0.3048 m/s
Density	$1.00\,kg/m^3 = 1.9404 \times 10^{-3}\,slug/ft^3$ $1.00\,slug/ft^3 = 515.36\,kg/m^3$
Viscosity	$1.00\,kg/(m\,s) = 20.886 \times 10^{2}\,lbf\,s/ft^2$ $1.00\,lbf\,s/ft^2 = 47.879\,kg/(m\,s)$
Specific heat	$1.00\,N\,m/(kg\,K) = 1.00\,J/(kg\,K) = 2.3928\,Btu/(lb_m\,°R) = 5.9895\,ft\,lb_f/(slug\,°R)$ $1.00\,ft\,lb/(slug\,°R) = 1.6728 \times 10^{-1}\,N\,m/(kg\,K) = 1.6728 \times 10^{-1}\,J/(kg\,K)$
Frequently used equivalents	
1 bhp	550 ft lb/s = 33 000 ft lb/min
1 kn	1.152 mi (stat.)/h
1 kn	1.69 ft/s
1 mi (stat.)/h	0.868 kn
1 mi (stat.)/h	1.467 ft/s
1 ft/s	0.682 mi (stat.)/h
1 ft/s	0.592 kn
1 km	0.621 mi (stat.)
1 km	0.539 mi (naut.)
1 mi (stat.)	1.609 km
1 mi (naut.)	1.854 km
1 rad	57.3°
Note that the preceding values are *equivalents*. The conversion factors are the reciprocals.	
Frequently used constants	
γ	1.4 (air)
Gas constant R (air)	287.05 N m/(kg K) = 1718 ft lb/(slug °R)
Specific heat c_p (air)	1004.7 N m/(kg K) (J/(kg K)) = 6006 ft lb/(slug °R)
Gravitational constant at sea level g_0	$9.80\,m/s^2 = 32.17\,ft/s^2$
Radius of the Earth r_0	6.378×10^{6} m = 20.92×10^{6} ft

mi (stat.) = statute mile, nmi = nautical mile, kn = nautical mile per hour

With these equations, only a defined variation of T with altitude is required to establish the standard atmosphere. The defined variation, based on experimental data, is shown in Fig. 24.8.

Once the temperature variation with altitude is defined, the characteristics of the standard atmosphere can be calculated directly.

The characteristics of the US standard atmosphere are presented in Table 24.3. From sea level to 36 089 ft, the temperature decreases linearly with altitude. This region is called the troposphere. Above 36 089 ft, the temperature is constant up to 65 617 ft in the region called the stratosphere. Above 65 617 ft, the temperature increases linearly to 100 000 ft, the upper level of interest for current or foreseeable aircraft.

Although the concept of geometric altitude, the altitude above sea level as determined by a tape measure, is most familiar, of prime importance for aircraft design and performance calculations is the pressure altitude, i.e., the geometric altitude on a standard day for which

Table 24.3 Characteristics of the US standard atmosphere

Altitude	Temperature		Pressure	Density	Density ratio	Kinematic viscosity	q/M^2	Sonic velocity	
(ft)	(°F)	(°R)	(psf)	(slug/cu ft)		(ft^2/s)	(lb/ft^2)	(ft/s)	(kn)
0	59.0	518.7	2116.2	0.0023769	1.0000	0.0001572	1481.0	1116.4	661.5
1000	55.4	515.1	2040.9	0.0023081	0.9710	0.0001610	1429.0	1112.6	659.2
2000	51.9	511.6	1967.7	0.0022409	0.9427	0.0001650	1377.0	1108.7	656.9
3000	48.3	508.0	1896.7	0.0021752	0.9151	0.0001691	1328.0	1104.9	654.6
4000	44.7	504.4	1827.7	0.0021110	0.8881	0.0001732	1279.0	1101.0	652.3
5000	41.2	500.9	1760.9	0.0020482	0.8616	0.0001776	1233.0	1097.1	650.0
6000	37.6	497.3	1696.0	0.0019869	0.8358	0.0001820	1187.0	1093.2	647.7
7000	34.0	493.7	1633.1	0.0019270	0.8106	0.0001866	1143.0	1089.3	645.4
8000	30.5	490.2	1572.1	0.0018685	0.7860	0.0001914	1100.0	1085.3	643.0
9000	26.9	486.6	1512.9	0.0018113	0.7619	0.0001963	1059.0	1081.4	640.7
10 000	23.3	483.0	1455.6	0.0017556	0.7385	0.0002013	1019.0	1077.4	638.3
11 000	19.8	479.5	1400.0	0.0017011	0.7155	0.0002066	979.8	1073.4	636.0
12 000	16.2	475.9	1346.2	0.0016480	0.6932	0.0002120	942.1	1069.4	633.4
13 000	12.6	472.4	1294.1	0.0015961	0.6713	0.0002175	905.6	1065.4	631.4
14 000	9.1	468.8	1243.6	0.0015455	0.6500	0.0002233	870.2	1061.4	628.8
15 000	5.5	465.2	1194.8	0.0014962	0.6292	0.0002293	836.0	1057.4	626.4
16 000	1.9	461.7	1147.5	0.0014480	0.6089	0.0002354	802.9	1053.3	624.0
17 000	−1.6	458.1	1101.7	0.0014011	0.5892	0.0002418	770.8	1049.2	621.6
18 000	−5.2	454.6	1057.5	0.0013553	0.5699	0.0002484	739.8	1045.1	619.2
19 000	−8.8	451.0	1014.7	0.0013107	0.5511	0.0002553	709.8	1041.0	616.7
20 000	−12.3	447.4	973.3	0.0012673	0.5328	0.0002623	680.8	1036.9	614.3
21 000	−15.9	443.9	933.3	0.0012249	0.5150	0.0002697	652.7	1032.8	611.9
22 000	−19.5	440.3	894.6	0.0011836	0.4976	0.0002772	625.6	1028.6	609.4
23 000	−23.0	436.8	857.2	0.0011435	0.4806	0.0002851	599.4	1024.5	606.9
24 000	−26.6	433.2	821.2	0.0011043	0.4642	0.0002932	574.1	1020.3	604.4
25 000	−30.2	429.6	786.3	0.0010663	0.4481	0.0003017	549.7	1016.1	601.9
26 000	−33.7	426.1	752.7	0.0010292	0.4325	0.0003104	526.2	1011.9	599.4
27 000	−37.3	422.5	720.3	0.0009931	0.4173	0.0003195	503.4	1007.7	596.9
28 000	−40.9	419.0	689.0	0.0009580	0.4025	0.0003289	481.5	1003.4	594.4
29 000	−44.3	415.4	658.8	0.0009239	0.3881	0.0003387	460.3	999.1	591.9
30 000	−48.0	411.9	629.7	0.0008907	0.3741	0.0003488	439.9	994.8	589.3
31 000	−51.6	408.3	601.6	0.0008584	0.3605	0.0003594	420.3	990.5	586.8
32 000	−55.1	404.8	574.6	0.0008270	0.3473	0.0003703	401.3	986.2	584.2
33 000	−58.7	401.2	548.5	0.0007966	0.3345	0.0003817	383.1	981.9	581.6
34 000	−62.3	397.6	523.5	0.0007670	0.3220	0.0003935	365.5	977.5	579.0
35 000	−65.8	394.1	499.3	0.0007382	0.3099	0.0004058	348.6	973.1	576.4
36 000	−69.4	390.5	476.1	0.0007103	0.2981	0.0004185	332.3	968.8	573.8
37 000	−69.7	390.0	453.9	0.0006780	0.2843	0.0004379	330.9	968.1	573.6
38 000	−69.7	390.0	432.6	0.0006463	0.2710	0.0004594	316.7	968.1	573.6
39 000	−69.7	390.0	412.4	0.0006161	0.2583	0.0004820	301.8	968.1	573.6
40 000	−69.7	390.0	393.1	0.0005873	0.2462	0.0005056	287.7	968.1	573.6
41 000	−69.7	390.0	374.6	0.0005598	0.2346	0.0005304	274.2	968.1	573.6
42 000	−69.7	390.0	357.2	0.0005336	0.2236	0.0005564	261.3	968.1	573.6
43 000	−69.7	390.0	340.5	0.0005087	0.2131	0.0005837	249.0	968.1	573.6
44 000	−69.7	390.0	324.6	0.0004849	0.2031	0.0006123	237.4	968.1	573.6
45 000	−69.7	390.0	309.4	0.0004623	0.1936	0.0006423	226.2	968.1	573.6
46 000	−69.7	390.0	295.0	0.0004407	0.1845	0.0006738	215.6	968.1	573.6
47 000	−69.7	390.0	281.2	0.0004201	0.1758	0.0007068	205.5	968.1	573.6
48 000	−69.7	390.0	268.1	0.0004004	0.1676	0.0007415	195.8	968.1	573.6
49 000	−69.7	390.0	255.5	0.0003818	0.1597	0.0007778	186.7	968.1	573.6
50 000	−69.7	390.0	243.6	0.0003639	0.1522	0.0008159	177.9	968.1	573.6

Table 24.3 (continued)

Altitude (ft)	Temperature (°F)	(°R)	Pressure (psf)	Density (slug/cu ft)	Density ratio	Kinematic viscosity (ft^2/s)	q/M^2 (lb/ft^2)	Sonic velocity (ft/s)	(kn)
51 000	−69.7	390.0	232.2	0.0003469	0.1451	0.0008559	169.5	968.1	573.6
52 000	−69.7	390.0	221.4	0.0003307	0.1383	0.0008978	161.6	968.1	573.6
53 000	−69.7	390.0	211.0	0.0003153	0.1318	0.0009418	154.0	968.1	573.6
54 000	−69.7	390.0	201.2	0.0003006	0.1256	0.0009879	146.8	968.1	573.6
55 000	−69.7	390.0	191.8	0.0002865	0.1197	0.0010360	139.9	968.1	573.6
56 000	−69.7	390.0	182.8	0.0002731	0.1141	0.0010871	133.3	968.1	573.6
57 000	−69.7	390.0	174.3	0.0002604	0.1087	0.0011403	127.1	968.1	573.6
58 000	−69.7	390.0	166.2	0.0002482	0.1036	0.0011961	121.1	968.1	573.6
59 000	−69.7	390.0	158.4	0.0002366	0.0988	0.0012547	115.4	968.1	573.6
60 000	−69.7	390.0	151.0	0.0002256	0.0841	0.0013161	110.0	968.1	573.6
61 000	−69.7	390.0	144.0	0.0002151	0.0897	0.0013805	104.8	968.1	573.6
62 000	−69.7	390.0	137.3	0.0002050	0.0855	0.0014481	99.9	968.1	573.6
63 000	−69.7	390.0	130.9	0.0001955	0.0815	0.0015189	95.2	968.1	573.6
64 000	−69.7	390.0	124.8	0.0001834	0.0777	0.0015932	90.8	968.1	573.6
65 000	−69.7	390.0	118.9	0.0001777	0.0740	0.0016712	86.5	968.1	573.6
70 000	−67.3	392.4	92.7	0.0001376	0.0579	0.0021219	82.4	971.0	575.3
75 000	−64.6	395.1	73.0	0.0001077	0.0453	0.0026938	64.9	974.4	577.3

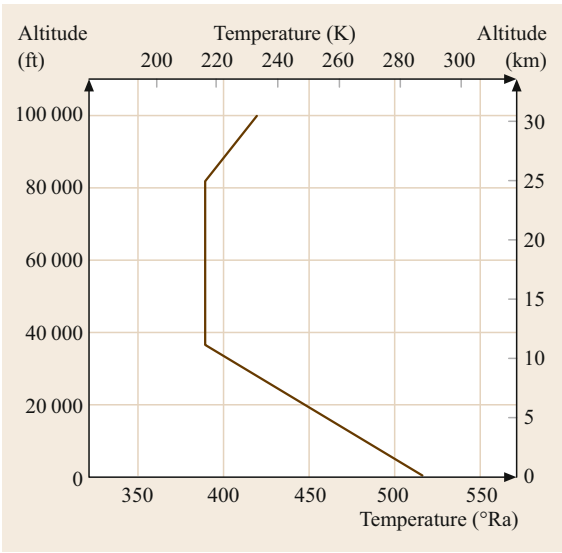

Fig. 24.8 Temperature variation with altitude in the US standard atmosphere

the pressure is equal to the ambient atmospheric pressure. Aircraft altimeters are pressure gages calibrated to read pressure altitude. Also important is the density altitude, the geometric altitude on a standard day for which the density is equal to the ambient air density. Pressure altitude, density altitude, and temperature are related through the equation of state $p = \rho RT$.

It should be noted that another standard atmosphere has been defined by the International Civil Aviation Organization (ICAO). The ICAO standard atmosphere and the US standard atmosphere are identical up to 65 617 ft. Beyond 65 617 ft, the ICAO standard atmosphere maintains a constant temperature up to 82 300 ft, while the US standard atmosphere reflects an increasing temperature with a constant gradient to beyond 100 000 ft.

24.5.3 Axis Systems

The airplane design process, with respect to achieving performance objectives of altitude, speed, range, payload, and take-off and landing distances, requires analysis of the airplane in motion. The Newtonian laws of motion state that the summation of all external forces in any direction must equal the time rate of change of momentum, and that the summation of all of the moments of the external forces must equal the time rate of change of the angular momentum, all measured with respect to axes fixed in space. However, if the motion of the airplane is described relative to axes fixed in space, the mathematics becomes extremely unwieldy, as the moments and products of inertia vary from instant to instant. To overcome this difficulty, use is made of moving or Eulerian axes that coincide in some particular manner from instant to instant with a definite set of axes fixed with respect to the airplane. The most common choice is to select a set of mutually perpendicular axes defined within the airplane as shown in Fig. 24.9, with their origin at the airplane's center of gravity (c.g.). The airplane's motion in space is defined by six components of velocity. This is a right-handed axis system with the positive x- and z-axes in the plane of symmetry and the x-axis point-

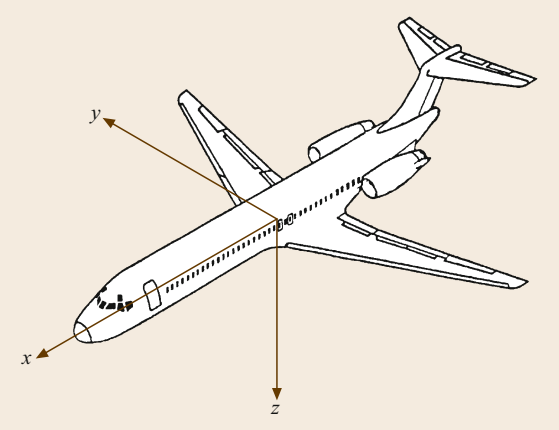

Fig. 24.9 Airplane axis system

ing out of the nose of the airplane along the flight path. This is called a wind axis system, since the x-axis always coincides with the airplane's velocity vector. The z-axis is perpendicular to the x-axis, positive downward, while the positive y-axis is out the right-hand wing, perpendicular to the plane of symmetry.

For most aircraft design analyses, the airplane is considered to be a rigid body with six degrees of freedom: three linear velocity components along these axes, and three angular velocity components around these axes. The angular motion around the y-axis is called pitch; the angular motion about the x-axis is called roll; and the angular motion about the z-axis is called yaw. Nearly all airplane motions encountered in preliminary aircraft design and performance analyses are in the plane of symmetry. The other three components of the airplane's motion lie outside the plane of symmetry. The symmetric degrees of freedom are referred to as the longitudinal motion, and the asymmetric degrees of freedom are referred to as lateral-directional motion.

In the plane of symmetry (Fig. 24.10), the inclination of the flight path to the horizontal is the flight path angle γ while the angle between the flight path and the airplane reference line is the angle of attack α. The angle between the airplane reference line and the horizontal is the airplane's pitch angle θ.

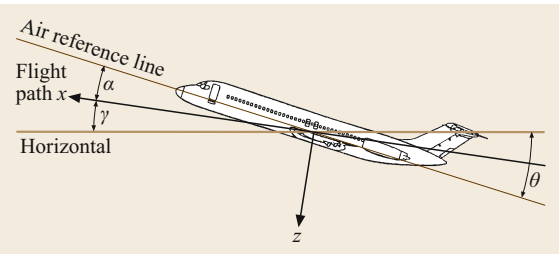

Fig. 24.10 Axis system in the plane of symmetry

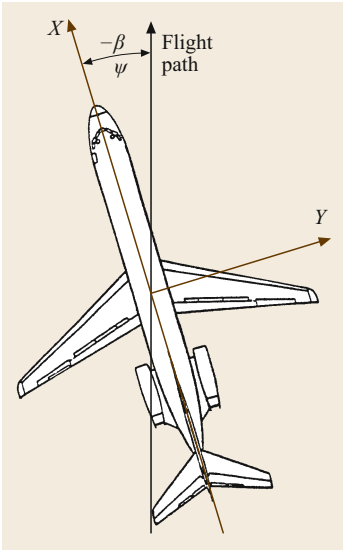

Fig. 24.11 Axis system in asymmetric flight

When the flight path does not lie in the plane of symmetry (Fig. 24.11), the angle between the flight path and the airplane's centerline is the yaw angle ψ. For straight flight in this situation, the yaw angle is equal in magnitude but opposite in sign to the sideslip angle β. In roll about the flight path, the angle between the y-axis and the horizontal is the roll or bank angle. A summary of all of the angles involved in flight performance and flight mechanics calculations is presented in Table 24.4.

The other three components of the airplane's motion lie outside the plane of symmetry. The symmetric degrees of freedom are referred to as the longitudinal motion, while the asymmetric degrees of freedom are referred to as lateral-directional motion. In the plane of symmetry (Fig. 24.10), the inclination of the flight path to the horizontal is the flight path angle γ and the angle between the flight path and the airplane reference line is the angle of attack α.

Table 24.4 Summary and definition of angles involved in flight performance and flight mechanics calculations

In the plane of symmetry		
γ	Flight path angle	Angle between the horizon and the velocity vector
θ	Pitch angle	Angle between the airplane reference line and the horizon
α	Angle of attack	Angle between the airplane reference line and the velocity vector
In asymmetric flight		
β	Angle of sideslip	Angle between the airplane centerline and the velocity vector
φ	Angle of roll	Angle between the airplane's y-axis and the horizon

24.5.4 Aerodynamic Forces and Moments

The aerodynamic forces acting on an aircraft consist of two types: pressure forces, which act normal to the aircraft surface, and viscous or shear forces, which act tangentially to the aircraft surface.

The physical parameters that govern the aerodynamic forces and moments acting on an aircraft have been developed through a method called dimensional analysis. This procedure is treated in detail in many textbooks on aerodynamics, and will only be summarized here. Dimensional analysis considers the dimensions or units of the physical quantities involved in the development of aerodynamic forces and moments, and divides them into two groups: fundamental and derived. The fundamental units are mass, length, and time, and all physical quantities have dimensions that are derived from a combination of these three fundamental units. Equations that express physical relationships must have dimensional homogeneity; that is, each term in the equation must have the same units in order for the equation to have physical significance. The broad physical relationships are postulated by logic, reason, or perhaps some experimental evidence, then the specific relationships are derived by dimensional analysis. For aerodynamic forces and moments acting on an aircraft in the plane of symmetry, the broad physical relationships are postulated as

$$F_{\text{aero}},\ M_{\text{aero}} = f(\text{shape, size, altitude, velocity, fluid properties})\ .$$

The specific relationship for aerodynamic forces, derived from dimensional analysis, is

$$F_{\text{aero}} = K\rho V^2 L^2 f\left(\alpha, \frac{\rho VL}{\mu}, \frac{V}{a}\right)\ ,$$

where K is a constant of proportionality or dimensionless coefficient, V is the velocity of the aircraft, L is an arbitrary characteristic length, ρ is the air density, μ is the coefficient of viscosity for air, α is the attitude of the airplane with respect to the flight path, $\rho VL/\mu$ is a dimensionless quantity called the Reynolds number (Re), a is the speed of sound in air, and V/a is a dimensionless quantity called the Mach number (Ma) [24.9].

The aerodynamic forces and moments acting on the airplane in the plane of symmetry are shown in Fig. 24.12. The resultant of the aerodynamic forces is resolved into the lift component, acting perpendicular to the flight path or velocity vector, and the drag component, acting parallel to the velocity vector. The lift and drag components are defined as acting at the airplane's center of gravity, while all of the moments acting on the airplane are lumped into one couple acting around the airplane's center of gravity. The equations for the lift and drag on the airplane may be written as

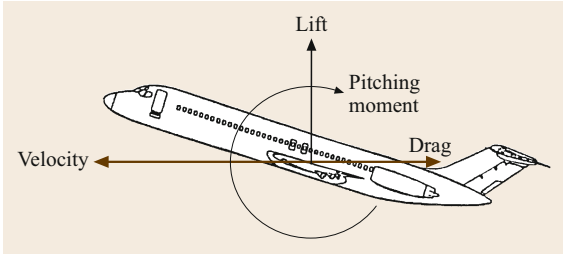

Fig. 24.12 Aerodynamic forces and moments in the plane of symmetry

$$\text{lift} = C_{\text{L}}\frac{\rho}{2}V^2 S\ ,$$

$$\text{drag} = C_{\text{D}}\frac{\rho}{2}V^2 S\ ,$$

where C_{L} and C_{D} are the lift and drag coefficients, respectively, and the area term in the equation is arbitrarily taken to be the wing area, S. To make the equation for the aerodynamic moment about the center of gravity dimensionally correct, the length of the wing mean chord, c, i.e., the mean distance from the leading edge to the trailing edge at the wing, is arbitrarily selected. The moment equation in the plane of symmetry is

$$\text{Moment} = M_{\text{cg}} = C_{\text{m}}\frac{\rho}{2}V^2 Sc\ ,$$

where C_{m} is defined as the pitching moment coefficient. As noted above, while the primary relationship between the physical quantities involved in the development of aerodynamic forces and moments is expressed in terms of the dimensionless coefficients, these coefficients are functions of both the Reynolds and Mach number. The aerodynamic forces and moments acting on the airplane in asymmetric flight are shown in Fig. 24.13. The side force acts normal to the airplane centerline, while the aerodynamic moments acting around the z-axis through the c.g. are lumped together and called the yawing moment. In addition, the aerodynamic moments acting around the x-axis are lumped together and are called the rolling moment.

The equations for the side force, yawing moment, and rolling moment are

$$\text{side force} = C_{\gamma}\frac{\rho}{2}V^2 S\ ,$$

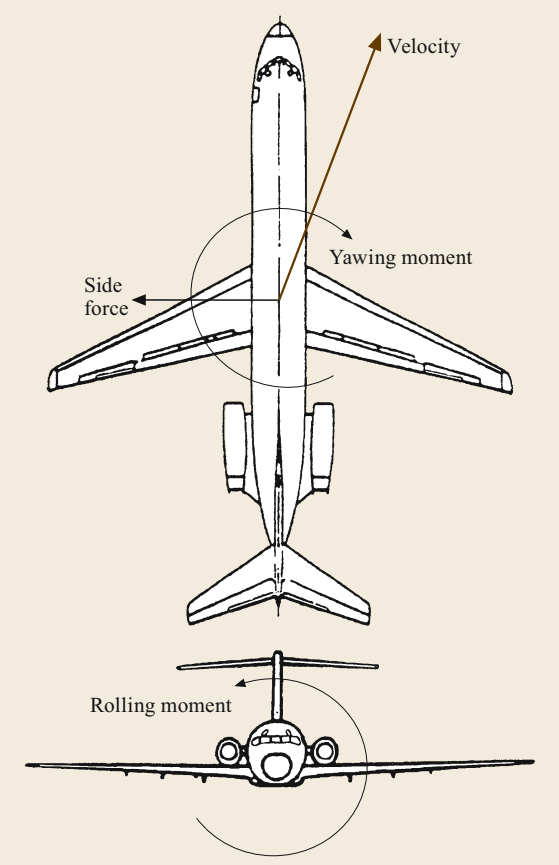

Fig. 24.13 Aerodynamic forces and moments in asymmetric flight

$$\text{yawing moment} = C_\text{n}\frac{\rho}{2}V^2Sb\,,$$

$$\text{rolling moment} = C_\text{l}\frac{\rho}{2}V^2Sb\,,$$

where C_γ, C_n, and C_l are the side force, yawing moment, and rolling moment coefficient, respectively, and b is the airplane wing span, selected as more appropriate than the wing mean chord for use with the asymmetric moment coefficients.

In summary, then, there are three defined aerodynamic forces acting along the airplane axes, and three aerodynamic moments acting around the airplane axes (Table 24.5).

24.5.5 Relative Wind

Up to now, the aerodynamic forces acting on the airplane have been defined in terms of the airplane velocity vector. It should be noted that the aerodynamic forces and moments depend only on the relative velocity between the airplane and the air that it is flying through. The same aerodynamic forces are generated if the airplane moves through the air with a velocity, V, or if the airplane is held fixed in space, as in a wind tunnel, and the air moves past the airplane, coming from the direction of the relative wind, opposite to the flight path, with a velocity, V, equal and opposite to the actual velocity, as shown in Fig. 24.14.

Table 24.5 Aerodynamic forces acting along and moments acting around the airplane axes

Axis	Force along	Moment around
x	Drag	Rolling moment
y	Side force	Pitching moment
z	Lift	Yawing moment

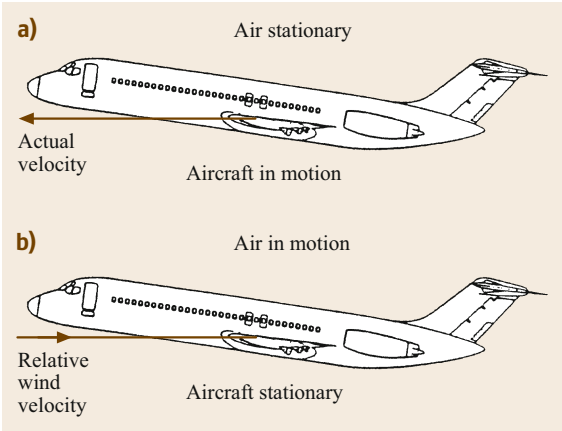

Fig. 24.14a,b **(a)** Actual velocity and **(b)** relative wind velocity

24.5.6 Dynamic Pressure

In the discussion on aerodynamic forces and moments, the expressions for all of them show a dependence on the quantity $(\rho V^2)/2$. This quantity, which appears throughout aerodynamic theory, is equal to the kinetic energy of a unit volume of air, and is defined as the dynamic pressure

$$q = \frac{\rho}{2}V^2\,.$$

Another form of the equation for dynamic pressure which is especially useful in aircraft design and performance calculations is

$$q = \frac{\gamma}{2}p\text{Ma}^2,$$

where γ is the ratio of specific heats for air, equal to 1.4, p is the ambient pressure, and Ma is the flight Mach number.

24.5.7 Airspeed Terminology

Since the very early days, airplanes have been equipped with airspeed indicators, which operate based on the difference between two pressures sensed by devices mounted on the airplane. One pressure used in airspeed measurement is the impact or total pressure, usually sensed by a Pitot or total head tube (Fig. 24.15a), which has an open hole at the front end to capture the total pressure. The other pressure used is the static pressure, that is, the ambient pressure at the operating altitude of the airplane, usually sensed by small flush holes located on a static tube (Fig. 24.15b). On many airplanes, the Pitot tube and the static tube are integrated into one device called the Pitot–static tube (Fig. 24.15c). On larger aircraft, the static pressure is sensed by flush holes in the fuselage called static ports (Fig. 24.15d), which are located in an area where the static pressure is equal to the ambient static pressure. Airspeed indicators are calibrated to read the airspeed as a function of the difference between the total and static pressure. To develop some meaningful definitions of airspeed over a range of aircraft operational altitudes, some specific terminology has been adopted as follows.

Indicated Airspeed (IAS)

This is the airspeed registered on the cockpit instrument, corrected for any instrument calibration errors.

Calibrated Airspeed (CAS)

This is the indicated airspeed reading corrected for static source position errors. Usually it is not possible to locate a Pitot–static tube or a static port in a place that senses the exact ambient static pressure, so corrections for this so-called position error are made. Calibrated airspeed refers to the fact that airspeed indicators are calibrated in airspeed units, usually knots, through the difference between total and static pressure at sea-level standard day conditions by [24.10]

$$V_{\text{cal}} = \sqrt{\frac{2\,(P_{\text{total}} - P_{\text{static}})}{\rho_{\text{sea-level}}}}\,V_{\text{true}}\,.$$

Equivalent Airspeed (EAS)

This is the calibrated airspeed adjusted for what are termed compressibility effects. Equivalent airspeed is a very important parameter in aircraft preliminary design and performance calculations. Equivalent airspeed is defined as

$$V_{\text{EAS}} = \sqrt{\frac{\rho_{\text{ambient}}}{\rho_{\text{sea-level}}}}\,V_{\text{true}}\,.$$

The idea behind equivalent airspeed is that, for any flight condition, i.e., any combination of true airspeed and ambient density, and therefore dynamic pressure, there is an equivalent airspeed at sea-level standard day conditions that produces the same dynamic pressure. In equation form

$$q = \frac{\rho_{\text{ambient}}}{2}V_{\text{true}}^2 = \frac{\rho_{\text{sea-level}}}{2}V_{\text{EAS}}^2\,.$$

A chart showing the relationship between V_{EAS} and V_{true} for the US standard atmosphere is shown in Fig. 24.16

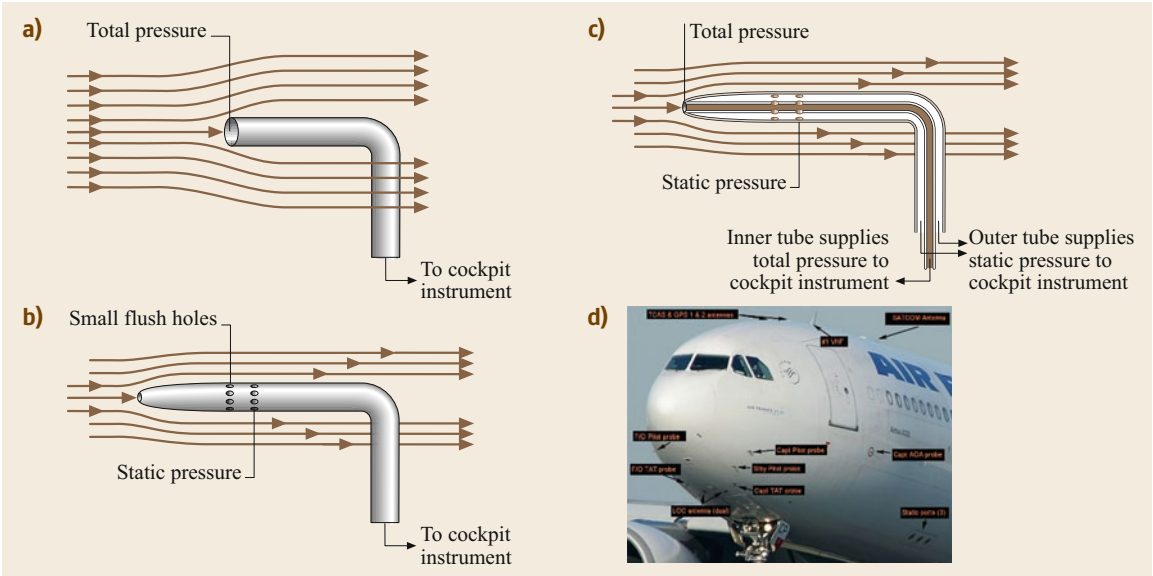

Fig. 24.15a–d Airspeed sensors. **(a)** Pitot tube, **(b)** static tube, **(c)** Pitot–static tube, **(d)** static ports

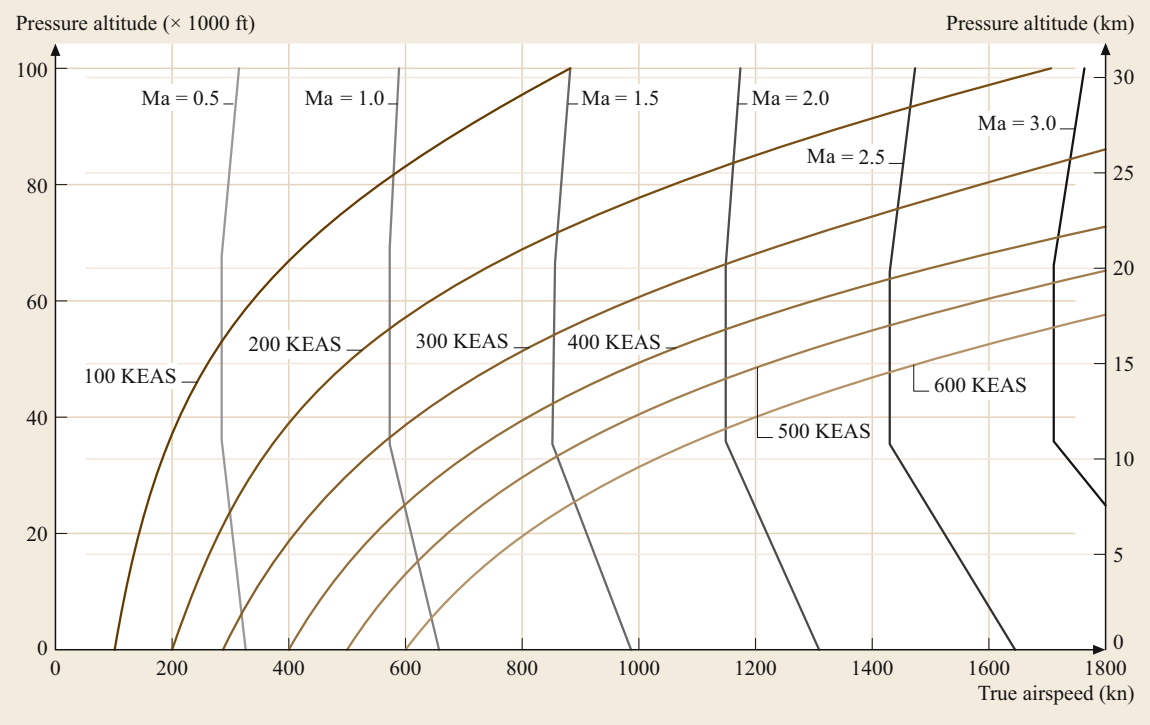

Fig. 24.16 Relationship between V_{EAS} and V_{true} for the US standard atmosphere

[24.11]. Equivalent airspeeds are reasonably close to the indicated airspeeds shown by the cockpit instrument.

The difference is the compressibility correction to the CAS in order to obtain the EAS. The compressibility increment, ΔV_C, is a function of both the Mach number and altitude, as shown in Fig. 24.17. This correction arises as follows.

For a compressible fluid such as air,

$$P_{total} - P_{static} = \frac{\gamma}{2} p \mathrm{Ma}^2 \left(1 + \frac{\mathrm{Ma}^2}{4} + \frac{\mathrm{Ma}^4}{40} + \frac{\mathrm{Ma}^6}{1600} + \dots\right).$$

Since the CAS is directly related to $(P_{total} - P_{static})$ and the EAS is directly related to the dynamic pressure q, the correction is the Mach number series in the brackets [24.12].

True Airspeed (TAS)

The true airspeed is the actual airspeed of the airplane at ambient conditions in the atmosphere, and may be obtained by converting or correcting the equivalent airspeed as follows

$$V_{true} = V_{EAS} \sqrt{\frac{\rho_{sea\text{-}level}}{\rho_{ambient}}}\,.$$

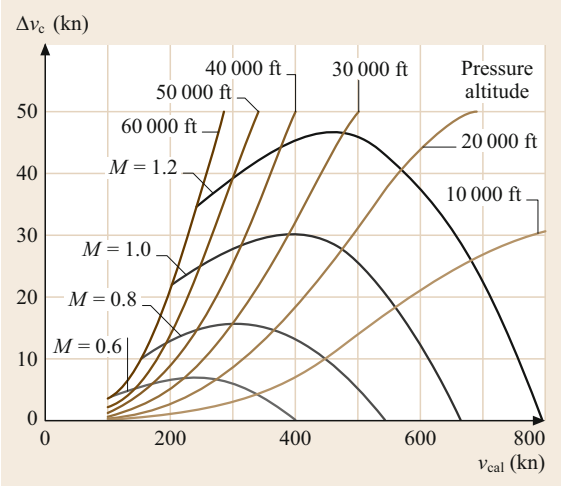

Fig. 24.17 Airspeed compressibility correction: subtract the compressibility from CAS to obtain EAS

At sealevel and at lower speeds where constant air density can be assumed, V_{true} equals CAS. At speeds above 100 kn (190 km/h), V_{true} is calculated by a flight computer or can be estimated by adding 2% to CAS for each 1000 ft (30.5 m) of altitude.

24.6 Flight Performance Equations

In order to examine the major characteristics of an airplane's performance, equations involving the summation of forces and moments in the plane of symmetry have been developed, so that Newton's laws of motion may be utilized. For unaccelerated symmetric flight along a straight path, the complete forces and moments are as shown in Fig. 24.18.

The summation of the forces and moments for static equilibrium may be written as

$$\sum F_x = T\cos\alpha - D - W\sin\gamma = 0\,,$$
$$\sum F_z = W\cos\gamma - L - T\sin\alpha = 0\,, \quad \sum M_{cg} = 0\,.$$

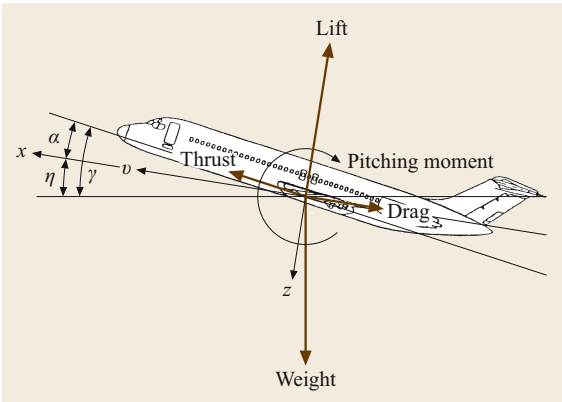

Fig. 24.18 Aerodynamic forces and moments in unaccelerated straight flight

If the assumption is made that the angle of attack is always a relatively small angle, then $\cos\alpha = 1$ and $\sin\alpha = 0$. With this assumption, the force equations reduce to

$$T - D = W\sin\gamma\,, \qquad L = W\cos\gamma\,. \tag{24.1}$$

With the small-angle assumption of $\sin\gamma = \gamma$, (24.1) may be transformed into an expression for the gradient of climb, that is the gain in altitude over a given distance covered in the horizontal direction.

The climb gradient is $\gamma = (T-D)/W$ and the climb velocity, or rate of climb, is

$$\frac{R}{C} = \frac{(T-D)}{W}V\,. \tag{24.2}$$

If this is expressed in terms of the lift coefficient, then

$$C_L = \frac{W}{Sq}\cos\gamma\,,$$

or with the small-angle assumption ($\cos\gamma = 1$)

$$C_L = \frac{W}{Sq}\,.$$

24.7 Airplane Aerodynamic Characteristics

The concepts associated with the aerodynamic forces and moments acting on an airplane give rise to some of its important aerodynamic characteristics.

24.7.1 Airplane Lift Curve

In the discussion of aerodynamic forces and moments, it was noted that the lift coefficient is primarily a function of the angle of attack α. The variation of the lift coefficient with the angle of attack is a very important aerodynamic characteristic of an airplane, and is described in a plot such as that shown in Fig. 24.19, called the airplane lift curve.

It was also noted that the airplane lift coefficient is also dependent on the Mach and Reynolds numbers, which are discussed below, but for now, we focus on the lift curve for a specific Mach number and Reynolds number corresponding to full-scale airplane operation.

As seen from Fig. 24.19, the lift curve has a zero value at some, usually negative, angle of attack, a linear region with a well-defined slope $dC_L/d\alpha$, and a departure from the linear slope as the maximum lift coefficient $C_{L_{max}}$ is approached. The characteristics of the lift curve, namely the zero-lift angle, the slope $dC_L/d\alpha$, and $C_{L_{max}}$, depend on certain geometric characteristics of the airplane and its components, as shown below. The airplane lift curve has a special relationship to its operation in steady, unaccelerated flight. As we have seen for these steady conditions, the variation of the lift coefficient required to balance the weight at various steady flight speeds is as shown in Fig. 24.20. The lowest steady flight speed is called the stalling speed V_{stall} and corresponds to the operation of the airplane at its maximum lift coefficient $C_{L_{max}}$. At high flight speeds, and hence dynamic pressures, the lift coefficient required to balance the weight reduces as $1/q$ or $1/V^2$. Therefore,

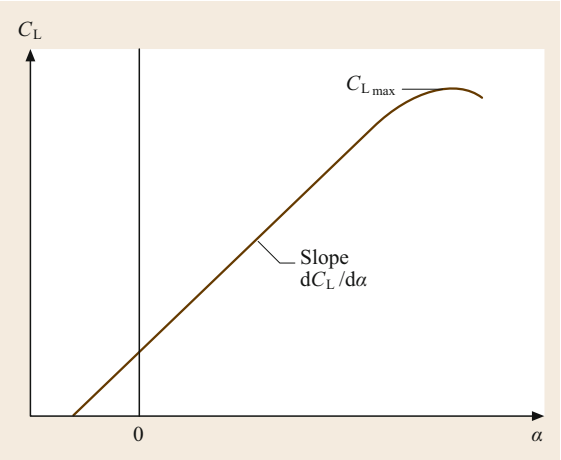

Fig. 24.19 Airplane lift curve

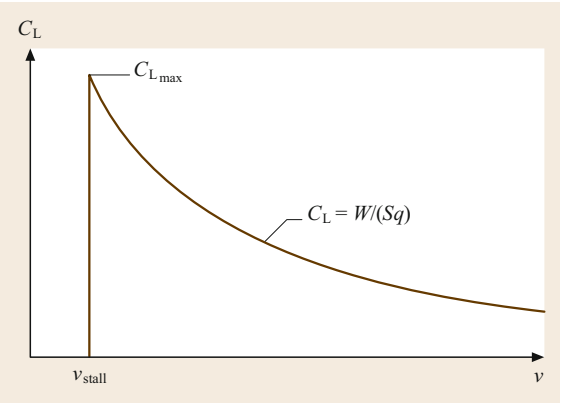

Fig. 24.20 Variation of C_L with airspeed in unaccelerated level flight

the airplane's speed along shallow, unaccelerated flight paths is primarily a function of the lift coefficient, or angle of attack. In order to control the airplane's speed, the pilot must be able to control the equilibrium lift coefficient or angle of attack.

Going back to (24.2), it can be seen that whether the airplane climbs or descends at a given speed depends on the difference between the thrust and drag at that speed. If the thrust just equals the drag ($T = D$), then the rate of climb will be zero and the airplane will be in level flight. Since the thrust is basically a function of the cockpit throttle setting, under steady unaccelerated flight conditions, the airplane speed is determined by the value of the equilibrium lift coefficient, and the rate of climb or descent is regulated primarily through the throttle [24.13]. For very large angles of climb or descent, this simple picture does not correspond to actuality, but for the performance methods presented in this chapter, it is a valid concept.

24.7.2 Airplane Drag Curve

Another aerodynamic characteristic of the airplane which is important for its range and climb performance is the drag curve or drag polar, viz. a plot of the drag coefficient versus the lift coefficient. As noted above, the drag varies with the angle of attack α, but since in the normal operating range of angle of attack C_L varies linearly with α, it has been found to be more convenient to describe the drag coefficient as a function of the lift coefficient instead of the angle of attack. The airplane drag curve, shown schematically in Fig. 24.21, has a value of C_D at zero C_L, called the zero-lift or parasite drag coefficient, C_{D_p}. At higher C_L, the drag coefficient exhibits a parabolic variation with C_L, due to the induced drag or drag due to the lift coefficient, C_{D_i}, which varies as the square of the lift coefficient. As is the case with the lift curve, the drag curve varies in shape with both the Mach number and Reynolds number, but for now we focus on the drag curve that is typical for full-scale airplane operation at one particular Mach number and Reynolds number.

A summary of the physical makeup of airplane drag is presented in Table 24.6.

An important parameter in the cruise performance of an airplane, as well as certain aspects of its climb performance, is the lift-to-drag ratio L/D. This ratio can be visualized from the drag polar as shown in Fig. 24.22. At any point on the drag curve, L/D is defined by the ratio C_L/C_D at that point, and also by the slope of a line from the origin to the point in question.

If the L/D values are determined at various points along the airplane drag curve, a plot of the airplane L/D ratio versus the lift coefficient C_L can be constructed. The L/D value is zero at $C_L = 0$, reaches a maximum value of $(L/D)_{max}$ at some C_L, then decreases at higher

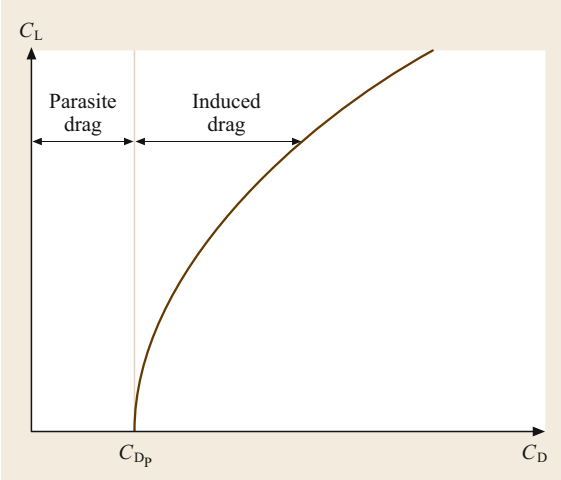

Fig. 24.21 Airplane drag curve

Table 24.6 Physical definition of airplane drag elements

Cruise speed of Ma = 0.5 or less	
Zero-lift drag	Skin friction plus pressure drag
Drag due to lift	Subsonic induced drag
Cruise speed between Ma = 0.5 and Ma = 1.0	
Zero-lift drag	Skin friction plus pressure drag
Drag due to lift	Subsonic induced drag
Compressibility drag	Drag from local shock waves
Cruise speed greater than Ma = 1.0	
Zero-lift drag	Skin friction plus pressure drag Supersonic wave drag
Drag due to lift	Supersonic wave drag due to lift Subsonic induced drag

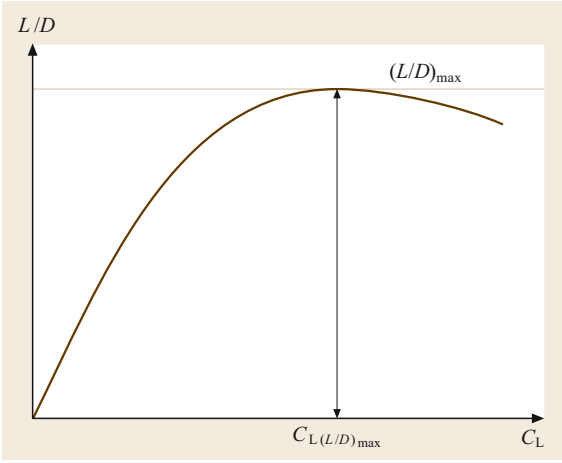

Fig. 24.22 Airplane L/D curve

C_L values. Both the value of $(L/D)_{max}$ as well as the C_L value at which it occurs, i.e., $C_{L(L/D)_{max}}$, are important aerodynamic characteristics of the airplane [24.11].

24.7.3 Mach Number Effects on Lift and Drag Curves

As noted in the section on flight speed terminology, the characteristics of the airflow around the airplane change dramatically as the flight Mach number is increased due to the compressible nature of air. These changes in the airflow have a significant effect on the airplane lift and drag curves in the various Mach number ranges. For airplanes that operate entirely within the subsonic speed range, there are no significant effects of the compressibility of air on the airplane lift and drag curves, and a single lift curve as shown in Fig. 24.19 and a single drag curve as shown in Fig. 24.21 describe the lift and drag characteristics of the airplane. For airplanes that operate at high subsonic speeds, i.e., in the transonic speed region, the airplane lift and drag curves will vary as the flight Mach number is increased due to the compressible nature of air, so there is a family of lift curves

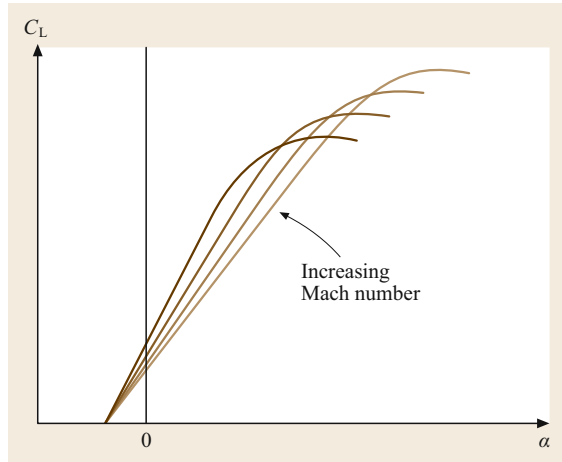

Fig. 24.23 Airplane lift curves at high subsonic Mach numbers

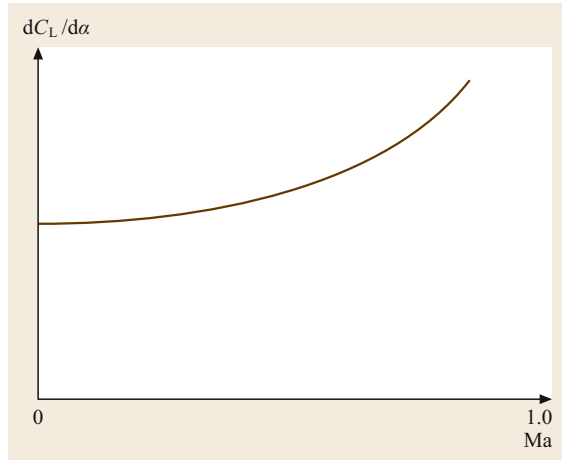

Fig. 24.24 Mach number effect on lift curve slope at high subsonic speeds

and a family of drag curves, one for each flight Mach number of interest. The family of lift curves is characterized by an increase in the slope of the lift curve $dC_L/d\alpha$ and a decrease in the maximum lift coefficient $C_{L_{max}}$ as the Mach number is increased in the high subsonic region, as shown schematically in Fig. 24.23.

The Mach number effects can be shown more specifically by plotting the significant parameters as a function of the Mach number; For example, the effect of the Mach number in increasing the lift curve slope is shown in Fig. 24.24, while the effect of the Mach number in decreasing the maximum lift coefficient $C_{L_{max}}$ is shown in Fig. 24.25.

The family of drag curves are characterized by increases in the parasite drag coefficient, C_{D_p}, and significant increases in the drag coefficient at higher C_L values as the Mach number is increased, as shown in Fig. 24.26.

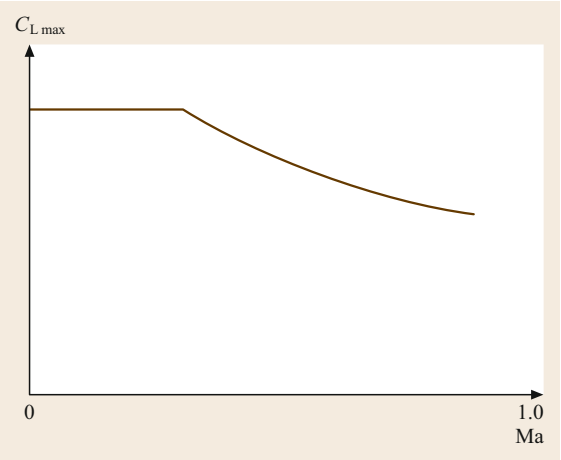

Fig. 24.25 Mach number effect on maximum lift coefficient at high subsonic speeds

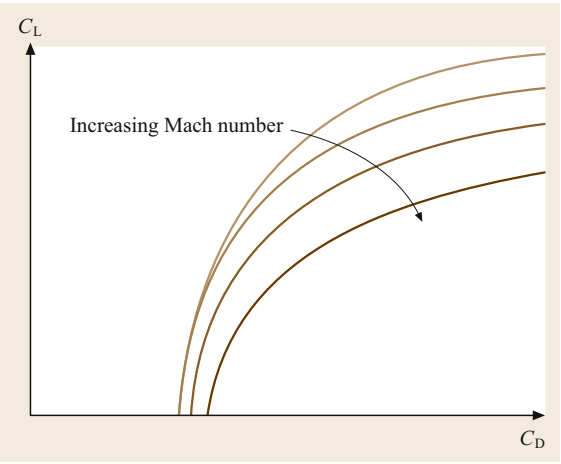

Fig. 24.26 Airplane drag curves at high subsonic speeds

For the drag curves, the Mach number effects are usually shown in the form of C_D versus the Mach number for various values of the lift coefficient, as shown in Fig. 24.27.

An explanation for these Mach number effects on the lift and drag curves has been derived from the theory of compressible flow [24.12], and confirmed by experimental data obtained in wind tunnels and from flight tests. It can be shown that, for an airplane at a given angle of attack, the lift coefficient will increase as the Mach number increases, because the suction on the wing upper surface and the pressure on the wing lower surface tend to grow with the Mach number, roughly by a factor of $1/\sqrt{1-\mathrm{Ma}^2}$ in the high subsonic speed range, which results in the increase in the lift curve slope as shown in Figs. 24.23 and 24.24. Also, as the Mach number increases, at some flight Mach number, the local velocities on the wing near the leading edge, at high angles of attack near the maximum lift coefficient, become supersonic, which leads to local shock waves and separation, limiting the attainable maximum lift coefficient as shown in Fig. 24.25. In the drag curves, the Mach number effects are due to the development of local supersonic flow around the wing, which eventually produces normal shock waves, and finally separated flow. Because of the energy loss in the shock wave, and the added pressure drag due to the separated flow, there are significant increases in the drag coefficient at a given lift coefficient as the flight Mach number is increased, as shown in Fig. 24.27. The development of these conditions for a wing airfoil section typical of those used on many current jet transports and business jets is shown in Fig. 24.28. There are some important concepts and definitions associated with the sketches in Fig. 24.28. At the condition shown in Fig. 24.28b, the condition of the lift coefficient and the flight Mach number where the maximum local velocity on the wing surface is equal to the sonic velocity is called the critical Mach number Ma_C. At a higher Mach number, in the conditions shown in Fig. 24.28c, with a local region of supersonic flow terminated by a normal shock wave, and the very beginning of flow separation behind the normal shock, the drag begins to rise abruptly. This condition is called the drag divergence Mach number Ma_{DIV}, for that particular lift coefficient. At higher flight Mach numbers (Fig. 24.28d,e), the supersonic zones are larger, the normal shocks are stronger, and the drag continues to rise very strongly. Although the wing is the primary source of local supersonic flow, shock waves, and the associated drag increase, all parts of the airplane, i.e., the fuselage, tail surfaces, and engine nacelles, will eventually experience these conditions as the flight Mach number approaches 1.0.

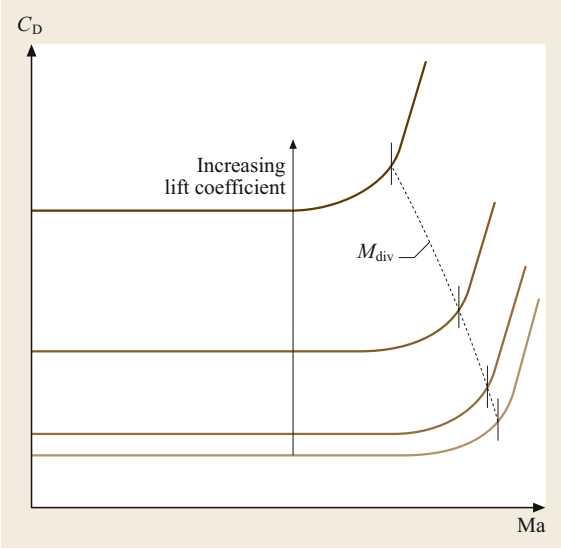

Fig. 24.27 Mach number effect on drag curves at high subsonic speeds

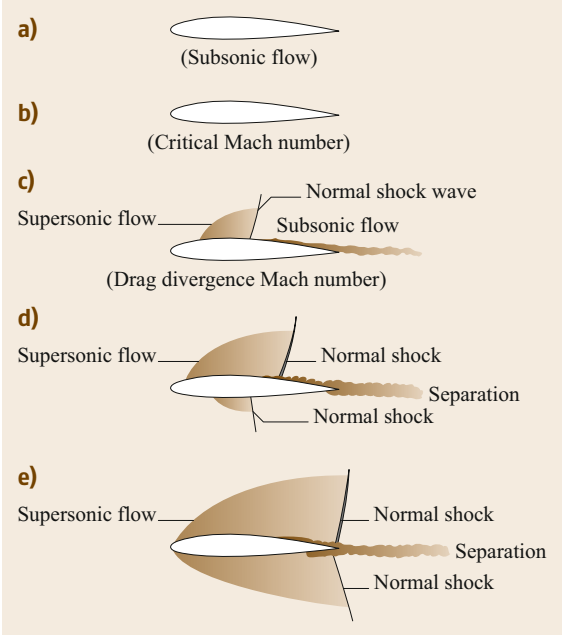

Fig. 24.28a–e Development of flow conditions around a wing airfoil section at high subsonic speeds. **(a)** Maximum local velocity is less than sonic; **(b)** maximum local velocity is equal to sonic; **(c)** supersonic velocities upper surface; **(d)** supersonic velocities upper and lower surfaces; **(e)** all velocities are supersonic

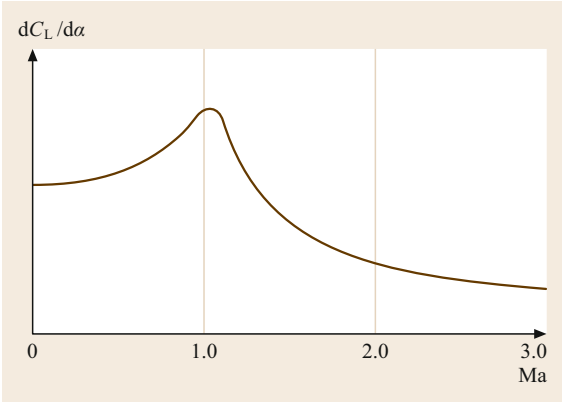

Fig. 24.29 Mach number effects on lift curve slope at subsonic and supersonic speeds

For airplanes that are designed to operate at supersonic speeds, the lift and drag curves also vary with the flight Mach number. The slopes of the curves are similar to those of subsonic speed designs, but the significant parameters show a different trend at supersonic speeds. The pressure on the wing upper and lower surfaces tend to reduce as the Mach number is increased supersonically, roughly by a factor of $1/\sqrt{\mathrm{Ma}^2-1}$, so that the lift curve slope, which increases at high subsonic speeds, decreases beyond Mach 1.0, as shown in Fig. 24.29. The maximum lift capability supersonically is described in terms of the maximum usable lift coefficient, which results from detached shock waves and unsteady flow at high angles of attack [24.14]. The drag curves at supersonic speeds are basically parabolic in shape, but with very high values of parasite drag coefficient because of the added element of supersonic wave drag, as shown in Fig. 24.30, and very high drag levels at operating lift coefficients due to the wave drag element that increases with the lift coefficient. The presence of wave drag at supersonic speeds has a significant impact on the maximum lift-to-drag ratio $(L/D)_{\max}$ referred to in Fig. 24.22. Because of this added drag element, the $(L/D)_{\max}$ values at supersonic speeds are usually less than half of the values at subsonic speeds, for any specific configuration.

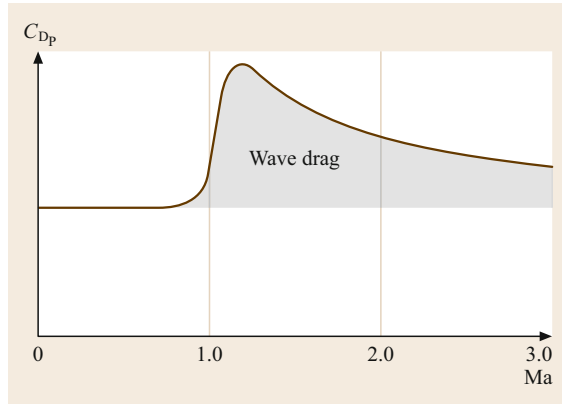

Fig. 24.30 Mach number effects on parasite drag coefficient

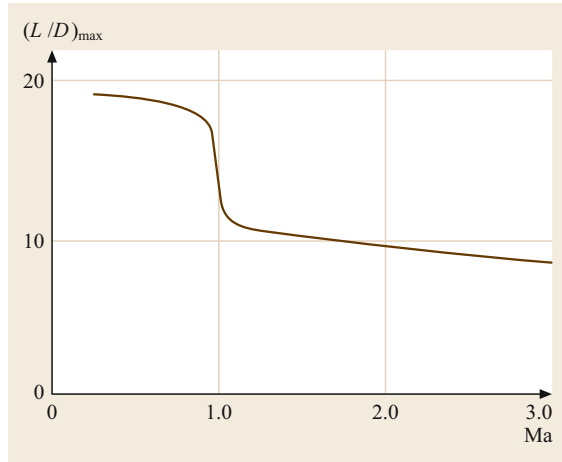

Fig. 24.31 Mach number effects on maximum lift-to-drag ratio

For jet transports, the $(L/D)_{\max}$ values subsonically are just under 20, while the best supersonic transport values are less than 10, as shown in Fig. 24.31.

24.8 Airplane General Configurations

Airplanes are often described by their general configuration. Figure 24.32 shows various aircraft types classified by the number of wings, their location on the fuselage, and the number of engines [24.15].

24.8.1 Aircraft Component Nomenclature

The various components of an airplane have unique names. Figure 24.33 indicates the names of the various components of a modern commercial transport aircraft.

Some specific geometric characteristics are defined in Table 24.7 and shown schematically in Fig. 24.34.

24.8.2 Wing Geometric Characteristics

The wing geometric characteristics include the wing area, aspect ratio, taper ratio, airfoil sections, thickness distribution, sweepback angle, aerodynamic twist, and dihedral angle. Other important elements that are incorporated into the geometric definition of the wing are high-lift system devices and lateral control system components.

Wing Area

The wing area is usually taken to be the total planform area of the wing from the fuselage centerline to the wing tip, including the area encompassed by the fuselage, as shown in Fig. 24.34.

Aspect Ratio

The wing aspect ratio (AR) is defined as the square of the wing span b divided by the wing area S

$$\mathrm{AR} = \frac{b^2}{S} \,.$$

Aspect ratio selection is basically a compromise between aerodynamic efficiency, in the form of high cruise L/D, and wing structural weight associated with the bending moments due to air loads for a given wing area.

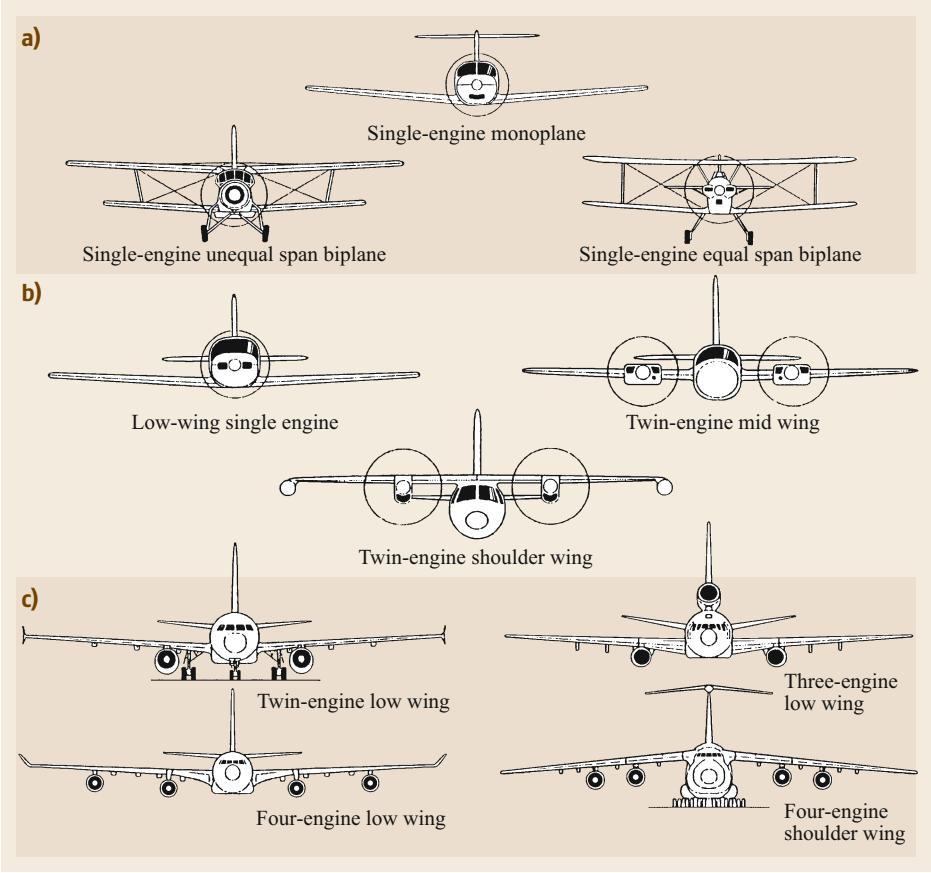

Fig. 24.32a–c Aircraft general configurations classified by the **(a)** number of wings, **(b)** their placement, and **(c)** the number and placement of engines

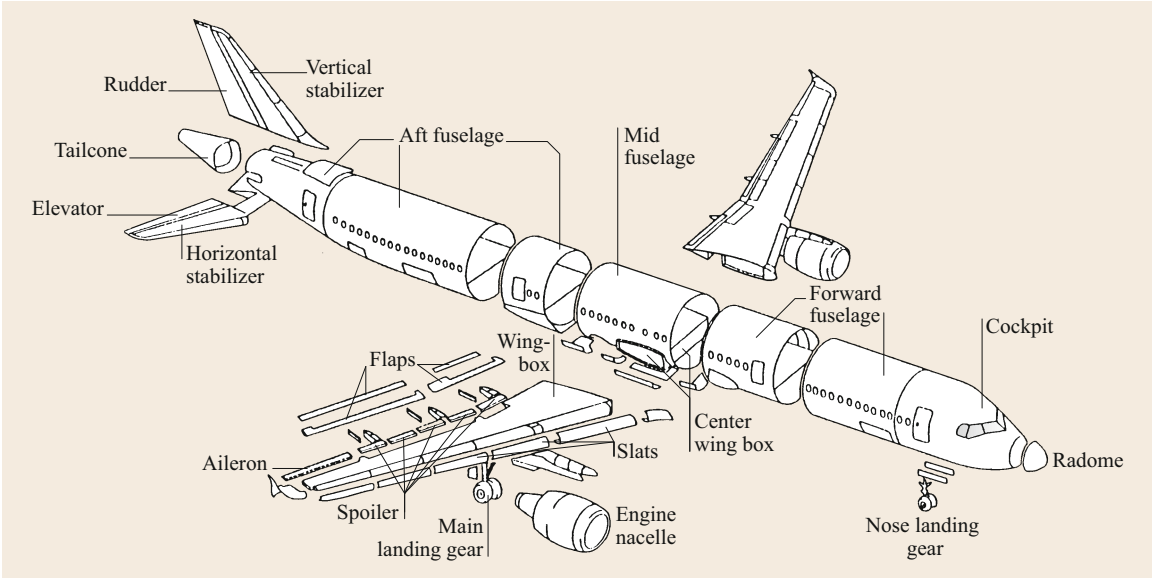

Fig. 24.33 Airplane component nomenclature

Table 24.7 Airplane geometric definitions

b	Wing span
$b/2$	Wing semispan
S	Wing area
b_H	Horizontal tail span
S_H	Horizontal tail area
l_H	Horizontal tail length
S_V	Vertical tail area
l_V	Vertical tail length
c	Wing mean aerodynamic chord
c_H	Horizontal tail mean aerodynamic chord
c_V	Vertical tail mean aerodynamic chord
l_{oa}	Overall length
l_{fus}	Fuselage length
h	Height
V_H	Horizontal tail volume
V_V	Vertical tail volume

Taper Ratio

The taper ratio λ is defined as the ratio of the chord at the tip of the wing to the chord at the airplane centerline, called the root chord

$$\lambda = \frac{c_t}{c_r} .$$

The taper ratio is also a compromise between aerodynamic considerations, primarily the span load distribution, which is important for cruise efficiency, stall characteristics, and bending moments due to air loads and structural considerations primarily associated with the bending moments.

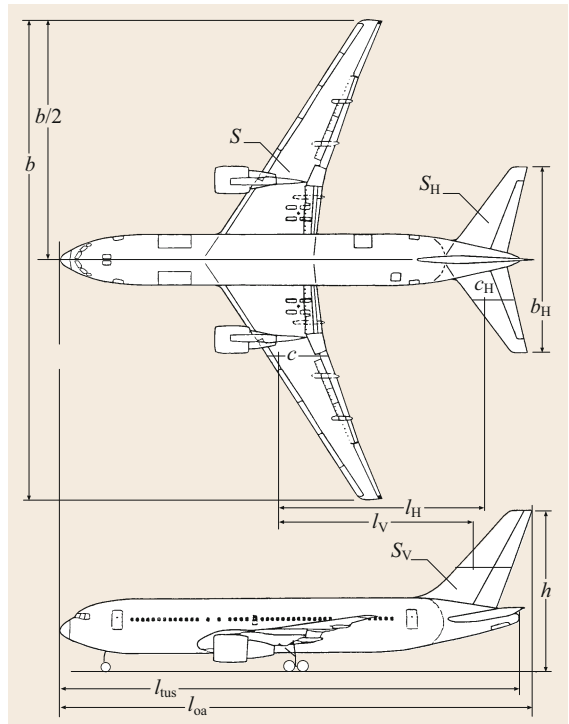

Fig. 24.34 Airplane geometric characteristics

Airfoil Sections

The wing airfoil sections are the cross-sectional shapes of the wing in planes parallel to the airplane centerline and normal to the wing reference plan. The wing airfoil sections provide the wing lift by creating suction

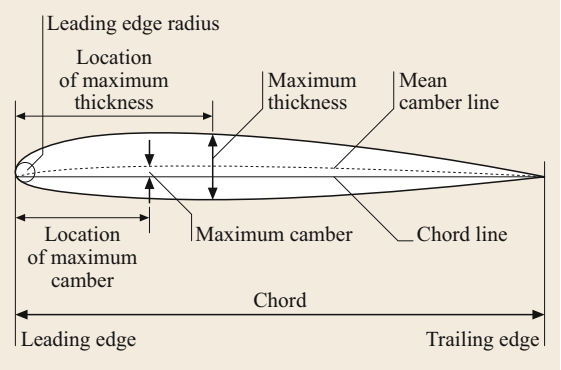

Fig. 24.35 Airfoil section geometric parameters

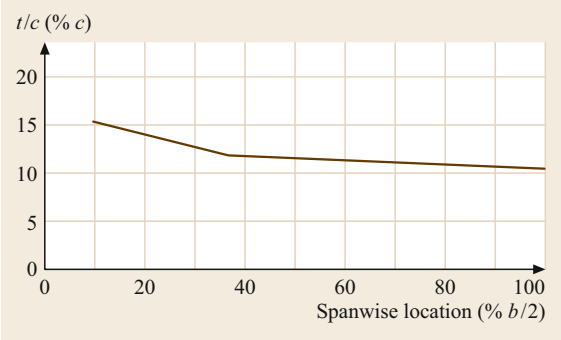

Fig. 24.37 Typical wing thickness distribution for a jet transport

on the wing upper surface and pressure on the lower surface. The wing airfoil geometry determines the detailed pressure distribution on the wing upper and lower surfaces, which in turn may have a significant influence on some of the important aerodynamic characteristics of the wing. Airfoil geometric parameters are defined in Fig. 24.35 [24.16].

Mean Aerodynamic Chord

An important wing geometric parameter is the mean aerodynamic chord (m.a.c.). The m.a.c. is the chord of an imaginary wing with a constant chord which would have the same aerodynamic characteristics as the actual wing. The m.a.c. can be defined graphically as shown in Fig. 24.36.

The wing span b is $b = \sqrt{\mathrm{AR}S}$, where AR is the wing aspect ratio and S is the reference wing area.

The root chord length is $C_{\mathrm{root}} = 2S/[b(1+\lambda)]$, where λ is the wing taper ratio.

The tip chord length is $C_{\mathrm{tip}} = \lambda C_{\mathrm{root}}$.

For trapezoidal planforms, the wing m.a.c. length is

$$\overline{C} = \left(\frac{2}{3}\right) C_{\mathrm{root}} \frac{1+\lambda+\lambda^2}{1+\lambda} .$$

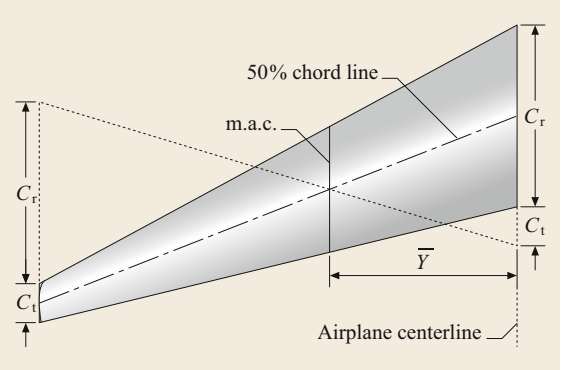

Fig. 24.36 Wing m.a.c. determination

The distance from the centerline to the m.a.c. location is

$$\overline{Y} = \left(\frac{b}{6}\right) \frac{1+2\lambda}{1+\lambda} .$$

Thickness Distribution

Another wing geometric characteristic is the variation of the airfoil thickness ratio across the span of each wing panel. Of course the simplest wing geometry, still found on many small personal/utility airplanes, is a constant-chord constant-thickness-ratio configuration. More sophisticated personal/utility aircraft, as well as commuters, regional turboprops, business jets, and jet transports, have wing designs in which the airfoil section thickness ratio (t/c) varies across the span, primarily to obtain greater depth for the airfoil sections at the wing root. This greater depth provides for a more efficient structural beam to resist the bending moments due to wing air loads. For straight-wing propeller-driven aircraft, the wing is usually defined by two airfoil sections, one at the wing root, and one at the wing tip, connected by straight-line elements through the constant-percentage chord points.

For business jets and jet transports which cruise at high subsonic speed, the wing is usually defined by three or more airfoil sections, one at the side of the fuselage, one at the tip, and one or more at intermediate spanwise locations. The purpose of the additional defining airfoils is to produce wing upper-surface pressure distributions that maintain as far as possible uniformly swept lines of constant pressure (isobars) at cruise conditions, so that the entire wing reaches its $\mathrm{Ma}_{\mathrm{DIV}}$ at the same point. A typical wing thickness distribution for a commercial jet transport is shown in Fig. 24.37.

Sweepback Angle

Two very important wing geometric parameters, especially for airplanes that cruise at high subsonic speeds,

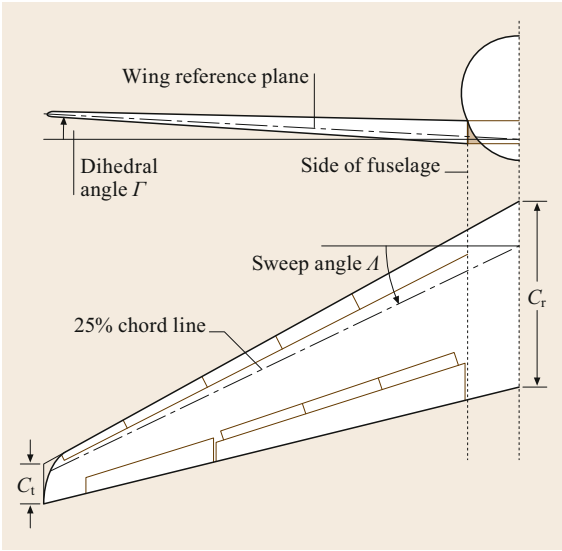

Fig. 24.38 Wing planform parameters

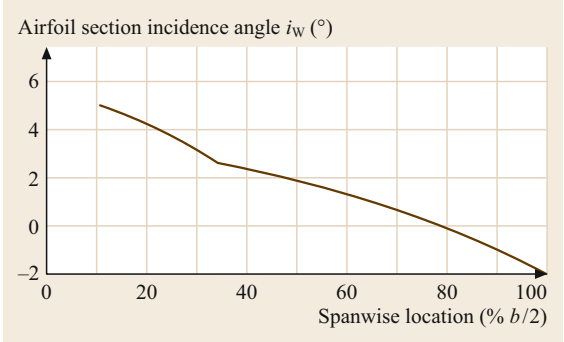

Fig. 24.39 Typical wing twist distribution for a jet transport

are the wing sweepback angle and the average thickness. The wing sweepback or sweep angle is defined in the plan view as the angle between a line perpendicular to the airplane centerline and the constant 25% chord line of the wing airfoil sections, as shown in Fig. 24.38. Nearly all high-subsonic-speed aircraft have wings with some amount of sweep, because sweep increases the wing drag divergence Mach number Ma_{DIV} for a given streamwise airfoil thickness.

Geometric Twist

Nearly all wing designs incorporate some degree of geometric twist, that is, a change in the orientation of the airfoil section chord lines from root to tip, with the tip airfoils having less of an angle of incidence than the root, as shown in Fig. 24.39. This geometric twist is used to avoid initial stalling at the wing tip as the airplane $C_{L_{max}}$ is reached. Typical values of wing twist vary from 3° for personal/utility, commuters, and regional turboprops to as much as 7° for business jets and jet transports. Supersonic military fighter/attack aircraft usually have little or no twist, depending on other means to provide satisfactory stall characteristics.

Dihedral Angle

The dihedral angle is defined in the front view of the airplane as the angle between the horizontal and a line midway between the upper and lower surfaces of the wing, as shown in Fig. 24.38. The dihedral angle primarily affects the lateral stability characteristics of the airplane. If the wing tips are higher than the wing root, the wing is said to have positive dihedral, which produces effective lateral stability. For low-wing airplanes with low horizontal tails, nearly all of the lateral stability comes from the wing dihedral angle, which is usually set around 5° for these types. For low-wing airplanes with high-mounted horizontal tails (tee tails), a significant amount of lateral stability is generated by the intersection between the horizontal and vertical tail sections, so that the wing dihedral angle for these types is usually reduced to around 2°. For high-wing airplanes, especially those with tee-tail arrangements, there is sufficient lateral stability generated by the wing–fuselage intersection and the horizontal tail–vertical tail intersection that the wing dihedral angle can be set at negative angles ranging from −2° to −5° [24.17].

Spar Locations

The front and rear spars, along with the upper and lower wing skins, are the major elements of the wing structural *box*, which resists the applied wing loads in bending and torsion. The distance between the wing spars is important structurally, but also has a significant impact on the space available for high-lift and lateral control devices, and on the volume available for internal wing fuel tankage. Typical locations for the front spar are 16–22% of local chord, while typical rear spar locations range from 60% to 75% of the local chord.

High-Lift Systems

Nearly all modern aircraft incorporate devices that fit within the wing to increase the maximum lift coefficient in the take-off and landing configuration. These devices are collectively called the high-lift system. High-lift devices fall into two categories: trailing-edge devices located at the rear portion of the wing, and leading-edge devices located at the forward portion of the wing. Trailing-edge devices include single-,

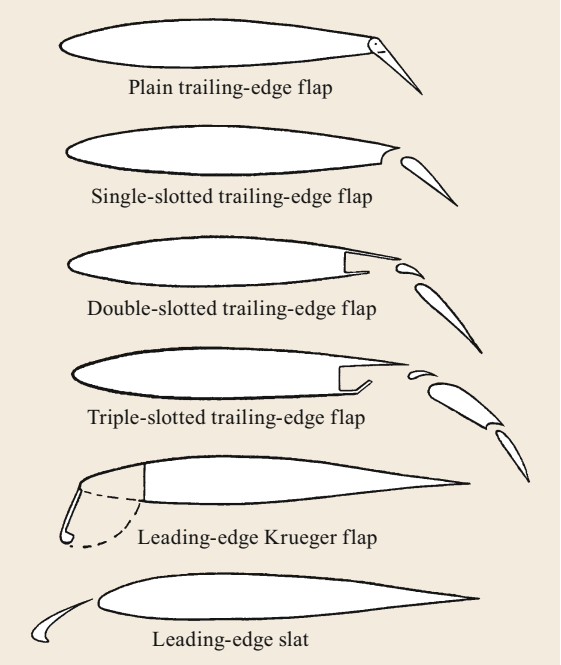

Fig. 24.40 Typical high-lift devices

double-, and triple-slotted flaps, as shown in Fig. 24.40. Single-slotted flaps are standard for personal/utility airplanes. Single-slotted flap chords are usually in the range of 25–30% of chord, and have a maximum deflection of 35°. For commuters, regional turboprops, business jets, and jet transports, more powerful double-slotted trailing-edge flaps are usually employed. Double-slotted flap chords are in the range of 30–35% chord with maximum deflections of 45°–50° [24.18, 19]. Some jet transports with design mission specifications that call for extremely low landing approach speeds and short landing distances have utilized triple-slotted trailing-edge flaps to achieve very high $C_{L_{max}}$ values in the landing configuration. Flap chords up to 40% may be used in triple-slotted flap designs, with maximum deflections of the aft flap segment of up to 55°. The effectiveness of trailing-edge flaps can be enhanced by selecting a large percentage of chord dimension for the flap, and utilizing as much flap span as possible, considering the need for lateral control ailerons on the outboard wing trailing edge.

Significant increases in $C_{L_{max}}$ can also be achieved through the application of leading-edge high-lift devices. The simplest leading-edge device is the plain leading-edge flap, used on a number of military fighter/attack aircraft. Some jet transports have used leading-edge Krueger flaps. A more effective, but more complicated, leading-edge device is the slat, which is used on all modern jet transports. The maximum effectiveness of leading-edge flaps and slats is usually achieved with flap and slat chords of 12–15%, and deflections ranging from 20° for slats to 30° for plain leading-edge flaps to 60° for Krueger flaps. Leading-edge flaps and slats must extend for the full span of the wing to be effective in increasing $C_{L_{max}}$. Typical high-lift devices are shown in Fig. 24.40.

Lateral Control Devices

An additional consideration during preliminary wing design is the provision of lateral control devices which produce rolling moments about the airplane's x-axis. The most common lateral control devices are ailerons, essentially a plain trailing-edge flap, and spoilers, basically a portion of the wing upper surface, hinged at its leading edge, which reduces the lift in the affected area of the wing when the spoiler is deflected. When deflected asymmetrically, spoilers can produce significant rolling moments, especially if they are located ahead of deflected trailing-edge flaps. Spoilers have additional uses when deflected symmetrically as drag-producing devices to allow the airplane to slow down in level flight, or to increase the rate of descent at the end of cruise. Spoilers are also used symmetrically to reduce the airplane's lift during landing ground roll, which improves braking effectiveness.

For personal/utility, commuters, and regional turboprops, the usual lateral control device is the aileron, with aileron spans ranging from 55% to 90% of the wing semispan. For business jets and jet transports, spoilers are generally used in conjunction with ailerons. Furthermore, since ailerons located on the outer part of the wing trailing edge tend to twist the wing as they are deflected to produce rolling moments at high dynamic pressure, or high-q conditions, thereby reducing there effectiveness, most jet transports utilize smaller ailerons located further inboard in addition to the outboard ailerons for high-q lateral control and trim.

Inboard Trailing-Edge Extensions

Wing inboard trailing-edge extensions are often used on business jets and jet transports with wing sweep angles greater then 30°. The need for an inboard trailing-edge extension arises from the required main landing gear leg upper pivot point location, which would be very near the wing trailing edge on a trapezoidal planform. By incorporating an inboard trailing-edge extension, a suitable structural arrangement may be designed to provide the necessary gear pivot location. This situation is shown in Fig. 24.41.

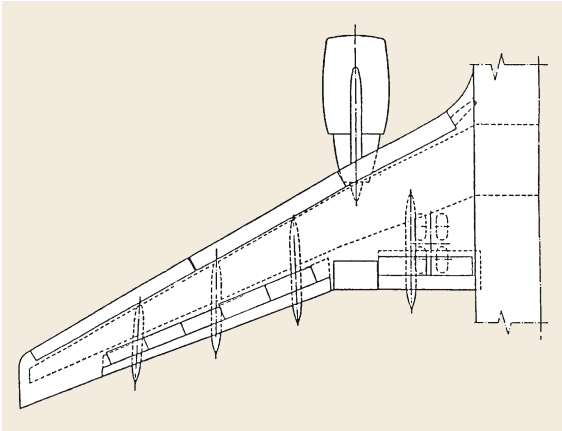

Fig. 24.41 Inboard wing trailing-edge extension

24.8.3 Fuselage Geometry

Primary requirements for the fuselage are to provide accommodation for the crew station, passengers, other payload to be carried in the fuselage, and for some designs the engine/propulsion system as well. For single-engine propeller-driven airplanes, the fuselage accommodates the engine/propeller installation forward, the pilot and passenger cabin next, followed by the aft fuselage, which serves mainly as a convenient structure for locating the horizontal and vertical tail well aft of the wing. For larger transport airplanes, the fuselage is made up of three distinct sections:

(1) the nose section
(2) a constant-section passenger compartment, and
(3) the afterbody or tail cone.

The nose section on larger airplanes usually contains the crew station, with crew seats, control yoke and wheel, or control stick, rudder pedals, instrument panel, glare shield, plus a variety of levers, knobs, and switches to operate various aircraft systems. Specific requirements for pilot field of view and downward vision from the defined pilot design eye position are contained in the Federal Air Regulations (FARs) and the military specifications (Mil Specs). The constant-section passenger compartment for larger airplanes is usually pressurized, and circular or near-circular in cross section, because of the structural weight efficiency of this shape for pressure vessels. For larger-capacity long-range jet transports, two aisles are provided for greater passenger mobility, and for ease of entry and exit from multiple adjacent seats. These larger circular cross sections provide significant space below the passenger deck to carry large amounts of revenue cargo, either in special containers or stacked on flat pallets. A typical cross section for a twin-aisle transport is shown in Fig. 24.42.

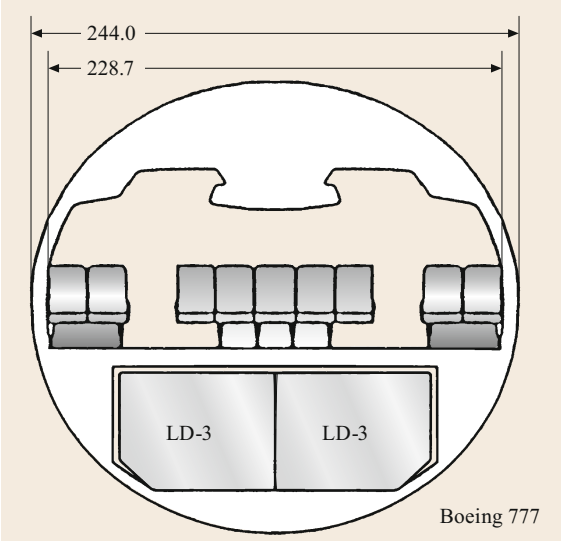

Fig. 24.42 Twin-aisle transport fuselage cross section

The length of the passenger compartment must be sufficient to accommodate the required number of passengers, allow for galley space, lavatories, coat rooms, plus passenger entrance doors, and emergency exits.

There are specific requirements in the FARs for emergency exits to be used in survivable accidents. The aft fuselage or afterbody is influenced by conflicting requirements of aerodynamic performance and structural weight. The afterbody should be long enough to avoid severe curvature and separation drag, while being as short as possible to avoid limiting the airplane pitch attitude on the ground during normal take-offs, as well as avoiding excessive weight from a long afterbody.

24.8.4 Empennage Geometry

For conventional aft-tail configurations, the horizontal and vertical tail arrangement, called the empennage, is the major element for providing both static aerodynamic stability in pitch and yaw as well as aerodynamic control moments in pitch and yaw. For unconventional configurations such as *flying wings* or forward horizontal tail *canards*, the static aerodynamic stability and control are provided by other means.

The aft horizontal tail is the major contributor to static aerodynamic stability in pitch. This is quite logical, since static longitudinal stability involves the generation of aerodynamic restoring moments which are dependent on an aerodynamic force from the horizontal tail (proportional to the horizontal tail area) and a moment arm (proportional to the distance from the

airplane center of gravity to the horizontal tail m.a.c.). The horizontal tail also provides the aerodynamic control moments to allow the pilot to achieve equilibrium in pitch at any desired lift coefficient, allowing the control of airspeed in steady unaccelerated flight, and the curvature of the flight path in accelerated flight. Longitudinal control is usually provided through the hinged, movable, aft portion of the horizontal tail called the elevator, although some designs move the entire horizontal tail about a fixed pivot point. This arrangement is called an all-movable horizontal, or a stabilator.

24.8.5 Landing Gear

Most modern airplanes use a tricycle landing gear configuration, that is, one with two main wheels aft of the c.g. and one forward [24.20]. Except for small airplanes with low cruise speed, landing gears are usually retracted for climb and cruise flight. The landing gear wheels and tires must be adequate to handle a variety of taxi, take-off, and landing loads prescribed by the FARs, as well as spreading the reaction loads from the gear sufficiently so as not to overstress the runway pavement. The landing gear also has to house the brakes.

24.8.6 Propulsion Systems

Propulsion systems for modern airplanes are of one of the following types [24.21]:

- Piston engine–propeller
- Turbine engine–propeller
- Turbojet engine
- Turbofan engine
- Turbofan engine with afterburner.

Small personal utility or acrobatic airplanes are usually powered by piston engine–propeller combinations, while larger personal utility and smaller commuter airplanes are usually powered by turboprop propulsion. Business jets and larger jet transports are powered by turbofans. High-performance military airplanes are usually powered by low-bypass turbofans equipped with afterburners. The key parameter for the propulsion system is the *specific fuel consumption* c, i.e., the amount of fuel burned per hour, per unit of output of the propulsion system [24.22].

For piston engines and turboprops, c is expressed in $\mathrm{lb}/(\mathrm{bh_p\,h})$, while for turbojets and turbofans, it is expressed in $\mathrm{lb}/(\mathrm{h\,lb_{thrust}})$.

24.9 Weights

The weight of an airplane, especially its empty weight, is a vital parameter in the performance and economics of the design. The following paragraphs provide information on the various aspects of aircraft weight.

24.9.1 Weight Definitions

Figure 24.43 shows a simple bar chart illustrating the elements of the weight buildup to the maximum take-off weight W_{to} required for a specific design mission. Also noted to the right of the bar chart are some important structural weight definitions that are related to the weight buildup, for a typical commercial jet transport. Other aircraft types have similar structural weight definitions.

Note that the operating weight empty includes both the manufacturer's weight empty (MWE), plus the operator's items, which include the flight crew, cabin crew, food, galley service items, drinkable water, cargo containers and pallets, plus life vests, life rafts, emergency transmitters, and the unusable fuel trapped in the fuel system and unavailable for use by the engines. When all the payload is loaded, that is, all available passenger seats are filled at the *standard* passenger + baggage weight and all the available revenue cargo volume is filled at some selected cargo density, the aircraft has reached its space limit payload (SLPL), which usually coincides with another key weight definition, the maximum zero-fuel weight (MZFW), the maximum design weight for the aircraft with no fuel on board. Loading

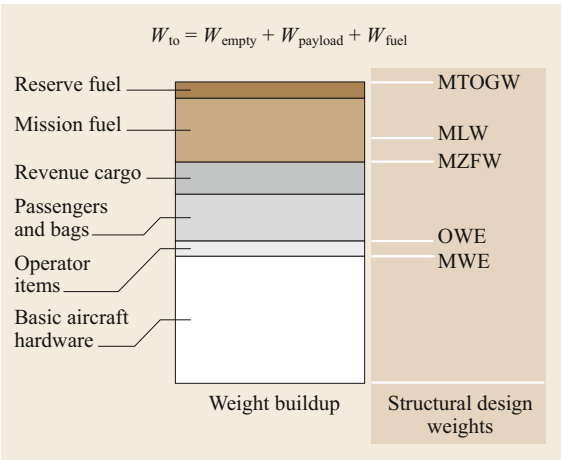

Fig. 24.43 Typical weight buildup – jet transport

on the fuel required for the mission, the mission fuel, plus the required reserves, brings the aircraft to W_{to}, the maximum take-off gross weight required to perform the specified design mission. The design maximum landing weight (MLW) for most smaller aircraft, such as private propeller-driven aircraft and short-range commuters, is usually the same as the MTOGW. However, for larger, long-range aircraft, where the mission fuel is a large percentage of the MTOGW, a somewhat lower MLW is selected to minimize the structural weight impact of designing all the structure to withstand the loads associated with landing at MTOGW. For this design choice, a fuel dump system, which allows fuel to be jettisoned overboard in an emergency following a high-gross-weight take-off, allows the aircraft to reduce its weight to the MLW without having to burn off large amounts of mission fuel. A summary of the airplane weight definitions is given in Table 24.8.

24.9.2 Weight Fractions

The maximum take-off weight required for a specific design mission (W_{to}) may be written as

$$W_{to} = W_{empty} + W_{payload} + W_{fuel}$$

or

$$\frac{W_{empty}}{W_{to}} + \frac{W_{payload}}{W_{to}} + \frac{W_{fuel}}{W_{to}} = 1 \,,$$

where

$$\frac{W_{empty}}{W_{to}} = \text{weight empty fraction} \,,$$

$$\frac{W_{payload}}{W_{to}} = \text{payload fraction} \,,$$

$$\frac{W_{fuel}}{W_{to}} = \text{fuel fraction} \,.$$

and W_{empty} is the operating weight empty (OWE), the basic aircraft hardware plus other items required to allow the aircraft to perform the design mission, $W_{payload}$ is the passengers + bags + revenue cargo (commercial) or bombs, missiles, cargo (military), and W_{fuel} is the total fuel on board for the mission, that is, fuel burned + reserve fuel.

24.9.3 Weight Estimation and Control

In order to begin design work on a specific aircraft project, there is a need to establish the weight of the various components and systems that make up the aircraft empty weight. This process, usually conducted by aircraft weight engineers, initially involves much reliance on empirical data from actual aircraft, correlated with appropriate physical parameters. These data are assembled into a group weight statement, a list of weights of the major elements that make up the MWE. Examples are shown in Table 24.9.

As the design work progresses, the group weights are updated as various parts of the aircraft are specifically defined. Major effort is required to ensure that the initial target weight for the entire aircraft is not exceeded during the design and manufacturing phase of the project.

24.9.4 Balance Diagram and C.G. Limits

The airplane balance diagram is used to ensure that the airplane center of gravity (c.g.) is in the proper location for all of the probable loading conditions considering the OWE c.g. location, fuel loading and usage, passenger loading, and cargo loading. The OWE c.g. is usually set by designers based on experience for a specific airplane design. Then the extreme excursions of the c.g. due to the most probable adverse loading conditions that move the c.g. forward and aft are examined by calculation to establish forward and aft limits for c.g. travel. The results of these calculations are plotted on a chart of airplane gross weight versus c.g. location so that appropriate c.g. limits can be established. Stability and control and structural design criteria must be met at these c.g. limits.

Table 24.8 Airplane weight definitions

Weight	Symbol	Definition
Manufacturer's weight empty	MWE	Airplane weight at the end of the manufacturing process
Operating weight empty	OWE	Airplane weight ready for operation, including flight crew, cabin crew, food, galley service items, potable water, cargo containers and pallets, life vests, life rafts, emergency transmitter, lavatory fluids, and unusable fuel
Maximum zero-fuel weight	MZFW	Airplane weight with maximum design payload on board, but no fuel; the design payload includes all passengers and their baggage, plus the maximum design cargo weight
Maximum landing weight	MLW	Airplane weight defined as the maximum for which the airplane meets all of the structural design requirements for landing, usually being somewhat higher than the MZFW
Maximum take-off gross weight	MTOGW	Airplane weight defined as the maximum for which the airplane meets all of the structural design and performance requirements for takeoff; this includes the maximum design payloads plus the fuel required to fly the design mission plus the required reserve fuel.

Table 24.9 Summary of group weight statements. Transport airlines in lb

Weight elements	DC-9-30	737-200	727-100	727-200	707-320	DC-8-55	DC-8-62	DC-10-10	L-1011-1	DC-10-30	747-100
Wing group	11 391	11 164	17 682	18 529	28 647	34 909	36 247	48 990	47 401	57 748	88 741
Tail group	2790	2777	4148	4142	6004	4952	4930	13 657	8570	14 454	11 958
Body group	11 118	11 920	17 589	22 415	22 299	22 246	23 704	44 790	49 432	46 522	68 452
Landing gear	4182	4038	7244	7948	11 216	11 682	11 449	18 581	19 923	25 085	32 220
Nacelle group	1462	1515	2226	2225	3176	4644	6648	8493	8916	9328	10 830
Propulsion group	2190	1721	3052	3022	5306	9410	7840	7673	8279	13 503	9605
Flight controls	1434	2325	2836	2984	2139	2035	2098	5120	5068	5188	6886
Auxiliary power	817	855	0	849	0	0	0	1589	1202	1592	1797
Instruments	575	518	723	827	550	1002	916	1349	1016	1645	1486
Hydraulic system	753	835	1054	1147	1557	2250	1744	4150	4401	4346	5067
Electrical system	1715	2156	2988	2844	3944	2414	2752	5366	5490	5293	5305
Avionics	1108	1100	1844	1896	1815	1870	2058	2827	2801	3186	4134
Furnishings	8594	9119	11 962	14 702	16 875	15 884	15 340	38 072	32 829	33 114	48 007
Air conditioning	1110	1084	1526	1802	1602	2388	2296	2386	3344	2527	3634
Antiicing system	474	113	639	666	626	794	673	416	296	555	413
Load and handling	57	–	15	19	–	55	54	62	–	62	228
Empty weight (less dry engine)	49 770	51 240	75 528	86 017	105 756	116 535	118 749	203 521	198 968	224 148	297 867
Dry engine	6160	6212	9322	9678	19 420	16 936	17 316	23 229	30 046	25 587	35 700
MWE	55 930	57 452	84 850	95 695	125 176	133 471	136 065	226 750	229 014	249 735	333 567
MTOGW	108 000	104 000	161 000	175 000	312 000	325 000	335 000	430 000	430 000	565 000	775 000

24.10 Aircraft Performance

Aircraft performance is the part of the subject of flight mechanics that deals with parameters such as speed, rate of climb, range, fuel consumption, and runway length requirements.

24.10.1 Level-Flight Performance

The simplest performance condition is steady level-flight cruise, when all forces are in equilibrium as the aircraft moves at a constant speed and altitude. From Fig. 24.18, equilibrium requires that

$$\text{lift } L = \text{weight } W = C_L \frac{\rho}{2} V^2 S\,, \quad C_L = \frac{W}{(\rho V^2/2)\,S}\,,$$

and

$$\text{thrust } T = \text{drag } D = C_D \frac{\rho}{2} V^2 S \quad \text{subsonic flight}\,.$$

For any given weight, C_L may be found and substituted into the induced drag term. ΔC_{D_C}, the empirical compressibility drag coefficient, is dependent on C_L and the Mach number.

Several fundamental airplane characteristics can be derived from the drag equation [24.23]. One major objective of airplane design is to minimize the drag for any required lift. At any altitude and speed, the ratio of drag to lift depends only on the ratio of C_D to C_L. At low Mach numbers, $\Delta C_{D_C} = 0$ and

$$C_D = C_{D_p} + \frac{C_L^2}{\pi e \mathrm{AR}}\,.$$

where AR is the aspect ratio and e is an efficiency factor. Generally, $e < 1$ but for elliptic wings $e = 1$.

For minimum drag, C_D/C_L is a minimum. Now

$$\frac{C_D}{C_L} = \frac{C_{D_p}}{C_L} + \frac{C_L}{\pi e \mathrm{AR}} .$$

At the value of C_L for which C_D/C_L is a minimum, $\mathrm{d}(C_D/C_L)/\mathrm{d}C_L = 0$. Then

$$\frac{\mathrm{d}\,(C_D/C_L)}{\mathrm{d}C_L} = -\frac{C_{D_p}}{C_L^2} + \frac{1}{\pi e \mathrm{AR}} = 0 .$$

And for $L/D =$ maximum,

$$C_{D_p} = \frac{C_L^2}{\pi e \mathrm{AR}} .$$

Thus, for minimum drag, the lift coefficient is the value for which the drag due to lift is equal to the parasite drag. For this condition,

$$C_{L_{(L/D)_{max}}} = \sqrt{C_{D_p} \pi e \mathrm{AR}} .$$

The value of L/D is

$$\frac{L}{D} = \frac{C_L}{C_D} = \frac{C_L}{C_{D_p} + C_L^2/(\pi e \mathrm{AR})} ,$$

for $L/D =$ maximum

$$C_L = \sqrt{C_{D_p} \pi e \mathrm{AR}}$$

and

$$C_{D_p} = \frac{C_L^2}{\pi e \mathrm{AR}} .$$

Thus,

$$\left(\frac{L}{D}\right)_{max} = \frac{\sqrt{C_{D_p} \pi e \mathrm{AR}}}{2C_{D_p}} .$$

To obtain this minimum drag in flight, one must fly at the speed corresponding to the C_L given above. This speed is designated as $V_{(L/D)_{max}}$. Then

$$\sqrt{\frac{2W}{\sqrt{C_{D_P} \pi e \mathrm{AR}}\rho S}} .$$

Propeller-driven airplanes achieve their best range at the lift coefficient and corresponding speed for $(L/D)_{max}$.

It is customary to study the performance of propeller-driven airplanes in terms of power, since they operate with engines that produce power rather than thrust. The thrust horsepower required for level flight is the drag times the distance covered per unit time, so

$$550\,\mathrm{thp}_{req} = \mathrm{DV} = C_{D_p}\frac{\rho}{2}V^3 S + \frac{C_L^2}{\pi e \mathrm{AR}}\frac{\rho}{2}V^3 S .$$

Then $V = \sqrt{2W/C_L \rho S}$, and we obtain

$$\mathrm{thp}_{req} = \frac{1}{550}\sqrt{\frac{2W^3}{\rho S}}\left(\frac{C_{D_p}}{C_L^{3/2}} + \frac{C_L^{1/2}}{\pi e \mathrm{AR}}\right) .$$

The constant 550 is included to keep the units in thrust horsepower and the other units in the corresponding English system units. The minimum power will be obtained when the term in parenthesis is a minimum. Taking the derivative of that term with respect to C_L, equating it to zero, and defining $C_{L_{mp}}$ as the lift coefficient for minimum power required leads to

$$-\frac{3}{2}\frac{C_{D_r}}{C_{L_{mp}}^{5/2}} + \frac{1}{2}\frac{1}{\pi e \mathrm{AR} C_{L_{mp}}^{1/2}} = 0 .$$

Therefore,

$$C_{L_{mp}}^2 = 3\pi C_{D_p} e \mathrm{AR} ,$$

and

$$C_{L_{mp}} = \sqrt{3\pi C_{D_p} e \mathrm{AR}} = \sqrt{3C_{L_{(L/D)_{max}}}} .$$

Substituting in the induced drag coefficient portion of the equation gives

$$C_{D_{imp}} = \frac{3\pi C_{D_p} e \mathrm{AR}}{\pi e \mathrm{AR}} = 3C_{D_p} .$$

At the minimum-power condition, the induced drag coefficient is three times as large as the parasite drag coefficient. This contrasts with the minimum drag condition, for which they are equal. Since, for a given total lift, the speed varies inversely as the square root of the lift coefficient, the speed for minimum power is lower than the speed for minimum drag by the ratio $1/3^{1/4} = 0.76$. Taking the inverse, the minimum drag speed is 1.32 times the minimum-power speed.

24.10.2 Climb and Descent Performance

Figure 24.18 illustrates the force on an airplane in steady-state constant-speed climb. The thrust is shown acting parallel to the flight path direction. In general, this is not quite true, but in conventional aircraft the

effects of an inclination of the thrust vector are small enough to be neglected.

Equating forces perpendicular and parallel to the flight path

$$L = W\cos\gamma\ ,$$
$$T = D + W\sin\gamma\ .$$

Then,

$$\sin\gamma = \frac{T-D}{W} = \frac{T}{W} - \frac{D}{W} = \frac{T}{W} - \frac{D}{L}\ ,$$

γ is the flight path angle or angle of climb. We may assume that γ is sufficiently small so that $\cos\gamma$ is approximately equal to 1.0. Then, $L = W$ and

$$\text{Rate of climb, RC} = V\sin\gamma = \frac{V(T-D)}{W}\ .$$

For propeller-driven aircraft, it is convenient to use power rather than thrust and drag. If RC is to be determined in feet per minute, the usual units, then with V in feet per second,

$$\begin{aligned}\text{RC (ft/min)} &= 60\left(\frac{\text{TV}-\text{DV}}{W}\right)\\ &= \frac{\text{thp}_{\text{avail}} - \text{thp}_{\text{req}}}{W}(33\,000)\\ &= \frac{\text{thp}_{\text{excess}}}{W}(33\,000)\ ,\end{aligned}$$

where $\text{thp}_{\text{excess}}$ is the thrust horsepower available for climbing; W is given in lb.

The preceding equations are based on an airplane climbing at constant true airspeed. In practical operations, climbing flight is done at constant indicated airspeed or constant Mach number. This provides the pilot with a simple guide to the proper climb speed, whereas a constant true speed would mean an ever-changing indicator reading as the altitude increases. A constant indicated speed essentially corresponds to a constant calibrated airspeed. At low Mach numbers, this is the same as a constant equivalent airspeed, since the compressibility correction to airspeed is very small.

With a constant equivalent airspeed, the airplane continually accelerates as the altitude increases. The equilibrium equation along the flight path must then include an inertial term. Thus

$$T = D + W\sin\gamma + \frac{W}{g}\frac{\mathrm{d}V}{\mathrm{d}t}\ .$$

Since

$$\frac{\mathrm{d}V}{\mathrm{d}t} = \frac{\mathrm{d}V}{\mathrm{d}h}\frac{\mathrm{d}h}{\mathrm{d}t} \quad \text{and} \quad \frac{\mathrm{d}h}{\mathrm{d}t} = V\sin\gamma\ ,$$

Table 24.10 Kinetic-energy correction factors for climb

Climb operation	Altitude (ft)	$(V/g)(\mathrm{d}V/\mathrm{d}h)$ (approx.)
Constant true speed	All	0
Constant v_{E}	Above 36 150	0.7Ma^2
Constant v_{E}	Below 36 150	0.567Ma^2
Constant Ma	Above 36 150	0
Constant Ma	Below 36 150	-0.133Ma^2

we can write

$$\sin\gamma = \frac{(T-D)/W}{1 + (V/g)\,(\mathrm{d}V/\mathrm{d}h)} = \frac{T-D}{W}\quad \text{(K.E. factor)}\ .$$

This equation differs from the previous rate-of-climb equation at constant true speed by the kinetic-energy correction factor $[1 + (V/g)(\mathrm{d}V/\mathrm{d}h)]^{-1}$. Approximate values of the term $(V/g)(\mathrm{d}V/\mathrm{d}h)$ are given as functions of the Mach number in Table 24.10 for various types of climb paths [24.24]. Note that, for constant-Mach-number climb below the isothermal atmosphere, the correction increases the rate of climb. In this region, constant Mach number means decreasing velocity as altitude increases, because the speed of sound is decreasing. The airplane is losing kinetic energy and trading it for an increased rate of climb. When applicable, the kinetic-energy correction factor is applied to gradient-of-climb and rate-of-climb calculations.

The foregoing equations include a surprisingly large amount of useful information. First, the Federal Air Regulations (FARs) specify minimum permissible performance for commercial aircraft in terms of minimum climb gradients, primarily after failure of one engine. A gradient is the tangent of an angle. For small to moderate flight path angles, the sine of the angle is essentially equal to the tangent, so

$$\begin{aligned}\text{gradient } \gamma &= \tan\gamma = \sin\gamma\\ &= \frac{T-D}{W}\quad \text{(K.E. factor)}\\ &= \left(\frac{T}{W} - \frac{D}{W}\right)\quad \text{(K.E. factor)}\ .\end{aligned}$$

Thus, the gradient depends on the thrust-to-weight ratio minus the inverse of the lift-to-drag ratio.

There are three conditions that are related to an airplane's climb performance. The first is the gradient of climb, which is important for clearing obstacles close to the ground. The second is the rate of climb, which is important for reaching cruise altitude as soon as possible. The third is the best economy of climb, climbing at a higher speed than the best rate of climb speed, but covering more distance in the climb for a given amount of fuel burned. These climb speeds are shown in Fig. 24.44.

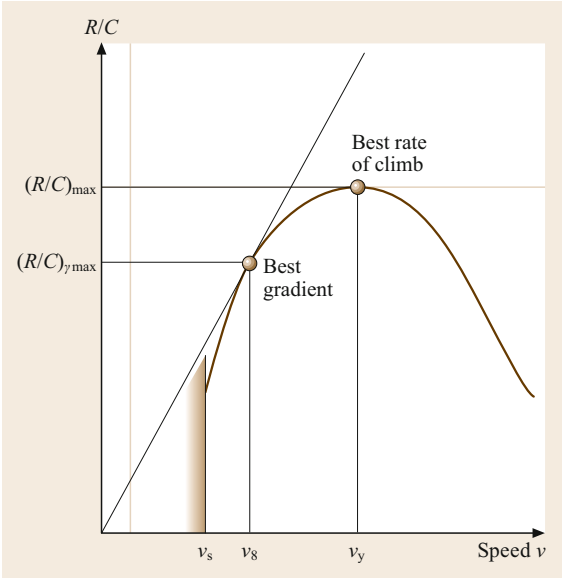

Fig. 24.44 Climb speed diagram

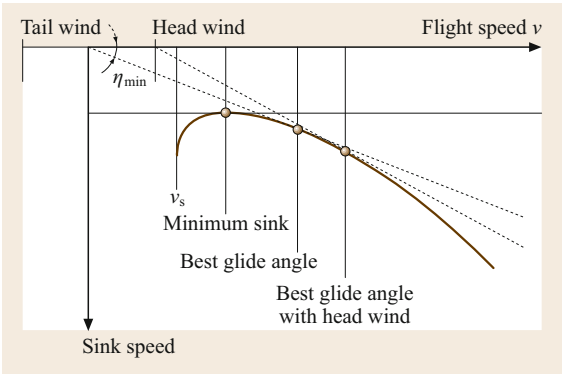

Fig. 24.45 Glider performance chart

Other important performance characteristics can be found from the climb gradient and rate-of-climb equations. If the thrust is zero, then the flight path gradient is the inverse of the L/D ratio, and the rate of descent or sink speed is given by the expression

$$\text{rate of descent} = \frac{V}{L/D} .$$

For gliders and sailplanes, these equations are used to develop charts such as the one shown in Fig. 24.45, which provide the essential performance data for these aircraft.

24.10.3 Range

The total range capability of an airplane consists of the climb, cruise, and descent segments. The cruise range is equal to the summation of the range increments obtained by multiplying the miles flown per pound of fuel used (mi/lb) at selected average weights by the appropriate incremental fuel quantity. The value of the miles per pound is called the specific range and is defined as follows.

For jet or turbofan aircraft,

$$\frac{\text{mi}}{\text{lb}} = \frac{\text{miles flown per hour}}{\text{fuel flow (lb/h)}} = \frac{V}{cT} = \frac{V}{cD} ,$$

where c is the specific fuel consumption (SFC) in pounds of fuel per pound of thrust per hour (lb/(lb h)).

The SFC used in the performance equations is the installed specific fuel consumption. *Installed* means that all adverse effects on SFC associated with the engine installation are included. A typical markup on engine specification SFC for jet and turbofan transports is 3% (i.e., installed SFC equals 1.03 times bare engine SFC). In some cases, for which the engine data are based on zero inlet and nozzle losses, the markup may be twice that amount.

Also,

$$D = \frac{W}{L/D} = \frac{D}{L} W$$

and thus

$$\frac{\text{nmi}}{\text{lb}} = \frac{V}{c(D/L)W} = \frac{V}{c}\frac{L}{D}\frac{1}{W} \quad \text{(jet)} .$$

The term $(V/c)(L/D)$ is called the range factor and is a measure of the aerodynamic and propulsive system range efficiency. If V is in knots, the range in miles per pound will be in nautical miles per pound of fuel.

For a propeller-driven airplane,

$$\frac{\text{nmi}}{\text{lb}} = \frac{V}{c\text{bhp}} ,$$

where c is the specific fuel consumption in pounds of fuel per horsepower per hour (lb/(bhp h)). Then the range in nautical miles per pound of fuel is

$$\frac{\text{nmi}}{\text{lb}} = \frac{V(\text{kn})}{c(\text{thp}/\eta)} = \frac{\eta}{c}\left(\frac{V(550)}{DV \times 1.69}\right) = 325\frac{\eta}{c}\frac{1}{D} = 325\frac{\eta}{c}\frac{L}{D}\frac{1}{W} \text{ (propeller)} .$$

For propeller-driven airplanes, the specific range depends only on the propeller efficiency, SFC, and L/D; speed is not a factor. Since the propeller efficiency and SFC are essentially constant in cruise, the range is determined by L/D.

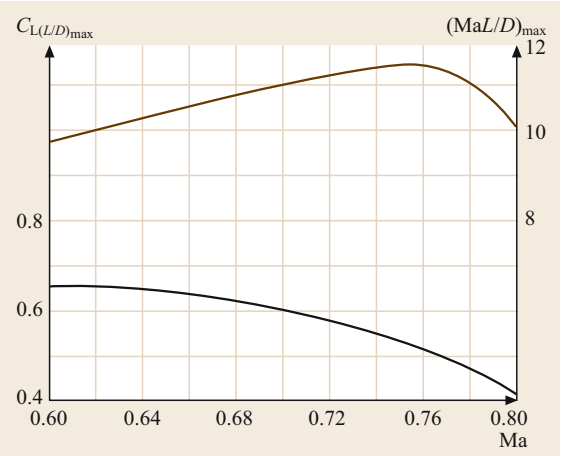

Fig. 24.46 $(MaL/D)_{max}$ and $C_{L(L/D)_{max}}$ for maximum range of jet airplanes (Ma is the cruise Mach number)

The specific range equation for jet airplanes can also be written as

$$\frac{\text{nmi}}{\text{lb}} = a\frac{\text{Ma}}{c}\frac{L}{D}\frac{1}{W} ,$$

where a is the speed of sound and Ma is the cruise Mach number. The expression (MaL/D) is a measure of the specific range capability due to the aerodynamic characteristics of jet-powered airplanes. Curves of (MaL/D) versus lift coefficient at various Mach numbers show that jet range is increased by high speed as well as high L/D up to the point where the adverse compressibility drag effect on L/D overpowers the beneficial effect of higher speed. This situation can be summarized on a chart such as that in Fig. 24.46, which shows that, if the SFC is constant with Mach number, the maximum mi/lb value for a jet airplane occurs at a Mach number and lift coefficient where the maximum value of (MaL/D) at each Mach number reaches its peak. However, the turbofan SFC increases slowly with Mach number, so that the optimum range will be obtained at a slightly lower Mach number than indicated in Fig. 24.46.

The total cruise range is given by

$$\text{range} = \int_{w_f}^{w_i} \frac{\text{nmi}}{\text{lb}} \mathrm{d}W .$$

If average values of η, c, and L/D can be chosen, the cruise range may be found analytically. For jets,

$$R\ (\text{nmi}) = \int_{w_f}^{w_i} \frac{\text{nmi}}{\text{lb}} \mathrm{d}W = \int_{w_f}^{w_i} \frac{V}{c}\frac{L}{D}\frac{\mathrm{d}W}{W}$$
$$= \frac{V}{c}\frac{L}{D}\ln\frac{W_i}{W_f} .$$

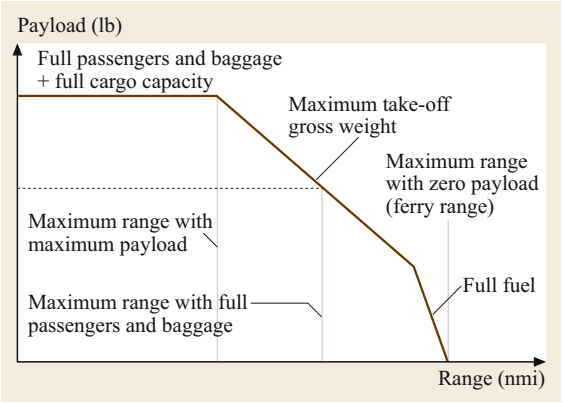

Fig. 24.47 Payload–range curve

For propeller-driven planes,

$$R\ (\text{nmi}) = \int_{w_f}^{w_i} 325\frac{\eta}{c}\frac{L}{D}\frac{\mathrm{d}W}{W}$$
$$= 325\frac{\eta}{c}\frac{L}{D}\ln\frac{W_i}{W_f} \quad \text{(Breguet formula)} ,$$

where η, c, and L/D are assumed constant throughout the flight or, more realistically, are taken as effective averages; V is in knots; and c is in lb/(lb h) or (lb/(bhp h)), as appropriate. The range formula for propeller-driven aircraft is called the Breguet formula, after its originator. The analogous jet formula is often similarly labeled.

The total range includes the cruise range plus the distance covered in climb and descent. For long flights, where the cruise portion is dominant, the lower mi/lb in climb due to the higher power being used, and the higher mi/lb in descent due to lower power being used, may be assumed to cancel, allowing the range to be estimated directly from the Breguet range equation, using the appropriate parameters chosen at an average weight. For short flights, where climb is a large portion of the total trip, this approximation may result in a significant error.

A summary of the payload–range characteristics of an airplane is shown in Fig. 24.47. The payload–range curve is one of the most important performance curves for a commercial transport or business jet. It establishes the envelope which shows how far the airplane can carry a given payload, or how much payload it can carry over a given range.

The payload–range curve applies to a specific airplane–engine combination (MWE, OWE, interior seating arrangement, fuel-tank configuration, MTOGW), operating under specific flight rules (cruise Mach number, altitude, altitude steps, alternate dis-

tance). The maximum payload is usually the volume or space limit payload (full passengers + bags and full cargo containers or pallets at some standard cargo density, i.e., 10 lb/ft^3) or the maximum zero-fuel weight limit payload, based on the structural limit of maximum zero-fuel weight. When operating on the maximum take-off weight limit, it is necessary to trade payload for fuel if greater range is desired. Operating on the fuel capacity limit line requires large reductions in payload to achieve small increases in range, due to modest improvements in cruise efficiency achieved by reductions in cruise weight. The key points on the payload range curve are calculated using the Breguet range equation for jet aircraft

$$R\ (\text{nmi}) = \left(\frac{V}{c}\right)\left(\frac{L}{D}\right)\ln\frac{W_\text{i}}{W_\text{f}}\,.$$

For a specific design on a particular cruise operation V, c, and L/D are usually taken as constants, and W_initial and W_final are derived from known weights, i.e., OWE, payload, reserve fuel, maximum take-off weight, and maximum fuel capacity. From this equation, it can be seen that the maximum range is achieved by cruising at a point where the quantity VL/D is a maximum.

Some key ideas about payload–range curves are as follows:

- Weight-limited payload = MZFW – OWE.
- Space-limited payload is slightly lower.
- Passengers + bags range is usually set by MTOGW.
- Greater passengers + bags range can be achieved by increasing MTOGW (allows more fuel to be carried).
- If passenger + bags range is limited by maximum fuel capacity, greater range can be achieved only through increased fuel capacity.

24.10.4 Endurance

The endurance problem is similar to the range problem except that we are trying to determine how long the aircraft will fly rather than how far it will fly. The quantity analogous to specific range is specific endurance, the hours flown per unit quantity of fuel. In the usual units, specific endurance is measured in hours per pound of fuel.

To maximize endurance, fuel flow per unit time must be minimized. Since the specific fuel consumption is nearly constant, the drag must be minimized for jet aircraft, while thrust horsepower must be as small as possible for propeller-driven aircraft. The endurance t_e for turbojet or turbofan aircraft is

$$\begin{aligned} t_\text{e} &= \int_{w_\text{f}}^{w_\text{i}} \frac{\text{h}}{\text{lb fuel}}\,\text{d}W = \int_{w_\text{f}}^{w_\text{i}} \frac{1}{Dc}\text{d}W \\ &= \int_{w_\text{f}}^{w_\text{i}} \frac{1}{[W/(L/D)]c}\text{d}W \\ &= \int_{w_\text{f}}^{w_\text{i}} \frac{1}{c}\frac{L}{D}\frac{\text{d}W}{W} = \frac{1}{c}\frac{L}{D}\ln\frac{W_\text{i}}{W_\text{f}}\,. \end{aligned}$$

Again, c and L/D are assumed to be constant throughout the flight, or taken as average values. Note the similarity between this equation and the jet range equation.

Endurance is simply range divided by speed. For the greatest endurance, the aircraft should obviously fly at the speed for minimum drag. This, of course, assumes that c is a constant with speed, a good assumption for jets but not quite true for turbofans. In addition, at very low engine thrust levels, c tends to increase as the thrust is decreased. This may also influence the speed for best endurance.

For propeller-driven aircraft, endurance is

$$\begin{aligned} t_\text{e} &= \int_{w_\text{f}}^{w_\text{i}} \frac{1}{\text{thp}\,c/\eta}\text{d}W = \int_{w_\text{f}}^{w_\text{i}} \frac{\eta}{c}\left(\frac{550}{DV\times 1.69}\right)\text{d}W \\ &= \int_{w_\text{f}}^{w_\text{i}} 325\frac{\eta}{c}\frac{L}{DV}\frac{1}{W}\text{d}W\,, \end{aligned}$$

where V is in knots and c is in pounds of fuel per brake horsepower per hour. We cannot assume that L/DV is a constant. L/DV is the ratio of lift to thrust power required, and we have shown that thp_req is a nonlinear function of weight. At any given lift coefficient, power required varies with $W^{3/2}$. However, it has been shown that, if V is expressed as $\sqrt{2W/(C_\text{L}\rho S)}$, t_e is given by [24.25]

$$t_\text{e}(s) = \frac{\eta}{c}\frac{C_\text{L}^{3/2}}{C_\text{D}}\sqrt{\frac{2\sigma S}{W_\text{i}}}\left[\left(\frac{W_\text{i}}{W_\text{f}}\right)^{1/2} - 1\right].$$

Here we see that, for best endurance, a propeller-driven airplane should be flown at the flight condition for maximum $C_\text{L}^{3/2}/C_\text{D}$. This is a maximum when the lift coefficient is $\sqrt{3}$ times the value for maximum lift-to-drag ratio. Since low speed as well as a particular lift

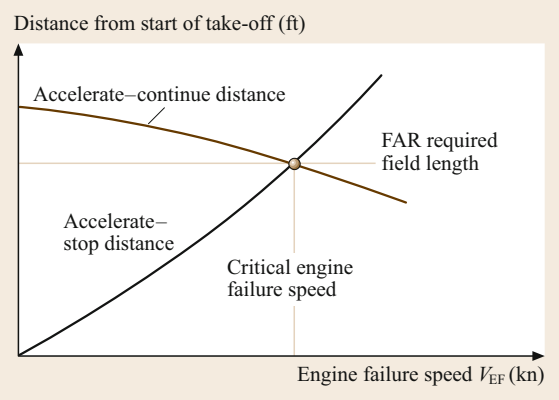

Fig. 24.48 Determination of FAR balanced field length with engine failure

coefficient is desirable for minimum power required, best endurance occurs at a high density (i.e., low altitude). Therefore, propeller aircraft endurance is best at low altitudes.

24.10.5 Take-Off Performance

The take-off performance problem is basically an acceleration to the required speed plus a transition to climb at a 35 ft height for civil turbine-powered transports, or a 50 ft height for piston-engine general aviation or military airplanes. The required runway length is defined as the distance from the start of take-off to the point where these *obstacle* heights are reached. The take-off field length required by FARs for jet transport operation is the greater of:

1. The all-engine take-off distance ×1.15
2. The take-off distance with an engine failure at the *most critical point* in the take-off.

The most critical point is where the distance to stop on the runway is equal to the distance to continue the take-off with one engine failed to a height of 35 ft. This situation is called the balanced field length concept. The most critical point in a given take-off, where the *accelerate–stop* distance is equal to the *accelerate–continue* distance, is found by plotting the accelerate–stop distance and accelerate–continue distance versus the engine failure speed, as shown in Fig. 24.48.

For propeller-driven transports, the FAR balanced field length concept is the same, but the speed at 35 ft is $1.15V_S$ for four or more engines, and $1.2V_S$ for two or three engines.

For single- and multiengine normal, utility, and acrobatic aircraft under 12 500 lb maximum gross weight, FAR 23 specifies only the all-engine take-off distance

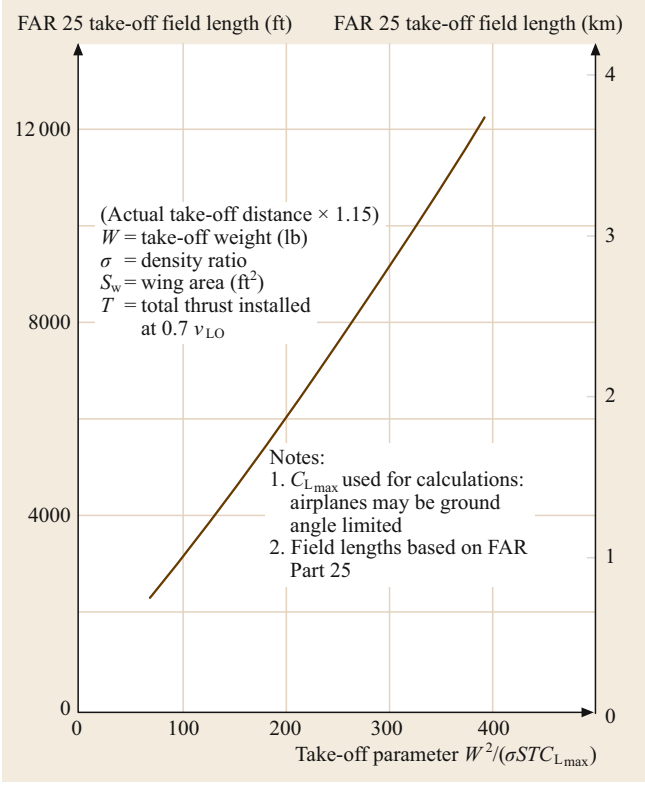

Fig. 24.49 FAR 25 all-engines-operating take-off field length to a 35 ft height

to a height of 50 ft with a speed equal to or greater than $1.3V_S$ at 50 ft. For FAR 23 commuter-category aircraft, the balanced field length concept is applied and the criteria for take-off are basically the same as for FAR 25, except that the take-off distance is defined to a 50 ft height, and the speed at 50 ft must be at least $1.3V_S$.

Analysis and flight tests suggest that the distance to liftoff is a function of several airplane factors, namely

$$d_{LO} = f\left(\frac{W^2}{\sigma S C_{L_{max}} T}\right) ,$$

where $\sigma = \rho/\rho_s$ and T is the thrust at $0.7V_{LO}$ [24.11]. Since the ground run distance to lift-off is about 80% of the total distance to the 35 ft height, it has been shown that this parameter works very well in correlating the required runway length results for many aircraft. Figure 24.49 shows the FAR all-engines-operating take-off field length to a 35 ft height d_{35} for jet or turbofan aircraft as a function of $W^2/(\sigma S C_{L_{max}} T_{0.7V_{LO}})$. This chart applies to normal take-off without engine failure and includes a 15% increase above the actual performance in accordance with the air transport requirements of FAR 25.

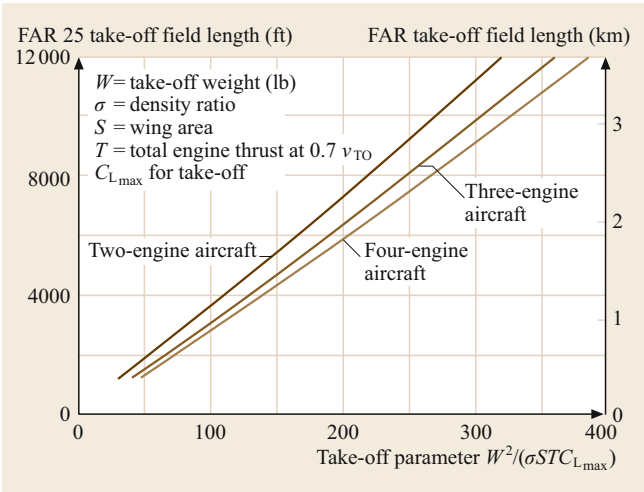

Fig. 24.50 FAR 25 one-engine-inoperative take-off field length. Two-, three-, and four-engine jet transports take-off distance to a 35 ft height balanced field length with engine failure

The actual distance is the distance determined from Fig. 24.49 divided by 1.15. Figure 24.50 shows the FAR one-engine-inoperative take-off field length for two-, three-, and four-engine transports.

For propeller-driven aircraft, a comparable analysis shows that take-off distance is a function of $W^2/(\sigma S C_{L_{max}} P)$, where P is the total brake horsepower. This is a less accurate approximation, since the effectiveness of the power depends on the propeller efficiency during take-off. Use of this parameter assumes that all propellers are designed to attain a similar level of efficiency in take-off.

24.10.6 Landing Performance

Landing distances consist basically of two segments: the air run from a height of 50 ft to the surface accompanied by a slight deceleration and flare, and the ground deceleration from the touchdown speed to a stop. Landing runway lengths are required by FAR 25 for commercial aircraft to be demonstrated by flight tests. The air distance d_{air} can be approximated by a steady-state glide distance d_{GL} plus an air deceleration distance d_{decel} at constant altitude, as shown in Fig. 24.51.

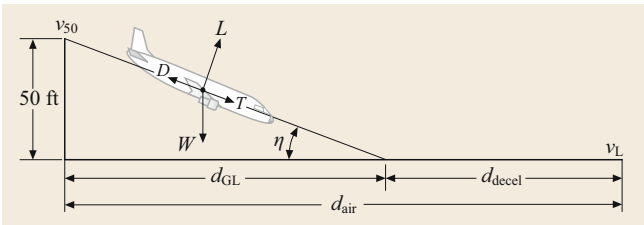

Fig. 24.51 Landing air distance

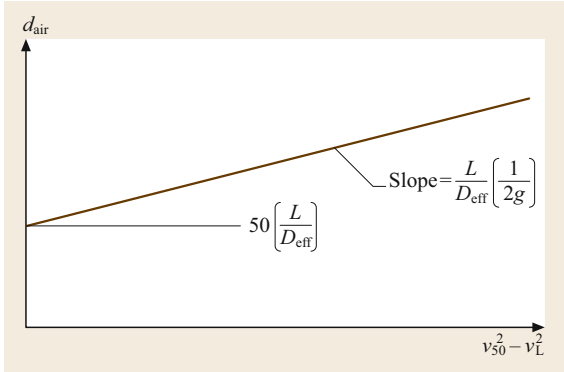

Fig. 24.52 Landing air run determination

V_{50} is the speed at the 50 ft height. In accordance with FAR 25, V_{50} must be at least $1.3V_S$. In practice, it is taken as equal to $1.3V_S$. V_L is the landing or touchdown speed and is usually about $1.25V_S$. The glide distance is

$$d_{GL} = 50\left(\frac{L}{D_{eff}}\right),$$

where $D_{eff} = D - T$,

$$d_{decel} = \frac{V_{50}^2}{2a} - \frac{V_L^2}{2a} = \frac{\frac{1}{2}\left(\frac{W}{g}\right)V_{50}^2 - \frac{1}{2}\left(\frac{W}{g}\right)V_L^2}{D_{eff}}.$$

Since lift is essentially equal to the weight,

$$d_{air} = 50\frac{L}{D_{eff}} + \frac{1}{2g}\left(V_{50}^2 - V_L^2\right)\frac{L}{D_{eff}}$$
$$= \frac{L}{D_{eff}}\left[50 + \frac{1}{2g}\left(V_{50}^2 - V_L^2\right)\right].$$

L/D_{eff} is the effective L/D ratio during the air run. It can be determined from flight test air runs by plotting flight test air run distances versus $(V_{50}^2 - V_L^2)$, as illustrated in Fig. 24.52.

The ground deceleration distance is

$$d_G = \frac{V_L^2}{2a} = \frac{V_L^2}{2\,[R/(W/g)]},$$

where R is the effective average resistance or total stopping force $= \mu(W-L) + D$, μ is the braking coefficient of friction (Table 24.11), and D is the drag, including the drag of flaps, slats, landing gear, and spoilers.

Note that both d_{air}, i.e., the air distance, and d_G, i.e., the ground stopping distance, are directly proportional to V_{50}^2 and/or V_L^2. Both V_{50}^2 and V_L^2 are fixed percentages above V_S for safety reasons. Thus, landing distance is linear in V_S^2 except for the glide distance from 50 ft, which depends only on the L/D ratio in the landing configuration. Thus, for similar airplanes with similar L/D values and equivalent braking systems (i.e., similar μ),

Table 24.11 Runway friction coefficients

Surface	μ typical values	
	Rolling (brakes off)	Brakes on
Dry concrete/asphalt	0.03–0.05	0.3–0.5
Wet concrete/asphalt	0.05	0.15–0.3
Icy concrete/asphalt	0.02	0.06–0.10
Hard turf	0.05	0.4
Firm dirt	0.04	0.3
Soft turf	0.07	0.2
Wet grass	0.08	0.2

landing distances can be expressed in the form

$$d_{\text{land}} = A + BV_S^2 ,$$

where $A = 50(L/D)_{\text{eff}}$.

The FAR 121 scheduled landing field length is defined as the actual FAR 25 demonstrated distance from a 50 ft height to a full stop on a dry, hard surface runway, increased by a factor of 1/0.60, i.e., a 67% increase. Curves of landing field length versus V_S^2 based on flight tests (Fig. 24.53) are linear, but vary between airplanes due to the effective L/D ratio in the air run, the effective coefficient of friction, and the drag in the ground deceleration. It should be noted that the FAR dry runway tests do not allow the use of engine thrust reversers. FAR dry runway distances must be increased by 15% for operation on wet runways.

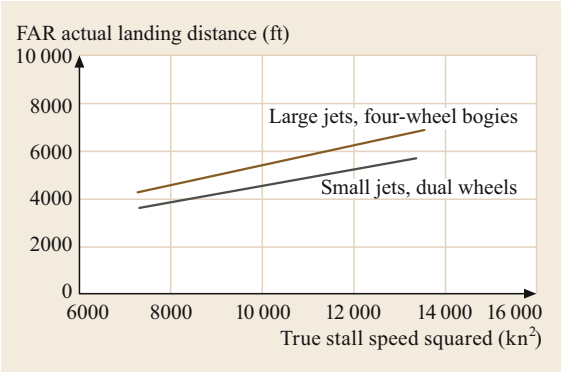

Fig. 24.53 FAR 25 demonstrated landing distance on dry, hard surface runways

24.11 Stability and Control

The subject of airplane stability and control deals with the ability of an airplane to fly straight with wings level without pilot input (stability) and the ability of the pilot to produce moments about the various airplane axes (control). *Static stability* refers to the initial tendency of the airplane to return or move away from its equilibrium position following a disturbance. *Dynamic stability* is concerned with the entire history of the airplane motion, in particular whether the motion subsides or diverges. In the following discussion, the airplane will usually be treated as a rigid body, a reasonable assumption for the majority of conditions studied. However, at high dynamic pressures, many of the structural elements deflect under aerodynamic loads, which further complicates stability and control analysis. The study of the behavior of the structural elements under load and the interaction with aerodynamic load is called *aeroelasticity*. Aeroelastic effects usually tend to reduce static stability. In extreme cases, this interaction may lead to dangerous undamped structural oscillations called *flutter*. The rigid-body motions of an airplane may be divided into two classifications: longitudinal and lateral motions. *Longitudinal motions* occur in the plane of symmetry, whereas *lateral motions* displace the plane of symmetry. For normal symmetric airplanes, with small displacements from equilibrium, these two types of motions are independent of each other.

24.11.1 Static Longitudinal Stability

Static aerodynamic stability in pitch, more commonly known as static longitudinal stability, is most easily achieved through the use of an aft-mounted horizontal tail. In concept, static longitudinal stability may be defined as the tendency of the airplane to return to its original flight condition without pilot input, when disturbed from steady, unaccelerated flight. While not an absolute requirement for sustained, controlled flight, static longitudinal stability has been found to be a desirable characteristic for ease of flight, since the variation of the airplane pitching moment coefficient C_m with the airplane lift coefficient C_L has a negative slope, as shown on the pitching moment diagram in Fig. 24.54.

It should be noted that the pitching moment coefficient is defined with respect to the airplane center of gravity (c.g.) location, expressed as a percentage of the wing mean aerodynamic chord (m.a.c.) aft of the leading edge. For example, with a c.g. location expressed as 25% m.a.c., the c.g. is located at a distance of 25% of the m.a.c. length aft of the leading edge of the m.a.c. Using the sign convention noted earlier, the negative slope of the pitching moment curve means that, for an airplane in equilibrium (pitching moment equal to zero) in steady, unaccelerated flight at a given lift coefficient, any disturbance which increases the airplane lift coef-

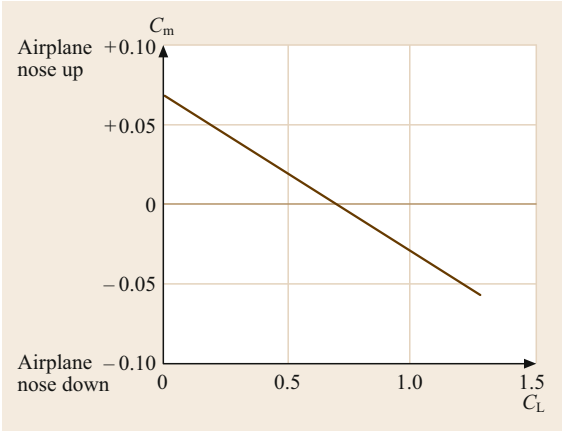

Fig. 24.54 Airplane pitching moment curve for a statically stable aircraft

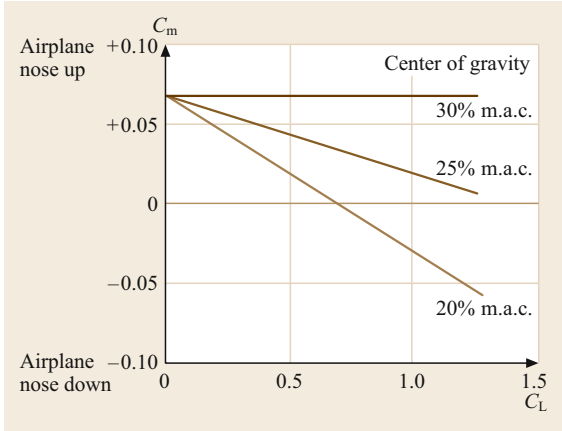

Fig. 24.55 Effect of c.g. location on airplane pitching moments

ficient will result in a negative, or airplane nose down (AND), pitching moment coefficient.

Effect of C.G. Location

It can be shown by analysis of the equation for the airplane pitching moment coefficient versus lift coefficient that the airplane c.g. location has a powerful effect on static longitudinal stability [24.26]. The results of this analysis show that, for every 1% of m.a.c. that the c.g. is moved forward, the slope of the pitching moment curve, dC_m/dC_L about that c.g. will become more negative by 0.01. This point is illustrated for a typical airplane configuration in Fig. 24.55. In this figure, the pitching moment curve with the c.g. located at 25% m.a.c. shows a negative (stable) slope of -0.05. If the c.g. is moved forward to 20% m.a.c., the pitching moment curve about this c.g. location shows a negative (stable) slope of -0.10, indicating that a 5% forward movement in the c.g. location results in a pitching moment curve that is more negative by 0.05. Similarly, if the c.g. is moved aft, the pitching moment curve will have a less stable (negative) slope about that c.g. location. In Fig. 24.55, if the c.g. location is moved aft to 30% m.a.c., then the slope of the pitching moment curve about this c.g. location is zero.

This situation illustrates another important concept in the discussion of static longitudinal stability, that of aerodynamic center.

Aerodynamic Center

From basic aerodynamics, the aerodynamic center location for any configuration is defined as the center of constant pitching moments, that is, the c.g. location where the pitching moment coefficient remains constant as the lift coefficient varies. In the illustration of Fig. 24.55, the aerodynamic center for the configuration shown is at 30% m.a.c., since for this c.g. location the pitching moment coefficient, C_m, is constant as the lift coefficient varies [24.27]. For any aircraft configuration, the criterion for achieving static longitudinal stability is that the aircraft c.g. must be located forward of the airplane aerodynamic center (a.c.). This criterion applies to all types of configurations, conventional aft-tail arrangements as well as canards, three-surface layouts, and even flying wings. However, as we shall see, this stability criterion is most easily met using a conventional aft-mounted horizontal tail. Again referring to Fig. 24.55, with the c.g. located at 25% m.a.c. and the a.c. located at 30% m.a.c., this configuration meets the criterion for static longitudinal stability, and with dC_m/dC_L equal to -0.05 is said to be stable by 5% m.a.c. With the c.g. located at 20% m.a.c. and the a.c. at 30% m.a.c., dC_m/dC_L is -0.10 and the configuration is said to be stable by 10% m.a.c. Expressed in equation form

$$\frac{dC_m}{dC_L} = X_{c.g.} - X_{a.c.} ,$$

where X is expressed in terms of a percentage of the m.a.c.

Aerodynamic Center Buildup

The aerodynamic center location for a complete airplane configuration is determined by the contribution of the various elements of the configuration in pitch. The contributions of these elements can be calculated with reasonable accuracy, but are usually verified by wind-tunnel model tests very early in the preliminary design phase. The major contributors to the complete configuration aerodynamic center are the wing, fuselage, engine nacelles, and horizontal tail. A typical wind-tunnel model

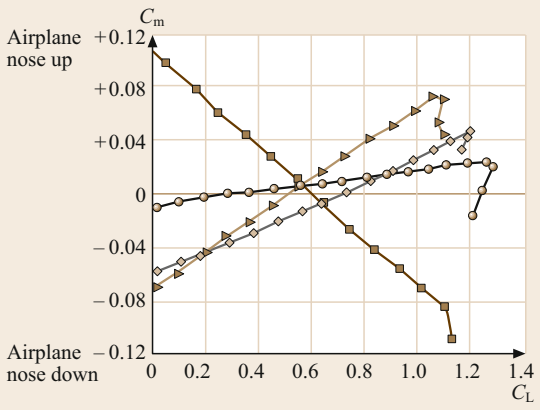

Configuration	p.m. curve slope dC_m/dC_L	a.c. location % m.a.c.	Effect of element on a.c. location
W	+0.024	22.6	–
W F	+0.087	16.3	$(-6.3\%)_{\text{fuselage}}$
W F N	+0.140	11.0	$(-5.3\%)_{\text{nacelles}}$
W F N H V	−0.177	42.7	$(+31.7\%)_{\text{horiz. tail}}$

Fig. 24.56 Aerodynamic center buildup. Straight wing, four-engine, propeller-driven transport model, center of gravity at 25% m.a.c.

buildup to determine the contributions of these elements to the complete configuration a.c. is shown in Fig. 24.56. These data are all referred to a c.g. location of 25% m.a.c. By measuring the slope of the pitching moment curve about this c.g., one can obtain the a.c. location for any configuration made up of the major elements that contribute to the a.c. location as

$$X_{\text{a.c.}} = 0.25 - \left(\frac{dC_m}{dC_L}\right) .$$

Figure 24.56 summarizes the a.c. locations for the various partial configurations, leading up to the complete configuration a.c. Also shown is the contribution of the various elements to the complete airplane a.c.

The wing-alone a.c. is at 22.6% m.a.c. The wing plus fuselage a.c. is at 16.3% m.a.c., indicating that the fuselage has a destabilizing or unstable contribution of 0.063 or 6.3% m.a.c. The wing plus fuselage plus engine nacelles have an a.c. location of 11.0% m.a.c., indicating that the nacelles have an unstable contribution of 5.3% m.a.c. to the a.c. location. The addition of the horizontal and vertical tails to the model results in an a.c. location for the complete configuration of 42.7% m.a.c. Since the vertical tail has no aerodynamic contribution in pitch, the horizontal tail provides a strong stabilizing contribution of 31.7% m.a.c. Some generalizations may be made from the data. First, the wing-only a.c. is usually around 25% m.a.c., not surprising since the a.c. for nearly all airfoil sections which make up the wing is within 1% m.a.c. or so of the 25% m.a.c. point. Wing sweep may also move the wing-alone a.c. by a percentage point or two, usually aft. Secondly, fuselages are destabilizing contributors, tending to move the a.c. location forward. The larger the fuselage relative to the wing, the more destabilizing its contribution to the complete airplane a.c. Forward-mounted nacelles, like the ones shown on the model in Fig. 24.56, are also destabilizing, although aft fuselage-mounted nacelles are usually stabilizing. Finally, the aft horizontal tail is a major stabilizing contributor to the complete airplane a.c. location. It can be shown that the horizontal tail contribution to static longitudinal stability is dependent on the distance between the 25% chord point on the wing m.a.c. and the 25% m.a.c. point on the horizontal tail, called the horizontal tail length l_H, and the horizontal tail area S_H. This is quite logical since static longitudinal stability involves the generation of aerodynamic restoring moments which are dependent on an aerodynamic force from the horizontal tail (proportional to the horizontal tail area) and a moment arm (proportional to the horizontal tail length).

24.11.2 Longitudinal Control

In addition to providing a major contribution to static longitudinal stability, the horizontal tail is also a source of longitudinal control moments. These control moments are used by the pilot to achieve equilibrium in pitch ($C_m = 0$) at any desired lift coefficient, allowing control of airspeed in unaccelerated flight, and the curvature of the flight path in accelerated flight. A typical pitching moment diagram illustrating the control moment required to balance the pitching moment at another lift coefficient is shown in Fig. 24.57.

This airplane is stable about its c.g. with a dC_m/dC_L equal to -0.10, and is in equilibrium ($C_m = 0$) at a lift coefficient $C_L = 0.5$. This means that the airplane will fly steadily at a speed corresponding to this lift coefficient, and its static longitudinal stability will resist any disturbances tending to deviate from this speed. If the pilot desires to slow the airplane down, and fly at

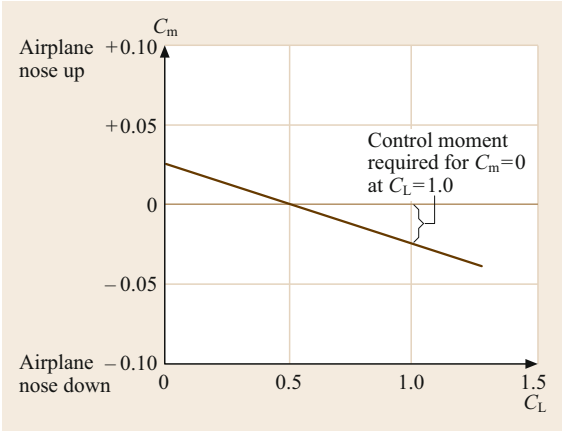

Fig. 24.57 Airplane pitching moment diagram, control moment requirement

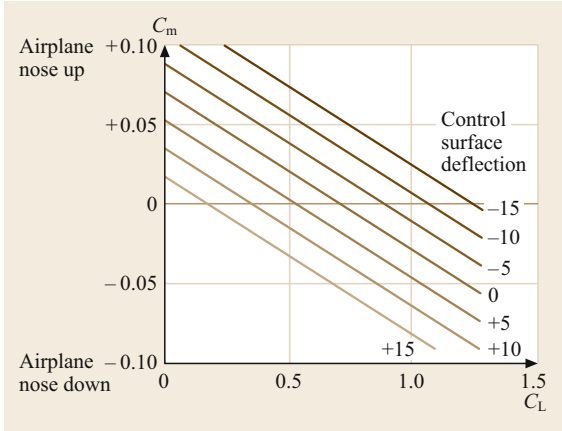

Fig. 24.58 Pitching moment diagram – effect of control deflections

a $C_L = 1.0$, he must be equipped with some type of control that can overcome the airplane nose-down moment coefficient of -0.05 at a $C_L = 1.0$, as shown in Fig. 24.57, in order to establish equilibrium at $C_L = 1.0$. Obviously, the more stable the airplane, the more control power must be provided to change the equilibrium lift coefficient. Thus, the designer must achieve a proper balance between the amount of static longitudinal stability provided and the amount of control power available. Longitudinal control power is usually provided through the hinged, movable aft portion of the horizontal tail (elevators), although in some designs the control power is provided by moving the entire horizontal tail about a fixed pivot point (all-movable horizontal tail or stabilator).

The longitudinal control capability for a specific configuration may be shown on a pitching moment diagram (Fig. 24.58), in which the pitching moment curves with various control surface deflections show the control deflection required to obtain equilibrium at various lift coefficients. Notice that a negative (trailing-edge-up) control deflection produces a positive (airplane-nose-up) pitching moment.

24.11.3 Static Directional Stability

Static directional stability for an airplane is defined as its tendency to develop restoring moments when disturbed from its equilibrium sideslip angle, normally zero. The static directional stability of an airplane is assessed from a chart of yawing moment coefficient, C_n, versus sideslip angle β as shown in Fig. 24.59. Using the sign convention of Figs. 24.11 and 24.13, a positive value of $dC_n/d\beta$ is required for static directional stability; i.e., a positive (airplane-nose-left) sideslip produces a positive (airplane-nose-right) yawing moment.

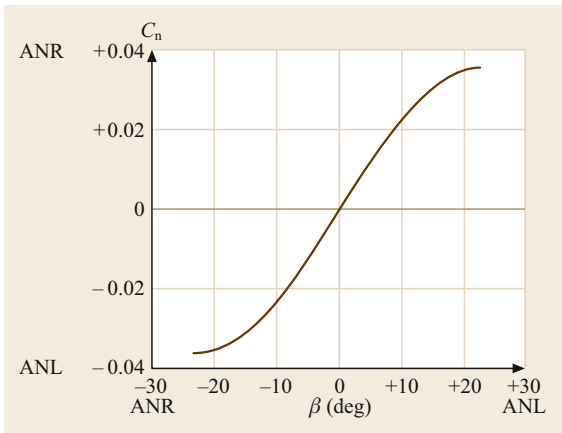

Fig. 24.59 Typical directional stability diagram (ANL = airplane nose left, ANR = airplane nose right)

Similar to the longitudinal case, the static directional stability of an airplane may be determined by adding up the contributions of the various elements of the configuration in sideslip. Analysis has shown that the main contributors to the airplane static directional stability are the fuselage and the vertical tail. The wing, a major element in longitudinal stability, has a negligible effect on the directional stability. This is due to the fact that an angle of sideslip produces very small cross-wind forces on the wing, whereas an angle of attack can produce very large lift forces. The fuselage is a major contributor to static directional stability, and its contribution is always unstable (destabilizing). The stabilizing contributor to static directional stability is the vertical tail, in reality a low-aspect-ratio wing attached to the aft fuselage. The contribution of the major elements is shown in Fig. 24.60. When a sideslip angle develops due to a disturbance, the vertical tail experi-

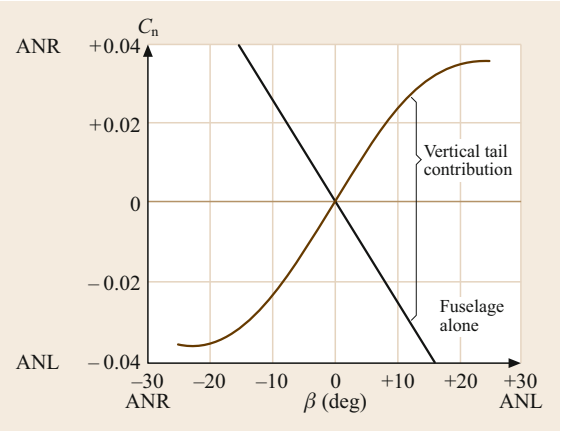

Fig. 24.60 Directional stability buildup (ANL = airplane nose left, ANR = airplane nose right)

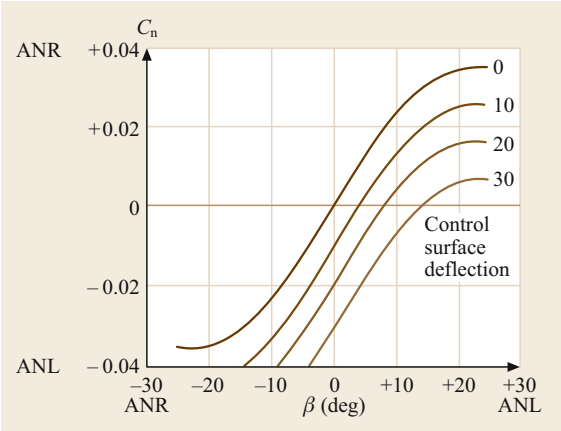

Fig. 24.61 Directional stability diagram – effect of control deflections (in degrees)

ences an increase in its angle of attack, and produces a restoring moment. The loss in directional stability at high sideslip angles, the *roundover* of the directional stability curve, is due to the vertical tail reaching its maximum lift capability, and stalling as the sideslip angle is increased. This roundover is not desirable and is often offset by the addition of a dorsal fin located at the intersection of the vertical tail leading edge and the fuselage. The magnitude of the restoring moment generated by the vertical tail depends on the distance from the airplane c.g. to the 25% m.a.c. point on the vertical tail, called the vertical tail length l_v and the vertical tail area S_v. For convenience, l_v is usually taken from the 25% m.a.c. point on the wing, rather than the c.g.

24.11.4 Directional Control

The vertical tail also provides the means for directional control. The predominant means is through a hinged, movable aft portion of the vertical tail (rudder), although some advanced military aircraft use all-movable verticals. As shown in Fig. 24.61, directional control is used to obtain equilibrium ($C_n = 0$) in steady sideslips. This figure shows that 30° of left rudder produces about 14° of positive sideslip.

Another requirement for directional control is to offset the asymmetric thrust moment which develops on a multiengine airplane when one engine becomes inoperative. In this situation, the aerodynamic moment from the vertical tail at or near zero sideslip with the control surface deflected must balance the thrust moment caused by the loss of one engine. This situation is most critical at low speeds during take-off. The minimum speed for which it is possible to maintain directional equilibrium ($C_n = 0$) during take-off with one engine inoperative is called the minimum control speed V_{mc},

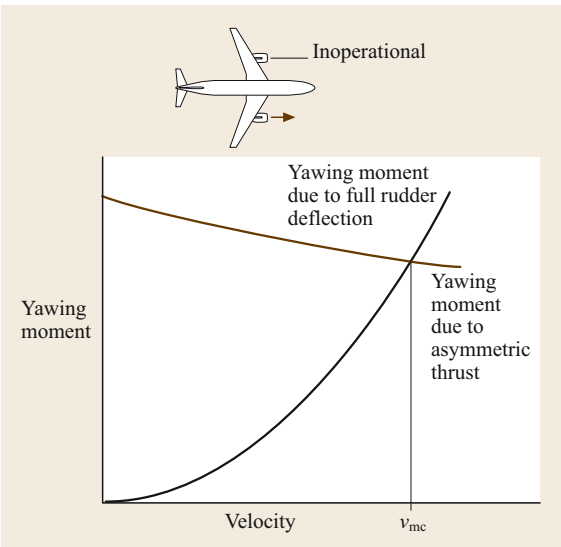

Fig. 24.62 Determination of ground minimum control speed

which may be obtained graphically by the intersection of the yawing moment due to the inoperative engine and the yawing moment due to full directional control, as shown in Fig. 24.62.

A summary of typical pilot control systems for airplanes is shown in Table 24.12.

24.11.5 Longitudinal Dynamics

In order to understand the requirements for static stability and control, it is necessary to study the dynamic characteristics of the airplane, investigating the types of motion that characterize the response of the airplane to a disturbance from some equilibrium flight condition

Table 24.12 Typical pilot control systems

Control about	Cockpit controller	Control direction	Airplane response
Lateral axis	Stick pull Stick push	Pitch	Nose up Nose down
Longitudinal axis	Stick right Stick left	Roll	Bank rwd Bank lwd
Vertical axis	Pedal right Pedal left	Yaw	Nose right Nose left

and the nature of the transient responses of the airplane to the movement of its controls. Dynamic systems in general have four different modes of motion when responding to a disturbance from an equilibrium condition. These modes are oscillatory or periodic, damped or undamped, as shown in Fig. 24.63.

The characteristic modes for nearly all airplanes are two oscillations, one of long period with poor damping, called the *phugoid*, and one of short period with heavy damping, called the *short period*. The *phugoid* oscillation is one in which there is a large-amplitude variation in airspeed, pitch angle, and altitude. The short period is a heavily damped oscillation in which the angle of attack varies at nearly constant speed.

24.11.6 Lateral Dynamics

There are two types of lateral dynamic motions. The first is called the *spiral mode*, which involves variations in bank angle and sideslip. This mode is usually a pure divergence, starting with a slow spiral in the direction of the disturbance, which if uncorrected, will develop into a high-speed spiral dive. The second motion is called the *Dutch roll*, because of its similarity to the well-known ice skating figure. This is an oscillatory motion involving variations in roll and yaw angles that for straight-wing propeller-driven airplanes is usually damped. However, for swept-wing airplanes, the Dutch roll oscillation is often lightly damped or mildly divergent, requiring the installation of a supplemental *yaw damper* system to provide satisfactory damping.

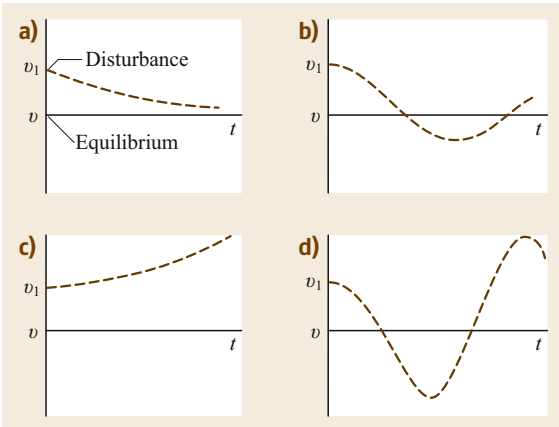

Fig. 24.63 Typical modes of motion. (a) Pure convergence; (b) damped oscillation; (c) divergence; (d) increasing oscillation

24.11.7 Maneuverability and Turning

The airplane flight path is controlled by varying the magnitude of the lift vector and by varying the output of the power plant. The magnitude of the lift vector is directly related to the lift coefficient through the angle of attack. The pilot can vary the angle of attack by controlling the pitching moment contributed by the control surfaces so that the pitching moment for the complete airplane is zero at the desired lift coefficient. From a steady unaccelerated level-flight condition, a maneuver in the plane of symmetry is initiated by a pilot control input to produce a positive nose-up pitching moment. This nose-up pitching moment will be balanced at some higher lift coefficient by the airplane's static longitudinal stability. If the longitudinal control input is made fairly rapidly, the speed will not have time to reduce to the speed required for equilibrium, and the lift will exceed the weight. With lift greater than weight, the airplane will experience a vertical acceleration. The maneuver just described is called an *abrupt pull-up* and may be the start of more complicated maneuvers. For a level-flight turn, referring to Fig. 24.64, the horizontal component of the lift vector accelerates the airplane laterally and curves the flight path. In a turn of radius R, the lateral force $L\sin\phi$, where ϕ is the angle of bank, must balance the centrifugal force on the airplane. Thus,

$$L\sin\phi = \frac{(W/g)V^2}{R}\,. \tag{24.3}$$

For a level-flight turn, the weight W must be equal to the vertical component of the lift $L\cos\phi$. Substitut-

Load factors in level flight turns

ϕ (deg)	$n = L/W = 1/\cos(\phi)$
0	1.000
15	1.035
30	1.155
45	1.414
60	2.000
75	5.464
90	∞

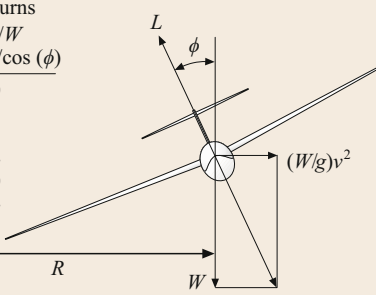

Fig. 24.64 Forces and load factors in level-flight turns

ing into (24.3), we obtain

$$L\sin\phi = \frac{[(L\cos\phi)/g]V^2}{R}\,, \quad \tan\phi = \frac{V^2}{\mathrm{gR}}\,. \quad (24.4)$$

Equation (24.4) specifies the angle of bank required for any speed and radius of turn. Conversely, the radius of turn is given by

$$R = \frac{V^2}{g\tan\phi}\,.$$

Also, since for a level-flight turn

$$W = L\cos\phi\,,$$

it follows that the lift for such a turn must be given by $L = W/\cos\phi$ and

$$\frac{L}{W} = \frac{1}{\cos\phi} = n\,.$$

As we shall see below, the quantity $n = L/W$ is an important parameter defined as the *load factor*.

24.12 Loads

Aircraft structures must be designed to withstand the most serious of the infinite number of possible combinations of external loads that may act on it in flight and when landing. Experience, accumulated over many years of design, analysis, and research, has led to the formulation of a very rational set of procedures that determine the design loads and define the airspeeds for which the design loads are imposed. For civil aircraft, these requirements and procedures are described in the FAR part 23 and part 25 *Airworthiness Standards, Airplanes*. For military aircraft, these requirements and procedures are described in MIL-A-8660, *Airplane Strength and Rigidity, General Specification For* and MIL-A-8661, *Airplane Strength and Rigidity, Flight Loads*. The requirements are, in most cases, nearly identical in both the civil and military documents. The information that follows is based on FAR 23 and 25, with information from MIL-A-8660 and MIL-A-8661 added where significant differences exist [24.26]:

- Flight conditions (FAR 25.331–25.459):
  - Maneuver load generated by intentional pilot application of controls
  - Gust load generated bya sudden change in angle of attack due to encountering a *gust*
- Landing conditions (FAR 25.473–25.511):
  - Level landing
  - Tail-down landing
  - One-wheel landing
  - Side load conditions
  - Braked roll conditions
  - Yawing conditions

24.12.1 Air Loads

Flight Load Factor

An important concept in the analysis of air loads imposed under various flight conditions is the flight load factor n, which is defined as

$$n = \frac{\text{aerodynamic force } \perp \text{ longitudinal axis}}{\text{aircraft weight}}\,.$$

For an aircraft in steady, level flight, the aerodynamic force perpendicular to the longitudinal axis is given by the lift, which is equal to the weight. Since the weight is due to the force of gravity, the aircraft is said to be in $1g$ flight. If the lift is four times the weight, the aircraft is subjected to $4g$. In a simpler form,

$$n = \frac{\text{lift}}{\text{weight}}\,.$$

V–n Diagrams

The analysis of the critical design air loads for an aircraft employs a chart known as the V–n diagram [24.26]. These charts show flight load factors as a function of equivalent airspeed and represent the maximum load factors expected in service, based on the requirements of the applicable specifications. These load factors are called *limit* load factors. The airplane structure must withstand these loads without damage. These limit loads are multiplied by a safety factor of 1.5 to define *ultimate* or failure loads. There are two types of V–n diagrams: one to define maneuver load factors, and one to define gust load factors.

V–n Diagram: Maneuver Envelope FAR 23.333 and FAR 25.333

The V–n diagram showing the maximum maneuver load factors that must be used for structural design (Fig. 24.65) is an envelope defined by various lines and points which have a specific relationship to the design load factors. A brief explanation of the key portions of the maneuvering envelope is given here.

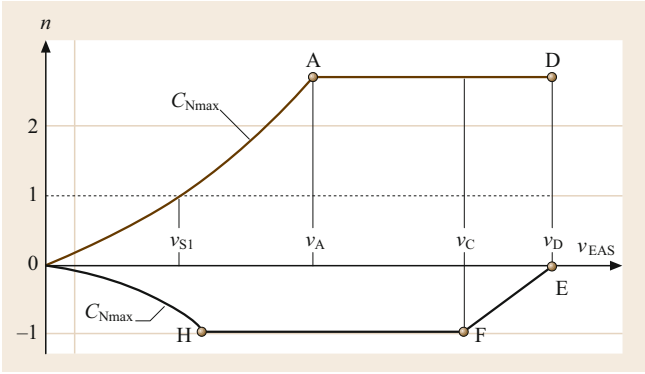

Fig. 24.65 *V–n* diagram: maneuvering envelope

Line O–A

This line describes the load factor that results when the aircraft is maneuvered to its maximum normal force coefficient $C_{N_{max}}$ in the clean or cruise configuration. Since this is the maximum normal force that can be generated by the aerodynamic characteristics of the configuration, it is the maximum load factor that can be generated by the pilot. The equation of this line is $n = C_{N_{max}} qS/W$.

Point A

This is the intersection of the pull up to $C_{N_{max}}$ with the maximum positive maneuver load factor specified in the requirements for the particular type of aircraft being designed. It should be noted that point A is not selected by the designer, but is determined uniquely by the aircraft parameters and the maneuver limit load factor for the type.

Table 24.13 Maximum maneuver load factors

Aircraft type	Max. positive	Max. negative
Normal	3.8	1.52
Acrobatic	6.0	3.00
Commuter	3.8	1.52
Utility	4.4	1.76

Line A–D

This is the maximum positive maneuver load factor for the type. The design limit load factors for various aircraft types were determined many years ago from flight tests of a number of airplanes of various types, each subjected to a number of typical maneuvers. These tests were made with an accelerometer placed at or near the airplane center of gravity, which recorded the imposed accelerations. Experience has indicated that these load factors result in highly satisfactory designs.

Line O–H

This line describes the load factor generated when the airplane is maneuvered to its maximum negative $C_{N_{max}}$ value. Since wing design is focused on using airfoils that have high values of positive $C_{N_{max}}$, the maximum values of negative $C_{N_{max}}$ are usually about 0.7 times the positive $C_{N_{max}}$ values.

Line H–F

This line describes the maximum negative maneuver load factor, again determined from flight tests as noted above.

The maximum maneuver load factors vary with aircraft type (Table 24.13). For FAR 23 aircraft, the maximum positive and negative maneuver load factors are listed in Table 24.14.

For FAR 25 aircraft, the maximum positive maneuver load factor varies with the design gross weight. The maximum value is 3.8 up to a gross weight of 4100 lb. At higher gross weights, the maximum value varies according to the relation up to a gross weight of 50 000 lb where the maximum becomes a constant value of 2.5. The maximum negative maneuver load factor for FAR part 25 aircraft is -1.0. Corresponding maneuver load factors for military aircraft are shown in Table 24.14.

V–n Diagram: Gust Envelope FAR 23.333 and FAR 25.333

In addition to the load factors imposed by intentional maneuvers controlled by the pilot, appreciable

Table 24.14 Design maneuver load factors for military airplanes

Aircraft type	Basic flight design weight		All weights	Max. design weight		Max. ordnance weight	
	Max.	Min. at V_H	Min. at V_H	Max.	Min. at V_H	Max.	Min. at V_H
Fighter/attack (subsonic)	8.00	−3.00	−1.00	4.00	−2.00	5.50	−2.00
Fighter/attack (supersonic)	6.50	−3.00	−1.00	4.00	−2.00	5.50	−2.00
Observation trainers	6.00	−3.00	−1.00	3.00	−1.00		
Utility	4.00	−2.00	0	2.50	−1.00		
Tactical bomber	4.00	−2.00	0	2.50	−1.00		
Strategic bomber	3.00	−1.00	0	2.00	0		
Assault transport	3.00	−1.00	0	2.00	0		
Conventional transport	2.50	−1.00	0	2.00	0		

increases in effective angle of attack result from entering a *gust*, or current of air having a velocity component normal to the line of flight. The resulting increase in load factor depends primarily on the vertical velocity of the gust, and especially for business jets and jet transports, it may exceed the maximum due to intentional maneuvers. These load factors are summarized on a *V*–*n* gust envelope diagram (Fig. 24.66).

The load factors produced by gusts vary directly with the equivalent airspeed, and are computed using the gust load factor equation given in FAR 23.341 and FAR 25.343.

The equation is

$$n = 1 + \frac{K_g U_{gE} V_E a}{498(W/S)} ,$$

where

$$K_g = \frac{0.88\mu_g}{5.3 + \mu_g} = \text{gust alleviation factor} ,$$

$$\mu_g = \frac{2(W/S)}{\rho \overline{C}_{ag}} = \text{airplane mass ratio} ,$$

U_{gE} = equivalent gust velocity (ft/s) ,

ρ = density of the air $\left(\text{slug/ft}^3\right)$,

$\frac{W}{S}$ = wing loading $\left(\text{lb/ft}^2\right)$,

$\overline{C}$ = mean geometric chord (ft) ,

g = acceleration due to gravity $\left(\text{ft/s}^2\right)$,

V_E = aircraft equivalent airspeed (kn) ,

a = slope of the airplane normal force curve per radian .

The *V*–*n* diagram for the gust envelope is shown in Fig. 24.66.

The designer must assume a symmetrical vertical gust of:

- 66 fps at V_B from sea level (S.L.) to 20 000 ft, decreasing to 38 fps at 50 000 ft
- 50 fps at V_C from S.L. to 20 000 ft, decreasing to 25 fps at 50 000 ft
- 25 fps at V_D from S.L. to 20 000 ft, decreasing to 12.5 fps at 50 000 ft.

The key points of the gust envelope are as follows.

Line 0–B′

As in the maneuver envelope, this line describes the maximum load factor that can be generated by a gust which causes the airplane to reach its $C_{N_{max}}$.

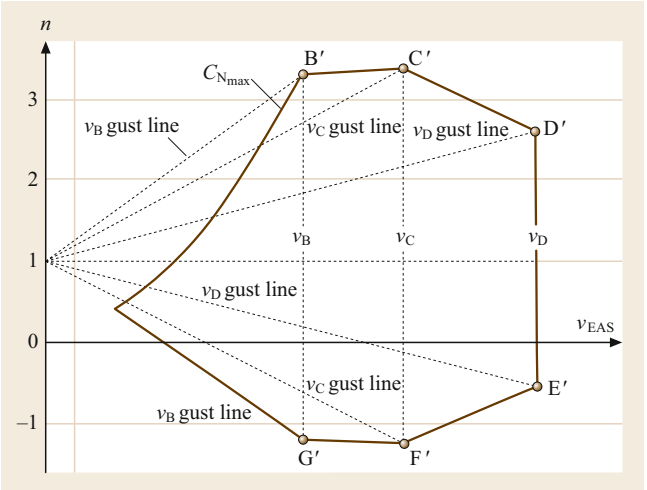

Fig. 24.66 *V*–*n* diagram: gust envelope

Point B′

This point is the intersection of the load factor for $C_{N_{max}}$ and the load factor for a 66 fps gust. This point determines V_B, the design speed for maximum gust intensity.

Point C′

This point is the intersection of the load factor due to a 50 fps gust and the design cruising speed V_C.

Point D′

This point is the intersection of the load factor due to a 25 fps gust and the design dive speed, V_D.

Points E′, F′, and G′

These points are the corresponding intersections for negative gusts at the designated speeds.

The maneuver and gust envelopes are superimposed to determine the highest load factors for design at all speeds within the flight envelope and the entire aircraft structure analyzed for these load factors.

In addition to these major air loads imposed on the airplane by intentional maneuvers and gusts, there are other conditions associated with abrupt control inputs in pitch, roll, and yaw that must be accounted for in the structural design.

24.12.2 Design Airspeeds

The airspeeds associated with the *V*–*n* diagram except for V_A and V_B are chosen by the designer, but must meet certain definitions and criteria contained in the FARs. The following list is a simplified summary.

Design airspeeds – EAS:

V_S Stalling speed or minimum steady flight speed
V_A Maneuver speed or full control deflection speed

V_B Design speed for maximum gust intensity
V_{FE} Design flap-extended speed
V_{LE} Design landing-gear-extended speed
V_{LO} Design landing-gear-operating speed (if different from V_{LE})
V_C Design cruising speed ($\geq V_B + 43$ kts)
V_{MO} Maximum operating limit speed (*barber's pole* speed)
V_{FC} Maximum speed at which flight characteristics requirements must be met
V_D Design dive speed, $\geq V_C/0.80$, or speed reached in 7.5° dive for 20 s from V_C, followed by 1.5g recovery.

The military speed definitions are basically the same, although MIL-A-8660B combines V_C and V_{MO} into a maximum level flight speed V_H, and replaces V_D with the *limit speed* V_L.

For subsonic airplanes, the design airspeeds are usually constant for the entire flight envelope. For high-subsonic and supersonic airplanes, the design airspeeds are varied throughout the flight envelope, since equivalent airspeeds that are appropriate at sea level and lower altitudes are beyond the performance capabilities of the airplane at higher altitudes. Therefore, the design airspeeds for these types are usually defined in terms of Mach number at higher altitudes; for example, the maximum operating limit speed is defined by a V_{MO}/Ma_{MO} line that is a function of altitude. As noted earlier, the design cruise speed (Mach number) need not be higher than the maximum speed in level flight at that altitude with maximum cruise power. This provision usually sets Ma_C. V_{MO} is usually set at or slightly above (0.01 or 0.02 Mach number) Ma_C, providing a margin on the order of 0.08 Mach number between the best long-range cruise Mach number and Ma_{MO}. The design dive Mach number is usually about 0.05 Mach number higher than Ma_{MO}.

24.12.3 Ground Loads

There are a range of take-off and landing conditions that must be considered in the structural design of the airplane. These conditions are described in detail in the appropriate sections of the Federal Aviation Regulations. These loads may be classified as vertical loads due to descent rates at touchdown and taxiing over rough surfaces, longitudinal loads caused by wheel spin-up loads on landing, braking loads, and rolling friction loads, and lateral loads caused by landing with some sideslip angle, cross-wind taxiing, and turning on the ground.

24.13 Airplane Structure

The structure of an aircraft must withstand the applied aerodynamic and ground reaction loads encountered in normal operation, as well as those that may be encountered very rarely. The essential character of aircraft structure is light weight, because weight plays such an important role in the performance and economics of the airplane. This critical significance of structural weight is the major difference between aircraft structural design and other types of structural design [24.28].

Overall aircraft structural loads consist of shear, bending, and torsion. Aircraft structural design has always sought to meet the applied load requirements with a minimum acceptable margin of safety and the least weight. However, the potentially disastrous effect of an aircraft structural failure requires that the structure must be designed for long life either with safe life criteria or fail-safe design. Safe life means that the stresses in a component are so low that fatigue failure is not possible over the anticipated life of the airplane, or at least until some period has passed after which a part replacement is required. Fail-safe means that the structure has alternate load paths so that no single failure of a part will be hazardous to the airplane. This is accomplished by designing the structure so that no one part carries most of the maximum load. Therefore, if one part fails, the remainder of the structure can still carry most of the maximum load. Since the maximum load is rarely encountered, and the structure has a safety factor of 1.5, the structure remains safe until the failure is found and repaired.

24.13.1 Structural Design

Aircraft structures are composed of three basic types of structural elements: stiffened shells, stiffened plates, and beams. The terms "stiffened shells" and "stiffened plates" refer to the fact that, under compressive loading, the thin skins of the shells and plates generally buckle before reaching the compressive failure stress of the material. To avoid this condition, stiffeners are attached to the thin skins. Stiffeners not only carry their own load, but by preventing early buckling of the skin, they increase the stress that can be supported in compression before buckling occurs. The primary wing structural element, the wing *box*, is essentially a hollow beam, consisting of the upper and lower wing skins, ribs, wing

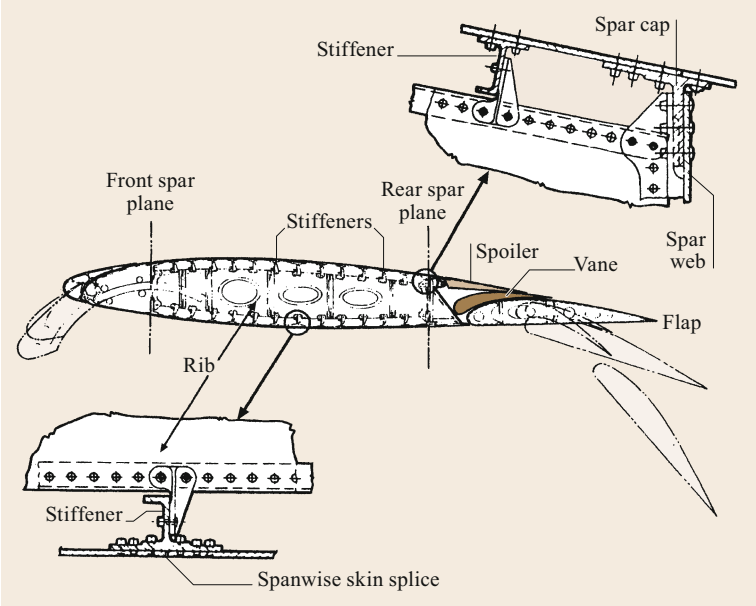

Fig. 24.67 Wing box structural elements

skin stiffeners, spar caps, and spar webs, as shown in Fig. 24.67.

The wing skins transfer the external air loads to the wing box structure. The fuselage is generally a semimonocoque structure (Fig. 24.68) that consists of frames which maintain the cross-sectional shape, to which are attached various longitudinal stiffeners called stringers or longerons. Loads on the fuselage floor are supported by floor beams, with other beam elements to accommodate cutouts in the fuselage shell. The horizontal and vertical tail structure is very similar to the wing structure, employing skins, ribs, stiffeners, spars, spar caps, and spar webs.

An overview of the semimonocoque construction of a Boeing KC-767a jet is shown in Fig. 24.69.

Another important aspect of structural design is the need to design for long fatigue life. Metals suffer gradual deterioration under repeated application and removal of loads. Modern commercial transports may fly for many thousands of hours and take-off and landing cycles, so that often fatigue life, rather than strength requirements, dominate the structural design. The number of load cycles a material can tolerate depends on the stress level. The lower the stress level, the greater the number of cycles that the part can withstand. The results of a typical fatigue test (Fig. 24.70) show the

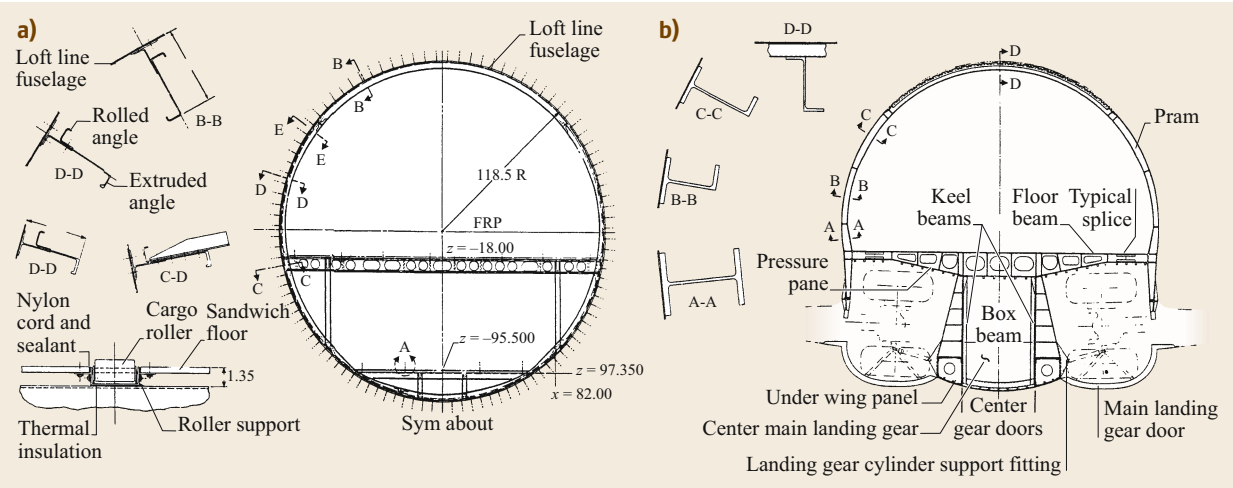

Fig. 24.68a,b Fuselage structural elements: **(a)** Typical fuselage cross section; **(b)** section through wheel wall

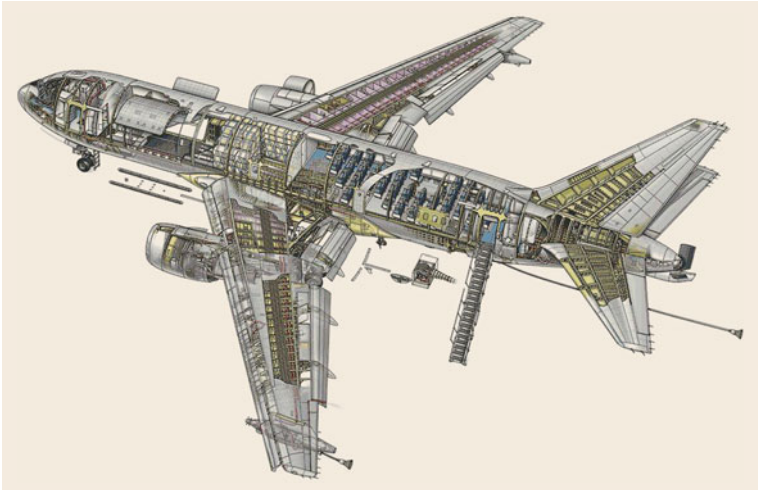

Fig. 24.69 Semimonocoque construction of a Boeing KC-767a jet (Flight International, © 2006 Reed Business Information)

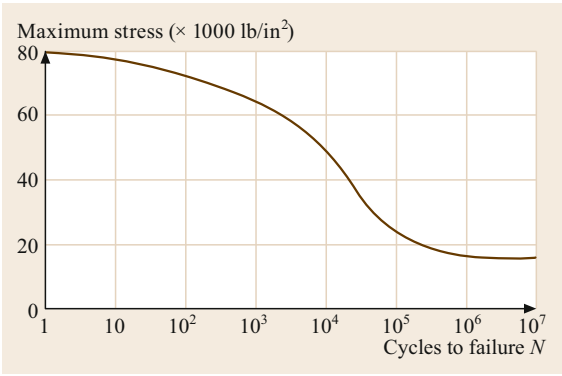

Fig. 24.70 Fatigue test results

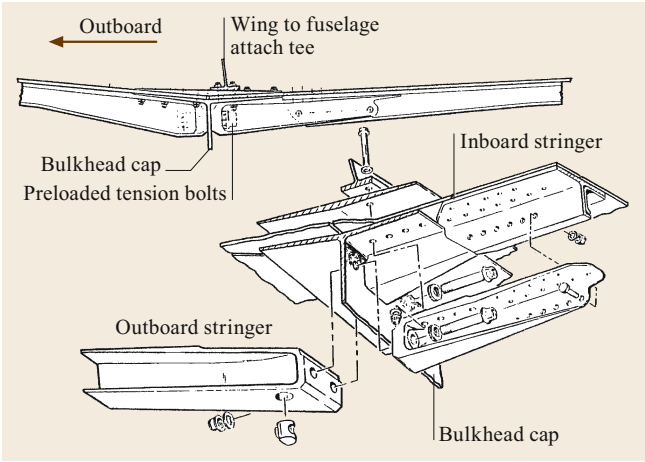

Fig. 24.71 Wing–fuselage joint fitting

tremendous improvement in fatigue life that can be obtained by limiting a material to cyclic stress levels that are well below the ultimate strength.

If fatigue is critical, a less strong material with better fatigue resistance may result in a lighter structure. Excessive stress levels conducive to early fatigue failure may arise not only from an overall high stress level, but also from stress concentrations at local points in the structure. Fittings and joints, which serve to carry loads from one structural component to another, may, if not designed very carefully, introduce increased local stresses leading to fatigue failure long before any problem occurs in the basic structure. A major part of the design of aircraft structure is the avoidance of stress concentrations by careful detail design. One approach is to lower the stress level approaching a hole or fitting by adding an extra sheet or thickness of metal called a *doubler* to the inside surface of a wing skin around an access hole or to the fuselage skin around a window. Special attention is given to fitting design (Fig. 24.71). In spite of the care taken in detailed structural design, a vital part of aircraft maintenance is the continuing search on a scheduled basis for structural cracks.

24.13.2 Structural Analysis

In the design and analysis of a real aircraft structure, which is usually a large assemblage composed of various structural elements such as stiffened shells, stiffened plates, and beams, the overall geometry becomes extremely complex and cannot be represented by a single mathematical expression. In addition, these built-up structures are characterized as having material and structural discontinuities such as cutouts, thickness variations in the members, as well as discontinuities in loading and support structures. It is apparent that classical methods can no longer be used, particularly those which require the formulation and solution of govern-

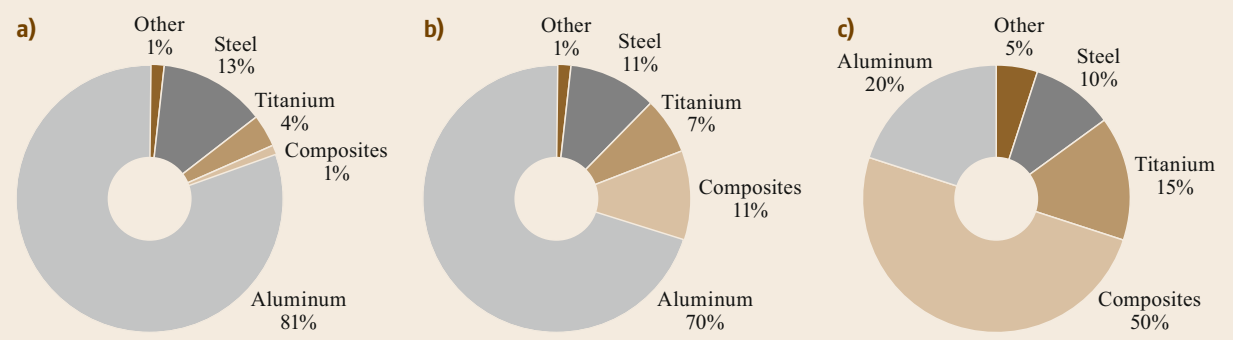

Fig. 24.72a–c Comparison of structural materials distribution – commercial transports. **(a)** Boeing 747, **(b)** Boeing 777, and **(c)** Boeing 787 Dreamliner

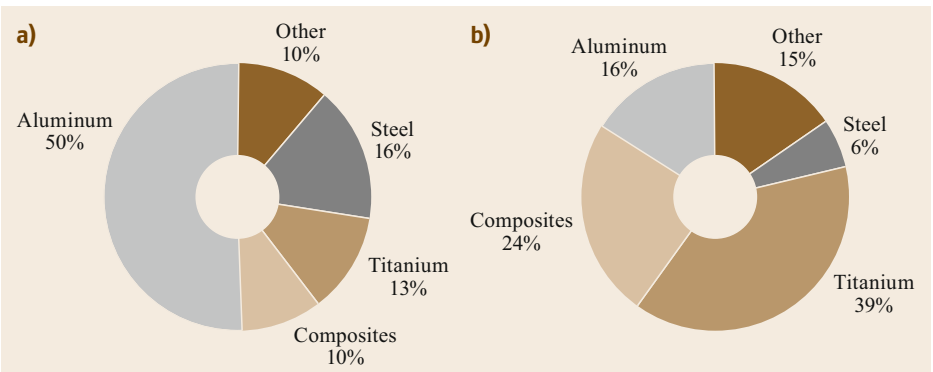

Fig. 24.73a,b Comparison of structural materials distribution – military fighters. McDonnel Douglas F-18, **(a)** Lockheed Martin F-22

ing differential equations. For complex structures, the preferred method of analysis is called the finite element stiffness method. With the advent of high-speed large-storage-capacity digital computers, finite element matrix methods have become the most widely used tools in the analysis of complex structures.

24.13.3 Structural Materials

Modern aircraft are constructed from a variety of materials, chosen based on considerations such as density, mechanical properties, corrosion resistance, ease of fabrication, and cost. The most used materials are the light metals, aluminum alloys, and titanium, although for some applications where high strength is required, steel alloys are used. Structural composite materials are being used more because of their low density and good mechanical properties. Composites generally consist of a plastic matrix of epoxy resin, reinforced by many high-strength fibers of carbon, Kevlar, glass, or boron. The distribution of materials used in aircraft construction has been changing over the years as materials science researchers have developed more attractive products. Figure 24.72 shows a comparison of the structural materials distribution between the Boeing 747 of 1969, the Boeing 777 of 1994, and the Boeing 787 of 2009. In the 40 years between the design of these three transport aircraft, the most notable difference in materials use is the large increase in composites and titanium, and a significant reduction in the use of aluminum.

An even more startling change in the structural materials distribution has taken place in military aircraft design. Figure 24.73 shows the distribution of structural materials in the McDonnell Douglas F-18 of 1978 and the Lockheed Martin F-22 of 2003. The most startling difference in the materials use between these two aircraft is the large reduction in the use of aluminum alloy and steel in the F-22 and the large increase in the use of titanium and composites.

In addition to the introduction of newer, nontraditional materials, several new processes for producing parts from these new materials have been introduced, which reduce the number of parts required and also reduce the amount of labor required to produce each part. Examples of these new processes are *resin transfer molding* (RTM) for producing composite parts, and *hot isostatic pressing* (HIP) for producing large high-quality castings.

24.14 Airplane Maintenance Checks

As noted earlier, in order to ensure safe operations, especially for commercial transport aircraft, regular formal maintenance checks are carried out on airplanes' systems and structure. These checks range from the very simple *preflight* check of the aircraft conducted by the flight crew prior to each flight, to the extensive, detailed maintenance inspection checks conducted by technical specialists at major maintenance facilities. A summary of the various types of maintenance checks that are conducted by airline operators is presented in Table 24.15.

Table 24.15 Summary of typical maintenance checks for transport airplanes

	B 737	B 747	A 300	A 320	Time required	Man-hours
A-Check	350 h	650 h	350 h	350 h	Overnight	20–130
B-Check	5.5 m	1800 h	1000 h	–	One day	200–1000
C-Check	15 m	18 m	18 m	15 m	A few days	600–1400
D-Check	22 000 h 25 000 ldg 108 m	31 000 h 72 m –	25 000 h 12 500 loading 108 m	– – 102 m	≈ 6 weeks	50 000

References

24.1 AIA: Manufacturing Workforce – Aerospace Industry Association Rep. (AIA, Arlington 2019), https://www.aia-aerospace.org/research-center/statistics/industry-data/workforce/

24.2 IATA: International Air Transport Association Rep. 62 (IATA, Geneva 2018), https://www.iata.org/en/pressroom/pr/2018-10-24-02/

24.3 P. Moran: Environmental Trends in Aviation 2050, FAA Office of Environment and Energy Report (2019), https://www.icao.int/Meetings/EnvironmentalWorkshops/Documents/Env-Seminars-Lima-Mexico/Mexico/08_UnitedStates_EnvironmentTrends.pdf

24.4 P. Argüelles, J. Lumsden, M. Bischoff: *European Aeronautics: A Vision for 2020* (Office for Official Publications of the European Communities, Luxembourg 2001)

24.5 D.P. Raymer: *Aircraft Design: A Conceptual Approach* (American Institute of Aeronautics and Astronautics, Reston 2006)

24.6 Federal Aviation Administration: *Code of Federal Regulations, Title 14, Aeronautics and Space* (Office of the Federal Register: Federal Aviation Administration, Washington 1997)

24.7 D. Küchemann: *The Aerodynamic Design of Aircraft* (Pergamon, Oxford 1978)

24.8 C.B. Millikan: *Aerodynamics of the Airplane* (Wiley, New York 1941)

24.9 A.M. Kuethe, J.D. Schetzer: *Foundations of Aerodynamics* (Wiley, New York 1950)

24.10 L.M. Nicolai: *Fundamentals of Aircraft Design* (METS, San Jose 1984)

24.11 R.D. Schaufele: *The Elements of Aircraft Preliminary Design* (Aries Publications, Santa Ana 2000)

24.12 H.W. Liepmann, A.E. Puckett: *Aerodynamics of a Compressible Fluid* (Wiley, New York 1947)

24.13 L.K. Loftin Jr.: *Subsonic Aircraft: Evolution and the Matching of Size to Performance* (NASA, Arlington 1980), (NASA Reference Publication 1060)

24.14 D.P. Raymer: *Aircraft Design: A Conceptual Approach* (AIAA, Washington 1989)

24.15 J. Roskam: *Airplane Design: Part I, Preliminary Sizing of Airplanes* (Roskam Aviation and Engineering, Ottawa 1989)

24.16 I.H. Abbott, A.E. Von Doenhoff: *Theory of Wing Sections* (Dover, New York 1959)

24.17 R.D. Schaufele, A.W. Ebeling: *Aerodynamic Design of the DC-9 Wiing and High Lift System, SAE Paper No. 67-0846* 1967), (Aeronautics and Space Engineering Meeting, Los Angeles)

24.18 Anonymous: *The DC-9 Handbook* (Douglas Aircraft, Long Beach 1991)

24.19 Anonymous: *The DC-10 Handbook* (Douglas Aircraft, Long Beach 1986)

24.20 N.S. Currey: *Aircraft Landing Gear Design: Principles and Practices* (AIAA, Washington 1988)

24.21 J. Roskam: *Airplane Design, Part IV; Layout Design of the Landing Gear and Systems* (Roskam Aviation and Engineering, Ottawa 1989)

24.22 A.P. Fraas: *Aircraft Power Plants* (McGraw-Hill, New York 1943)

24.23 Anonymous: *Brief Methods of Estimating Airplane Performance, Report No. SM-13515* (Douglas Aircraft, Santa Monica 1949)

24.24 Anonymous: *DC-9-30 Performance Handbook* (Douglas Aircraft, Long Beach 1969)

24.25 R.S. Shevell, I. Kroo: *Introduction to Aircraft Design Synthesis and Analysis, Course Notes* (Stanford Univ. Press, Palo Alto 1981)

24.26 C.D. Perkins, R.E. Hage: *Airplane Performance Stability and Control* (Wiley, New York 1949)

24.27 R.S. Shevell: *Fundamentals of Flight* (Prentice Hall, Englewood Cliffs 1989)

24.28 D.J. Peery, J.J. Azar: *Aircraft Structures* (McGraw-Hill, New York 1982)

Hamid Hefazi

Mechanical Engineering Department
State University of New York (SUNY)–Korea
Incheon, Republic of Korea
hamid.hefazi@sunykorea.ac.kr

Hamid Hefazi received the PhD degree in Aerospace Engineering from the University of Southern California in 1985. He is currently Professor and Chair of mechanical engineering department at SUNY-Korea. His research areas include computational fluid dynamics (CFD), aerodynamic design optimization, aeroacoustics, hydrodynamics, neural networks, and advanced optimization methods.